Universitat de Girona

OPERATION AND CONTROL OF HIGH RATE ACTIVATED SLUDGE PROCESS IN URBAN WASTEWATER TREATMENT PLANTS

Joan Canals Tuca

DOCTORAL THESIS

Operation and control of High Rate Activated Sludge process in urban wastewater treatment plants

Joan Canals Tuca

2024

DOCTORAL THESIS

Operation and control of High Rate Activated Sludge process in urban wastewater treatment plants

Joan Canals Tuca

2024

Supervised by

Dr. Hèctor Monclús Sales

Dra. Alba Cabrera Codony

Dra. Maria J. Martín Sánchez

Academic Tutor:

Prof. Manuel Poch Espallargas

Thesis submitted in fulfilment of the requirements for the degree of
Doctor from the University of Girona
Water Science and Technology Programme

HÈCTOR MONCLÚS SALES

Professor del Departament d'Enginyeria Química, Agrària i Tecnologia Agroalimentària de la Universitat de Girona.

ALBA CABRERA CODONY

Professor del Departament d'Enginyeria Química, Agrària i Tecnologia Agroalimentària de la Universitat de Girona.

MARIA J. MARTÍN SÁNCHEZ

Professor del Departament d'Enginyeria Química, Agrària i Tecnologia Agroalimentària de la Universitat de Girona.

Certifiquem:

Que el treball titulat **Operation and control of High Rate Activated Sludge process in urban wastewater treatment plants**, que presenta **Joan Canals Tuca** per a l'obtenció del títol de doctor, ha estat realitzada sota la nostra supervisió i que compleix els requisits per optar a Menció Industrial. I perquè així consti i tingui els efectes oportuns, signem aquest document.

Hèctor Monclús Sales Alba Cabrera Codony Maria J. Martín Sánchez

A Girona, 22 de març de 2024

Journal publication derived from this PhD Thesis:

Canals, J., Cabrera-Codony, A., Carbó, O., Torán, J., Martín, M., Baldi, M., Gutiérrez, B., Poch, M., Ordóñez, A., & Monclús, H. (2023). High-rate activated sludge at very short SRT: Key factors for process stability and performance of COD fractions removal. Water Research, 231. https://doi.org/10.1016/j.watres.2023.119610

Canals, J., Cabrera-Codony, A., Carbó, O., Baldi, M., Gutiérrez, B., Ordoñez, A., Martín, M. J., Poch, M., & Monclús, H. (2024). Nutrients removal by high-rate activated sludge and its effects on the mainstream wastewater treatment. Chemical Engineering Journal, 479. https://doi.org/10.1016/j.cej.2023.147871

This thesis was partially funded by Centre for the Development of Industrial Technology (CDTI) Spanish Ministry of Science, Innovation and Universities (MCIU).

LEQUIA has been recognized as "consolidated research group" (2021-SGR-1352) by the Catalan Ministry of Research and Universities.

Acknowledgments

En primer lloc, el meu agraïment a l'Hèctor, el meu director de Tesi, per la seva ajuda, rigor científic i coneixements aportats, a part de l'exquisit tracte amb que a tractat a un *tesinando* de setanta anys moldejat per tants anys d´ofici. Moltes gràcies, et desitjo lo millor.

Agraït a l´Alba (Déu meu! que jove!) per l´ajuda impagable d'introduir-me en el llenguatge científic i ensenyar-me a destriar el blat de la palla. Sense ella, els escrits d´aquesta tesi no serien el mateix.

Agraït a la Maria, per l´ajuda en el plantejament de mètodes i programes en la fase experimental del treball, i en el seu reconegut esperit crític, imprescindible per una Tesi.

Un agraïment molt especial al Manel, el meu tutor, al que vaig trair, canviant el tema de la Tesi. No et preocupis: el post-doc el faré sobre el teu tema.

Agraït l'Oriol Carbó i la Josefina Toran per la seva gran ajuda en el treball en la planta pilot. Quin luxe haver tingut aquests col·laboradors!

Agraït a l'Imre Tackacs i a l´Elénè Hauduc per la seva ajuda en el treball de modelització i pels consells per centrar el treball de Tesi.

Agraït a Bernard Wett pels seus consells en la visita al HRAS d'Strass paradigma de la recuperació d'energia en una EDAR.

Agraït a l'Antonio Ordoñez, la Merce Baldi i la Belen Gutierrez, responsables del treball de recerca a GSInima, i amics de llargues hores de discussions processistes.

Agraït a GSInima pel suport econòmic i moral en aquest treball.

Agraït al CEDTI per el seu suport econòmic.

Agraït al Consorci del Besòs Tordera per l´ajuda en la fase experimental del treball i molt especialment al personal d´explotació de l'EDAR de Montornès, durant els mesos de COVID inclosos.

Agraït al Jesús Colprim per haver donat continuïtat al treball del HRAS en la tesi de PN-Anammox.

Agraïment a les persones que en vàrem depositar confiança al llarg de la meva vida professional: Federico de Lora, Miquel Adroher, Miquel Rigola, Joan Galtes, Fernando Morcillo, Marta Verde, Carles Sola, Jaume Blasco i a tots el col·legues amb els que he participat per fer que les aigües d´aquest món siguin més netes.

Agraït al meu pare que em va afavorir el gust per la curiositat i a la meva mare el gust pel treball, dues característiques imprescindibles per fer una Tesi.

I per últim, el meu agraïment a la Neri, amb la que hem dedicat llargues hores d´estudi, ella a la higiene mental i jo a la higiene ambiental, som una parella exemplar!

Table of Content

List of acronyms

A/B	Adsorption-Bio-oxidation
AHO	A-Stage Heterotrophic Organisms
AOB	Ammonia Oxidizing Bacteria
APHA	Standard methods
BNR	Biological nutrient removal
BOD_5	Biochemical Oxygen Demand
CAS	Conventional activated sludge
CF	Constant flow
CEPT	Chemical enhanced primary treatment
CH_4	Methane
COD	Chemical Oxygen Demand
cCOD	Colloidal Chemical Oxygen Demand
pCOD	Particulate Chemical Oxygen Demand
rbCOD	Readily biodegradable COD
sCOD	Soluble Chemical Oxygen Demand
COD_{OUT}	Effluent COD
COD_{IN}	Influent COD
COD_W	Waste COD
COD_{OXID}	Oxidized COD
DO	Dissolved Oxygen
EPS	Extracellular Polymeric Substances
EC	Energy consumed
EP	Energy produced
GAO	Glycogen Accumulating Organisms
HRAS	High-Rate Activated Sludge
HRAS AS	HRAS A-Stage
HRAS-CS	HRAS Contact-Stabilization
HRAS-SBR	HRAS Sequencing Batch Reactor
HRT	Hydraulic retention time
IWA	International Water Association
kLa	Mass transfer coefficient
KO_2	Half-saturation of O_2
KS	Half-saturation of readily biodegradable substrate
MLSS	Mixed Liquor Suspended Solids
µMax	Maximum specific growth rate
NOB	Nitrite oxidizing bacteria
$N\text{-}NH_4^+$	Ammonium Nitrogen
OAV	Opening air valve
OFR	Overflow Rate
OHO	Ordinary Heterotrophic Organisms
OLR	Organic loading rate

OLR-sCOD	Organic Loading Rate soluble COD
ORR	Organic Removal Rate
OrgN	Organic nitrogen
OrgP	Organic phosphorous
ORP	Oxidation -reduction potential
OUR	Oxygen Uptake Rate
PAO	Polyphosphate Accumulating Organisms
PC	Primary clarifier
PHA	Polyhydroxyalkanoates
PHB	Polyhydroxybutyrate
PN/A	Partial nitritation/Anammox
$P\text{-}PO_4^{3-}$	Orthophosphates
SBP	Sludge blanket position
SBR	Sequential Batch Reactor
SD	Standard deviation
SER	Solids exchange rate
SFt	Total solids flux
SFg	Gravity solids flux
SFu	Bulk movement solids flux
SL	Solids Loading
SOC	Specific Oxygen Consumption
SOC-COD	Specific COD oxygen consumption
SOC-sCOD	Specific sCOD oxygen consumption
$SOC\text{-}BOD_5$	Specific BOD5 oxygen consumption
SRT	Solids retention time
SVI	Sludge volume index
SS	Suspended solids
T	Temperature
TKN	Total Kjeldahl Nitrogen
TN	Total Nitrogen
TP	Total phosphorous
TSS	Total Suspended Solids
VF	Variable flow
VFA	Volatile Fatty Acids
VL	Volume of water
VSS	Volatil Suspended Solids
VT	Volume of water + volume of air bubble
WWTP	Wastewater treatment plants
Y_H	Biomass synthesis yield
ZSV	Zone settling velocity
Θ	Temperature coefficient yield

List of Tables

List of Figures

Chapter 1: Introduction

Chapter 3: Materials and Methods

Chapter 4: COD fractions removal

Chapter 5: Nutrients removal

Chapter 6: Specific Oxygen Consumption in HRAS process

Chapter 7: HRAS Sludge Settleability

Chapter 8: General Discussion

Summary

The conventional activated sludge (CAS) process has indeed demonstrated remarkable efficacy and adaptability in meeting evolving effluent quality standards for wastewater treatment over the past century. However, it remains a high-energy-consuming process with significant environmental implications. Consequently, there has been a notable surge in the development of more sustainable technologies geared towards minimizing energy consumption. Currently, only approximately 40% of influent organic matter is removed by primary clarifiers (PC) and directed to anaerobic digestion for energetic valorization, while the remaining 60% proceeds directly to CAS, entailing the corresponding oxygen consumption. Enhancing the effectiveness of PC is therefore imperative to reduce the overall electricity usage.

In this framework, High Rate Activated Sludge (HRAS) process emerge as a potential substitute for primary clarifiers to mitigate energy consumption. The HRAS process, by reducing solid retention time (SRT), effectively minimizes COD oxidation and enables maximum energy recovery.

This thesis is motivated by several key objectives: i) to investigate HRAS's COD fractions removal efficiency and stability under low SRT, HRT, and DO conditions when treating raw wastewater without PC; ii) to assess the removal of TKN and TP fractions and their correlation with COD fractions removal, along with the operational factors; iii) to establish specific oxygen consumption and assess the most effective method for controlling the oxygen supply; iv) to evaluate the settleability of HRAS sludge and determine the influence of clarifier biomass inventory on the HRAS process; and v) to quantify the energy reduction achieved with HRAS.

To conduct this research, an industrial HRAS pilot plant (35 $m^3 \cdot day^{-1}$) was designed and operated over a 497-day period, treating wastewater from a WWTP 95000 eq. habitants. This study employed a combination of simulation and experimental tools, with the pilot plant operating at SRT of 0.2 days, HRT of 0.6hours, and DO of 0.5 $mg \cdot L^{-1}$ with variable flow rates. The pilot plant comprised two 0.8 m^3 biological reactors and two clarifiers of 1.0 and 1.4 m diameter, which were alternately operated. Continual monitoring of the operational parameters such as DO, ORP, influent, recirculation, and waste flow rates was conducted. Suspended solids in the influent, reactor, effluent, and recirculation flow were continuously analyzed using four digital sensors.

The main findings from the experimental pilot plant indicate that maintaining a stable MLSS concentration in the reactor ensures the process stability, even under significant influent variations and extreme operational conditions. The Solids Exchange Rate (SER) underscores the influence of incoming solids on HRAS solids inventory, challenging the conventional importance of SRT in HRAS design and control. Moreover, the different COD fractions removal underscores the significance of settling efficiency and stability in HRAS's removal efficiencies. HRAS serves as a filter for influent peak loads of COD, particularly the particulate COD, while its oxidation is primarily affected by soluble COD removal. The simulation model adopted using SUMO resulted in a good fit for the sCOD, while for the pCOD there was a good fit except for temperatures above 23 ºC.

A consistently low specific oxygen consumption (SOC) for COD, sCOD and BOD_5 removal underscore the HRAS's heightened energy efficiency at elevated influent concentrations, with SOC influenced by

influent concentration and biodegradability. High oxidation of COD is generated during periods of high influent soluble COD, suggesting the potential for additional oxygen control strategies using soluble COD online monitoring. The simulation model using SUMO fitted the SOC values with the exception of very low $sCOD_{IN}$ concentration.

The HRAS achieves higher TKN, $N\text{-}NH_4^+$, TP, and $P\text{-}PO_4^{3-}$ removal compared to PC, with removal rates correlated with influent nutrient concentrations. TKN and TP removal show positive correlations with COD and pCOD, highlighting the significance of adsorption and entrapment processes. TKN and TP removal were independent of COD_{OXID}. The superplus of sCOD removal suggests intracellular storage or the high nitrogen content in biomass in a heavily loaded HRAS.

Long-term analysis indicates that the short-cut nitrification/denitrification process in HRAS effluent, supplemented by Anammox in the sidestream, is the optimal pathway for downstream nitrogen removal.

Additionally, HRAS exhibits heightened energy efficiency at elevated influent concentrations, with specific oxygen consumption influenced by influent concentration and biodegradability.

The low SVI30, and high ZSV, of HRAS underscores its exceptional biomass settling properties, while high SSOUT indicates low flocculation quality. While HRAS clarifiers could be designed with a higher OFR than conventional clarifiers, a lower OFR is advisable for enhanced COD harvesting and increased process stability. Overall, the implementation of HRAS instead of PC, alongside Anammox in the sidestream, leads to a 40% reduction in WWTP electricity consumption, a 34% decrease in water line reactors volume, and an 11% increase in anaerobic digestion volumes, promoting cost-effective construction and footprint reduction.

.

Summary in Catalan

El procés convencional de fangs actius (CAS) ha demostrat una notable eficàcia i adaptabilitat per complir amb els estàndards de qualitat dels efluents en el tractament d'aigües residuals durant l'últim segle. No obstant això, segueix sent un procés d'alt consum energètic amb importants implicacions ambientals. Conseqüentment, hi ha hagut un notable augment en el desenvolupament de tecnologies més sostenibles orientades a minimitzar el consum d'energia. Actualment, només aproximadament el 40% de la matèria orgànica influent a les EDARs és eliminada pels clarificadors primaris i dirigida cap a la digestió anaeròbia per a la seva valorització energètica, mentre que el 60% restant es enviat directament al CAS, la qual cosa comporta un consum d'oxigen corresponent. Millorar l'eficàcia dels clarificadors primaris és necessari per reduir el consum general d'electricitat.

En aquest context, el procés de *High Rate Activated Sludge* (HRAS) emergeix com a substitut dels clarificadors primaris per mitigar el consum d'energia. El procés HRAS redueix el temps de residència cel·lular i hidràulic (TRC i TRH), minimitza eficaçment l'oxidació de la DQO i permet la màxima recuperació d'energia.

Aquesta tesi està motivada per diversos objectius clau: i) investigar l'eficiència i estabilitat de l'HRAS en l'eliminació de les fraccions de DQO sota condicions de baix TRC, TRH i oxigen dissolt (OD) en tractar aigües residuals sense decantador primari; ii) avaluar l'eliminació de les fraccions de nitrogen (TKN) i fòsfor (TP) i la seva correlació amb l'eliminació de les fraccions de DQO, juntament amb els paràmetres d'operació; iii) establir el consum específic d'oxigen i avaluar el mètode més efectiu per controlar el subministrament d'oxigen; iv) avaluar la decantabilitat dels llots del HRAS i determinar la influència de l'inventari de biomassa del decantador en el procés HRAS; i v) quantificar la reducció d'energia assolida amb HRAS.

Per dur a terme aquesta investigació, es va dissenyar i operar una planta pilot industrial (35 $m^3 \cdot dia^{-1}$) de HRAS durant un període de 497 dies, tractant aigües residuals de l'EDAR d'una població de 95000 habitants equivalents. Aquest estudi va emprar una combinació d'eines de simulació i experimentals, amb la planta pilot operant amb TRC de 0.2 dies, TRH de 0.6 hores i OD de 0.5 $mg \cdot L^{-1}$ amb taxes de flux variables. La planta pilot constava de dos reactors biològics de 0.8 m^3 i dos clarificadors de 1.0 i 1.4 m de diàmetre, que es van operar alternativament. Es va dur a terme un seguiment continu dels paràmetres operatius com OD, ORP, el potencial redox, els cabals influent, de recirculació i de purga. Els sòlids en suspensió en l'influent, reactor, efluent i recirculació es van analitzar contínuament mitjançant quatre sensors digitals.

Els principals resultats experimentals de la planta pilot indiquen que mantenir una concentració estable de MLSS en el reactor garanteix l'estabilitat del procés, fins i tot sota variacions significatives en l'influent i en condicions extremes d'operació. La Taxa d'Intercanvi de Sòlids (SER) subratlla la influència dels sòlids entrants en l'inventari de sòlids de l'HRAS, qüestionant la importància que s'ha atribuït convencionalment al TRC en el disseny i control de l'HRAS. A més, la diferent eficiència d'eliminació de les fraccions de DQO destaca la importància de la decantació i de l'estabilitat del procés en el rendiment de l'HRAS. L'HRAS actua com a filtre per a les altes càrregues de DQO a l'influent, especialment la DQO particulada, mentre que la seva oxidació es veu principalment afectada per

l'eliminació de la DQO soluble. La simulació realitzada mitjançant el software SUMO va permetre un bon ajust del resultats per la DQO soluble, mentre que per la DQO particulada l'ajust va ser correcte per temperatures sota els 23ºC.

El baix consum específic d'oxigen (SOC) per la DQO total, soluble i DBO_5 posa de manifest l'eficiència energètica elevada de l'HRAS. El SOC està influït tant per la concentració de l'influent i com per la seva biodegradabilitat. S'ha observat una alta oxidació de la DQO durant els períodes on la DQO soluble a l'influent és elevada, suggerint que estratègies de control de l'oxigen utilitzant la concentració de DQO soluble a l'influent poden ser apropiades per controlar l'oxidació de DQO. La simulació realitzada amb el software SUMO va permetre un bon ajust pels valors de SOC excepte amb valors molt baixos de DQO soluble a l'influent.

L'HRAS aconsegueix una major eliminació de TKN, $N\text{-}NH_4^+$, TP i $P\text{-}PO_4^{3-}$ en comparació amb el decantador primari, amb taxes d'eliminació correlacionades amb les concentracions de nutrients influents. L'eliminació de TKN i TP mostra correlacions positives amb el DQO total i la fracció particulada, destacant la importància dels processos d'adsorció, sent independent de l'oxidació de DQO. El superàvit d'eliminació de DQO soluble suggereix un possible emmagatzematge intracel·lular o un alt contingut de nitrogen en la biomassa de l'HRAS. L'anàlisi a llarg termini indica que la presència d'un procés de *short-cut* nitrificació/desnitrificació, complementat per ANAMMOX a la línia de retorn, és la via òptima per a l'eliminació de nitrogen en l'etapa següent de tractament. A més, l'HRAS exhibeix una major eficiència energètica a concentracions de l'influent elevades, amb un consum d'oxigen específic influenciat per la concentració influent i per la seva biodegradabilitat.

El baix índex de volum de fangs (SVI_{30}) i l'alta velocitat de sedimentació (ZSV) subratllen les propietats excepcionals de sedimentació de la biomassa de l'HRAS, mentre que els sòlids en suspensió alts en l'efluent indiquen una baixa qualitat de floculació. Tot i que els clarificadors de HRAS podrien dissenyar-se amb una velocitat del sobrenedant (*overflow rate,* OFR) més alta que els clarificadors convencionals, és recomanable un OFR més baix per aconseguir una major recuperació de DQO i una major estabilitat del procés. En general, la implementació de HRAS en lloc del decantador primari, juntament amb ANAMMOX en la línia de retorns, condueix a una reducció del 40% en el consum d'electricitat de l'EDAR, una disminució del 34% en el volum dels reactors de la línia d'aigua i un augment de l'11% en els volums de digestors anaerobis, aconseguint una reducció dels costos de construcció a més de la reducció de la petjada ambiental.

Summary in Spanish

El proceso convencional de fangos activados (CAS) ha demostrado una eficacia y adaptabilidad notable para cumplir con los estándares de calidad requeridos para los efluentes en el tratamiento de aguas residuales durante el último siglo. Sin embargo, sigue siendo un proceso de alto consumo energético con importantes implicaciones ambientales. Como resultado, ha habido un notable aumento en el desarrollo de tecnologías más sostenibles orientadas a minimizar el consumo de energía. Actualmente, solo aproximadamente el 40% de la materia orgánica influente es eliminada por los clarificadores primarios y dirigida hacia la digestión anaerobia para su valorización energética, mientras que el 60% restante es enviado directamente al CAS, lo que conlleva un consumo de oxígeno correspondiente. Mejorar la efectividad de los clarificadores primarios es necesario para reducir el consumo general de electricidad.

En este contexto, el proceso de *High Rate Activated Sludge* (HRAS) emerge como sustituto de los clarificadores primarios para mitigar el consumo de energía. El proceso HRAS, al reducir el tiempo de residencia celular (TRC), minimiza eficazmente la oxidación de la DQO y permite una recuperación máxima de energía.

Esta tesis está motivada por varios objetivos clave: i) investigar la eficiencia y estabilidad de eliminación de las fracciones de DQO y estabilidad del HRAS bajo condiciones de bajo TRC, TRH y oxígeno disuelto (OD) al tratar aguas residuales crudas sin PC; ii) evaluar la eliminación de las fracciones de nitrógeno (TKN) y fósforo (TP) y su correlación con la eliminación de las fracciones de DQO, junto con los parámetros de operación; iii) establecer el consumo específico de oxígeno y evaluar el método más efectivo para controlar el suministro de oxígeno; iv) evaluar la sedimentabilidad de los lodos del HRAS y determinar la influencia del inventario de biomasa del decantador en el proceso HRAS; y v) cuantificar la reducción de energía lograda con HRAS.

Para llevar a cabo esta investigación, se diseñó y operó una planta piloto industrial (35 $m^3 \cdot día^{-1}$) de HRAS durante un período de 497 días, tratando aguas residuales de una EDAR con 95000 habitantes equivalentes. Este estudio empleó una combinación de herramientas de simulación y experimentales, con la planta piloto operando a TRC de 0.2 días, TRH de 0.6 horas y OD de 0.5 $mg \cdot L^{-1}$ con tasas de flujo variables. La planta piloto constaba de dos reactores biológicos de 0.8 m^3 y dos clarificadores de 1.0 y 1.4 m de diámetro, que se operaban alternativamente. Se llevó a cabo un monitoreo continuo de los parámetros operativos como OD, ORP, potencial redox y caudales influente, de recirculación y de purga. Los sólidos en suspensión en el influente, reactor, efluente y recirculación se analizaron continuamente mediante cuatro sensores digitales.

Los principales hallazgos de la planta piloto experimental indican que mantener una concentración estable de MLSS en el reactor garantiza la estabilidad del proceso, incluso bajo variaciones significativas del influente y condiciones operativas extremas. La Tasa de Intercambio de Sólidos (SER) subraya la influencia de los sólidos entrantes en el inventario de sólidos de HRAS, relativizando la importancia que se ha atribuido al TRC en el diseño y control de HRAS. Además, la diferente eliminación de las fracciones de DQO pone de manifiesto la importancia de la eficiencia de la decantación y estabilidad del proceso en el rendimiento del HRAS. El HRAS actúa como filtro para las

cargas elevadas de DQO influente, especialmente la DQO particulada, mientras que su oxidación se ve principalmente afectada por la eliminación de la DQO soluble. El modelo de simulación realizado mediante el software SUMO obtuvo buenos resultados para la DQO soluble, mientras que para la DQO particulada el ajuste fue correcto para temperaturas por debajo de los 23 ºC.

El bajo consumo específico de oxígeno (SOC) para la DQO total, soluble y DBO_5 pone de manifiesto la elevada eficiencia energética del HRAS. El SOC está influenciado tanto por la concentración del influente como por su biodegradabilidad. Se ha observado una alta oxidación de la DQO durante los períodos en los que la DQO soluble en el influente es elevada, sugiriendo que estrategias de control de oxígeno utilizando la concentración de DQO soluble en el influente pueden ser apropiadas para controlar la oxidación de DQO. La simulación realizada con el software SUMO permitió un buen ajuste para valores de SOC excepto para valores muy bajos de DQO soluble en el influente.

El HRAS logra una mayor eliminación de TKN, $N\text{-}NH_4^+$, TP y $P\text{-}PO_4^{3-}$ en comparación con el decantador primario, con tasas de eliminación correlacionadas con las concentraciones de nutrientes influentes. La eliminación de TKN y TP muestra correlaciones positivas con el DQO total y la fracción particulada, destacando la importancia de los procesos de adsorción, siendo independiente de la oxidación de DQO. El exceso de eliminación de DQO soluble sugiere un posible almacenamiento intracelular o un alto contenido de nitrógeno en la biomasa del HRAS. El análisis a largo plazo indica que un proceso *short-cut* nirificación/desnitrificación, complementado por Anammox, en la línea de retornos, es la vía óptima para la eliminación de nitrógeno en la siguiente etapa del tratamiento. Además, el HRAS exhibe una mayor eficiencia energética a concentraciones influentes elevadas, con un consumo específico de oxígeno influenciado por la concentración influente y su biodegradabilidad.

El bajo índice de volumen de lodos (SVI_{30}) y la elevada velocidad de decantación (ZSV) subrayan las propiedades excepcionales de sedimentación de la biomasa del HRAS, mientras que los altos sólidos en suspensión en el efluente indican una baja calidad de floculación. Aunque los clarificadores de HRAS podrían diseñarse con un *overflow rate* (OFR) mayor que los clarificadores convencionales, es recomendable un OFR más bajo para conseguir una mayor recuperación de DQO y una mayor estabilidad del proceso. En general, la implementación de HRAS en lugar del decantador primario, junto con Anammox en la línea de retornos, conduce a una reducción del 40% en el consumo de electricidad de la EDAR, una disminución del 34% en el volumen de los reactores de línea de agua y un aumento del 11% en los volúmenes de digestión anaerobia, consiguiendo una reducción en los costes de construcción además de la reducción de la huella ambiental.

Chapter 1
INTRODUCTION

This chapter introduces the High-Rate Activated Sludge (HRAS) process, offering an overview of the current understanding through a comprehensive literature review. It delves into the key insights garnered from previous studies on HRAS, aiming to establish a thorough comprehension of the process. The literature review forms the basis for the research objectives, methodologies, and contributions to the field, setting the stage for the subsequent chapters.

1.1 HRAS as Sustainable Alternative to CAS Process

The conventional activated sludge (CAS) process has proven its efficacy and adaptability in meeting new effluent quality standards for wastewater for more than a century. However, it is a high-energy consuming process with a significant environmental impact. As a result, there has been a significant increase in the development of more sustainable technologies aimed at reducing energy consumption and environmental impacts. Only approximately 35-40% of the influent organic matter, measured as COD, is removed by primary clarifier PC (Crites and Tchobanoglous, 1998) and sent to anaerobic digestion for energetic valorisation as biogas; the remaining 60%-65% goes directly to CAS, with its corresponding oxygen consumption (Seeley, 1992). Improving the effectiveness of the PC is therefore crucial to reduce the overall electricity consumption (Huang and Li, 2000; Li, 1998; Ross and Crawford, 1985; Yetis and Tarlan, 2002).

Municipal wastewater with 500 $mg \cdot L^{-1}$ of COD contains around 1.9 $kWh \cdot m^{-3}$ of energy stored in the chemical bonds (Mccarty et al., 2011), while the energy required in conventional wastewater treatment plants (WWTPs) is in the range of 0.3-0.7 $kWh \cdot m^{-3}$ (Jose Jimenez et al., 2015). Therefore, there is a great potential for improving the energy recovery in WWTPs and several studies (Sancho et al., 2019) proposed to enhance the PC efficiency in order to derivate more COD to anaerobic digestion and reduce the organic load to the following conventional activated sludge.

Various technologies have been suggested for enhancing PC efficiency and carbon redirection, including i) physical processes (dynamic sand filtration, dissolved air flotation, membrane filtration), ii) chemical processes (chemical-enhanced primary treatment, CEPT), and iii) biological processes (adsorption bio-oxidation process, contact stabilization). Among technologies, a combination of physical and biological separation processes appears the most promising solution, as seen in High-Rate Activated Sludge (HRAS), that can be used as an alternative to the PC (Figure 1.1).

In 1997, Böhnke firstly proposed the implementation of the HRAS process as the initial stage of the Adsorption-Bio-oxidation (A/B) process in various wastewater treatment plants (WWTPs), including those in Strass, Salzburg, Krefeld, Nieuwveer, Utrecht, Dokhaven, and Groningen. These early HRAS applications demonstrated a substantial COD removal efficiency ranging from 53% to 74% (De Graaff et al., 2016). However, the technology faced challenges and debates, particularly concerning compliance with nitrogen removal requirements, given the difficulty in meeting the COD/TKN (Total Kjeldahl Nitrogen) effluent ratio of the HRAS (Figure 1.1).

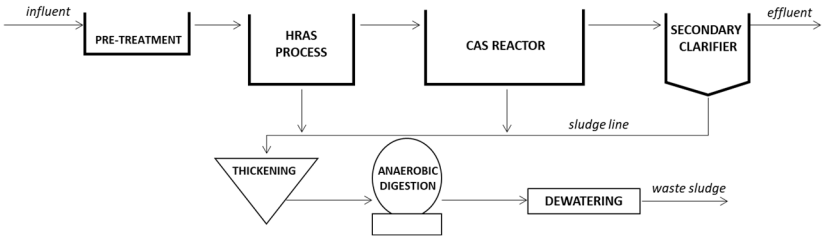

Figure 1.1 HRAS implementation in a wastewater treatment plant.

The introduction of the Anammox process in the return line provided a solution by reducing the influent nitrogen load, reigniting interest in the HRAS process. Over the last fifteen years, HRAS has been extensively researched as a potential replacement for primary clarifiers to reduce the energy consumption of WWTPs. Furthermore, recent years have seen a renewed focus on HRAS as a pretreatment for the PN/A process, known for its high energy efficiency towards neutrality and minimal emissions of nitrous oxide, a potent greenhouse gas (Ahn et al., 2010, Carbó et al. 2024).

1.2 HRAS Design and Operational Parameters

HRAS design parameters are typically characterized by a short solids retention time (SRT) of 0.1-1.0 days, a short hydraulic retention time (HRT) of 30-60 minutes, and a low dissolved oxygen (DO) concentration of 0.5-1.0 $mg \cdot L^{-1}$. These values are notably lower than those observed in conventional activated sludge (CAS) processes, which typically have SRTs of 6-18 days, HRTs of 6-18 hours, and DO concentrations of 1.0-2.0 $mg \cdot L^{-1}$. The intention behind these design parameters is to enhance carbon adsorption and storage in HRAS, prioritizing it over mineralization.

However, HRAS design parameters can vary based on the characteristics of the influent wastewater, e.g. when treating the PC o CEPT effluents. HRAS must operate at longer SRT and HRTs due to lower influent particulate and colloidal fractions. This is crucial for optimizing HRAS performance across different wastewater compositions (Carrera et al., 2022; Rey-Martínez et al., 2021; Zhang et al., 2021).

Furthermore, the use of short HRTs in HRAS entails lower influent flow dilution compared to CAS processes with HRTs of 6-18 hours. This results in a lower buffering capacity for influent variations (Miller et al, 2017). It is important to note that this characteristic does not contradict the fact that the HRAS process effectively reduces influent variations in subsequent nutrient removal processes.

Various HRAS configurations (Figure 1.2) have been developed, including HRAS A-stage and HRAS Contact-Stabilization (HRAS-CS). These configurations offer flexibility in design and operation, allowing for adaptation to different influent wastewater characteristics. The HRAS A-stage features a single contact reactor with HRT less than 60 minutes, while HRAS-CS involves two reactors, including a contact reactor (15 minutes HRT) and a stabilization (45 minutes HRT) (Meerburg et al., 2015; Rahman et al., 2017; Van Winckel et al., 2019). The contact-stabilization configuration induces feast-famine behavior in the contact and stabilization phases, respectively, promoting maximum organic matter adsorption in the contact reactor.

In their study, Rahman *et al.* (2017) proposed the use of the HRAS-CS process for influents with low organic matter concentrations, such as those from a chemically enhanced primary treatment (CEPT) process and recommended the use of HRAS A-stage for effluents with high organic concentrations, such as raw wastewater. Similarly, in laboratory pilot plants operating at SRT of 0.3 days and 20°C Rahman et al. (2016) observed that HRAS A-Stage exhibited higher pCOD and COD removal efficiency (74% and 67% respectively) compared to HRAS-CS, which showed pCOD 55% and COD 54% removal efficiency but similar results for sCOD (56-50%) and cCOD (35-25%). Additionally, Tirkey et al. (2022) investigated an anoxic HRAS for nitrogen removal (denitrification) and carbon recovery, while Wett et al. (2020) studied a HRAS Sequencing batch reactor (HRAS-SBR) with high thickening capabilities.

In terms of clarifier design, the sludge loading rate (SL) has been traditionally emphasized as a key parameter, but recent insights suggest that overflow rate (OFR) plays a predominant role in clarifier performance, particularly in relation to sludge floc formation behaviour (Mancell-Egala et al., 2017). The pilot plant operates with an SL of 113 ± 43 $Kg \cdot m^{-2} \cdot d^{-1}$ and OFR 0.8-1.7 $m \cdot h^{-1}$, which is consistent with values from previous research (SL 110 ± 29 $Kg \cdot m^{-2} \cdot$d-1 and OFR 1 ± 0.08 $m \cdot h^{-1}$, Van Winckel et al., 2019).

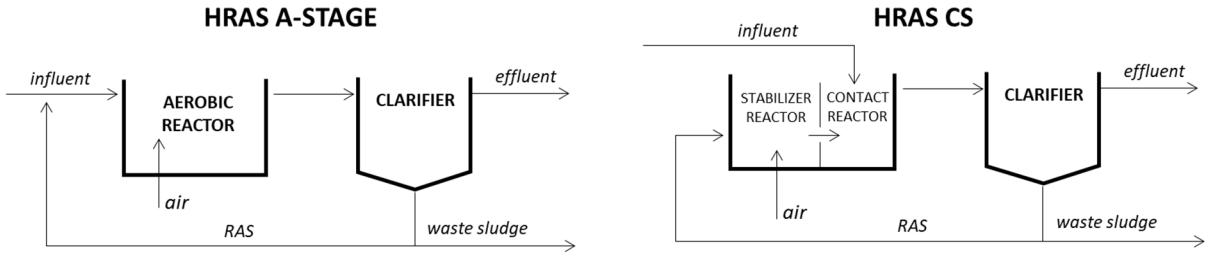

Figure 1.2 HRAS reactors typologies: HRAS A-Stage and HRAS-CS

1.3 Effect of Operating Parameters on HRAS Process Performance

Operational parameters play a crucial role in influencing both the biochemical and physical processes of the HRAS. Specifically, the SRT significantly impacts biofloculation, sludge settleability, and carbon oxidation. It is imperative to set the SRT to optimize Mixed Liquor Suspended Solids (MLSS) concentration, biomass yield, and overall system efficiency (Sancho et al., 2019).

Similarly, the Hydraulic Retention Time (HRT) plays a vital role in biofloculation and adsorption. It must be long enough to facilitate biomass development and the biosorption process, yet short enough to limit Chemical Oxygen Demand (COD) mineralization. Dissolved Oxygen (DO) levels should be kept as low as possible to minimize carbon mineralization and prevent anoxic conditions at the clarifier's bottom. MLSS concentration affects carbon adsorption and sludge settleability but has not been adequately studied to date.

To explore the effect of temperature on COD elimination, it is necessary to distinguish between soluble COD (sCOD) and particulate COD (pCOD). An increase in temperature generally leads to an increase in sCOD removal but a decrease in pCOD removal (Jose Jimenez et al., 2015).

Despite the complexity of presenting the impact of each specific parameter on HRAS process efficiency due to varying operational parameters and influent characteristics, we present results from an HRAS pilot plant working with raw municipal wastewater under different conditions. An optimal SRT exists where carbon capture is maximized, as demonstrated by Jimenez et al. (2015), who found that COD capture is maximized between 0.25-0.4 days of SRT. Below 0.2 days of SRT, less COD is oxidized, but only a small fraction is removed from the wastewater.

Miller et al. (2015) concluded that SRT is the primary control parameter. Below 0.5-1 day of SRT, the dominant COD removal mechanisms are assimilation and oxidation of readily degradable substrate and sedimentation of particulate matter. Between 0.5-1 days of SRT, COD removal becomes a function of hydrolysis, as adsorption of particulate and colloidal matter is maximized, although not complete due to limited adsorption sites. In a laboratory HRAS pilot plant study working at 0.25 days of SRT and 30 minutes of HRT, the following yields were achieved: 57% COD, 56% sCOD, 58% pCOD, and 76% suspended solids (SS) removal (Miller et al., 2013).

The absorption process and storage yield better results at low SRT and HRT. (Rosso et al., 2019) concluded that at 0.3 days of SRT and 30 days of HRT, there was greater cellular storage than at 0.5 days of SRT and 60 minutes of HRT. An increase in SRT leads to an increase in the elimination of sCOD, indicating that oxidation against cell storage prevails.

Regarding the main parameters related to clarifier efficiency, it is noteworthy that solids loading (SL) does not affect pCOD removal due to high sludge settling properties (low SVI_{30} of 49-67 $mL \cdot g^{-1}$ compared to 110-180 $mL \cdot g^{-1}$ in CAS processes, (Seeley, 1992)). However, variations in SL do affect effluent suspended solid (SS) concentrations, with the impact linked to the overflow rate (OFR). OFR, on the other hand, does not affect pCOD removal due to high sludge settling properties. Nonetheless, variations in OFR do affect effluent suspended solid SS_{OUT} concentrations, emphasizing the influence of sludge floc formation. Therefore, effluent suspended solids concentrations are primarily dictated by the efficacy of floc formation(Mancell-Egala et al., 2017).

One of the primary challenges in the HRAS process is controlling the effectiveness of COD elimination to achieve a COD/TKN ratio within acceptable limits for subsequent denitrification. In a pilot plant study, Miller et al. (2017) implemented a control strategy based on DO, SRT and MLSS values. While the strategy demonstrated effectiveness in mitigating variations in COD performance, it did not consistently maintain the COD/TKN ratio at the desired values.

The Total Suspended Solids (TSS) in HRAS effluent, with its high concentration, significantly influences the SRT. Attempts to control SRT using a controller that considered not only the MLSS in

the reactor but also the SS in the effluent proved challenging. This design failed as the controller exhibited high sensitivity to sensor accuracy (Zhigou Yuan et al., 2019).

1.4 COD removal and Energy Recovery in HRAS process

The HRAS process enhances the removal of particulate and colloidal COD (pCOD, cCOD), and even some of the soluble COD (sCOD), with a minimum energy consumption (Christian et al., 2008; Constantine et al., 2012; Jimenez et al., 2015; Nogaj et al., 2015; Rahman et al., 2019; Wett et al., 2007; Yeshi et al., 2014). HRAS removes the wastewater organic load using two different mechanisms (see Figure 1.3).

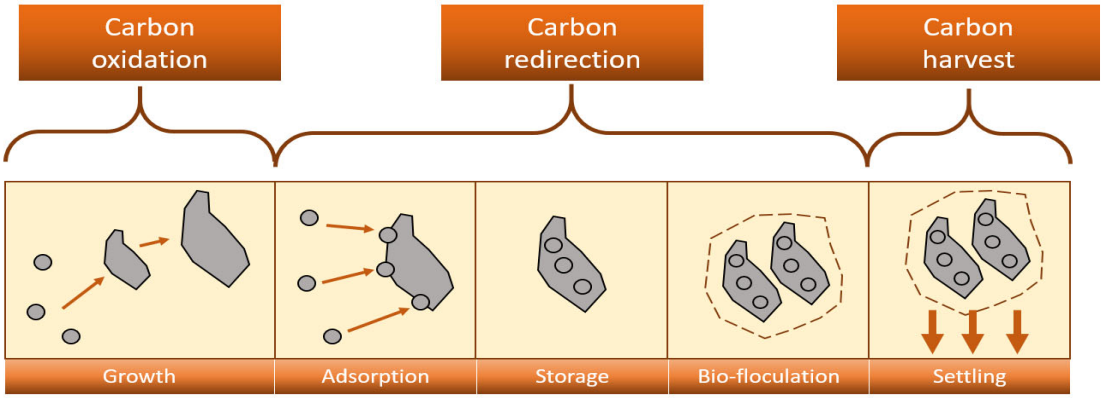

Figure 1.3 Carbon removal diagram

1) Carbon redirection, where particulate and colloidal fractions are removed by bioadsorption (bioflocculation) and redirected into the sludge matrix, while soluble biodegradable COD is removed by intercellular storage (bioaccumulation), microbial growth and carbon oxidation. The bioadsorption capacity is usually affected by the size of the organic compounds, the shear rate, the presence of available sorption sites on the sludge, the characteristics of the mixed liquor and the organic loading rate (OLR) (Modin et al., 2016).

2) Carbon harvesting, where redirected organic carbon is recovered through settling without having been metabolized by bacteria and sent to anaerobic digestion (Modin et al., 2016; Rahman et al., 2016; Rosso et al., 2019). One factor that limits carbon harvesting is the settling capability of the biological sludge. Meerburg (2016) compared the SVI of biological sludge at 1 hour and 8.45 hours HRT (achieving SVI values of 76 and 120 $ml \cdot g^{-1}$, respectively) and concluded that the lower the HRT was, the higher the settleability of biological sludge. Similar conclusions were drawn by Miller et al. (215) and Rahman et al. (2019). However, Jiménez et al. (2015) and Rosso et al. (2019) found that the low oxidation of organic matter due to the low SRT maximizes the organic matter redirection but decreases the settling of biomass and consequently worsens the harvesting.

1.4.1 Organic Matter Adsorption

Biological adsorption refers to the physicochemical adhesion of organic matter by biological flocs without immediate aerobic or anaerobic biodegradation. According to the International Water Association (IWA) Model for Activated Sludge processes, slowly biodegradable organic matters, including particles and colloids, are assumed to be instantaneously sorbed to activated sludge flocs (Henze et al., 2000). However, studies have demonstrated that not all particulate organics undergo sorption (Alexander et al., 1980). The process can be more accurately described using both instantaneous sorption and first-order kinetics (Jorand et al., 1995a; Modin et al., 2016)(Jorand et al., 1995; Modin et al., 2015). The low SRT and HRT in HRAS allow for adsorption before oxidation occurs (Rahman et al., 2014).

The adsorption capacity typically ranges from 40 to 100 $mg_{COD} \cdot g_{VSS}^{-1}$. Several factors may influence sorption, including the size of organic compounds (0.03-1.5 microns), the characteristics of the biological sludge, and the OLR. Only aerobic sludges exhibit a net absorption of organic matter, as reported by Modin et al (2016), who compared the adsorption capacity of Primary, Aerobic, and Anaerobic biological sludges. The adsorption of cCOD and pCOD is controlled by the production of Extracellular Polymeric Substances (EPS) generated in aerobic growth processes (Jimenez et al., 2015). However, at high organic loading rates, such as in HRAS, the EPS concentration is very low.

1.4.2 Intracellular Storage

Many microorganisms can store soluble, biodegradable organic compounds as insoluble polymers, forming intracellular inclusions. Activated sludge with a high capacity for storing Polyhydroxyalkanoates (PHA) can be obtained through enrichment under feast-famine conditions or Sequential Batch Reactor (SBR) processes (Majone et al., 1999). Low oxygen supply has been shown to direct a larger fraction of the organic substrate to storage products (Third et al., 2003).

Laboratory studies conducted by (Carucci et al., 2001) revealed the phenomenon of cell storage when urban wastewater contacts biological sludges. The formation of Polyhydroxybutyrate (PHB) is prominently observed in high-load HRAS processes, contributing to the elimination of quickly biodegradable COD (rbCOD) in the range of 18-22%. This suggests an additional mechanism for COD removal that must be considered and enhanced in HRAS processes.

In high-load processes like HRAS Contact-Stabilization (HRAS-CS), (Rahman et al., 2019) indicated that for raw wastewater, the elimination of sCOD can occur through different mechanisms depending on the process. This includes absorption/storage in the HRAS-CS process, attributed to the low-time 'feast-famine' regime in the contact reactor (10 minutes), and oxidation in the HRAS A-Stage process, which involves 30 minutes of aeration contact time.

Storage yields better results at low SRT and HRT. D. Rosso et al. (2019) concluded that at 0.3 days of SRT and 30 minutes of HRT, there was greater cellular storage compared to 0.5 days of SRT and 60 minutes of HRT. An increase in SRT leads to an increase in the elimination of sCOD, indicating that

oxidation against cell storage prevails. Finally, (Lim et al., 2016) noted that inactive biomass determines surface adsorption, while active biomass quantifies adsorption and storage. The percentage of active biomass in HRAS, unlike in CAS, is not constant due to the high influence of incoming suspended material in raw wastewater and internal returns of the WWTP.

1.5 Organic Loading Rate and Organic Removal Rate

The Organic Loading Rate (OLR), defined as the ratio of the organic loading applied to a biological process per day relative to the biomass, is a common parameter in CAS process design, typically ranging from 0.2 to 0.6 $Kg_{BOD5} \cdot Kg_{MLSS}^{-1} \cdot d^{-1}$ (Crites and Tchobanoglous, 1998). In the case of HRAS processes, the OLR is reported to be in the range of 2-3.5 $Kg_{BOD5} \cdot Kg_{MLSS}^{-1} \cdot d^{-1}$ or 6.4-8.3 $Kg_{BOD5} \cdot Kg_{MLSS}^{-1} \cdot d^{-1}$ (de Graaff et al., 2016).

However, the Organic Removal Rate (ORR), which represents the ratio between the organic loading removed by a biological process per day relative to the biomass, has not been commonly addressed in HRAS studies. The present research aims to analyze the correlation between OLR and Organic Removal Rate (ORR) for COD, BOD_5, and sCOD.

1.6 Oxygen Demand and Control in HRAS Process

The primary objective of the HRAS process is to maximize the recovery of organic matter for anaerobic digestion while minimizing oxygen consumption, ultimately generating renewable biogas. While prior research on HRAS has predominantly centered on determining the relationships between operational conditions such HRT, SRT, DO, and the removal efficiency of various COD fractions. Jetten (1997), Demoulin, (1998), Jimenez et al., (2015), Meerburg (2016), Rahman et al. (2019), Rosso et al. (2019) among others provided experimental data on SOC. The present research conducted during the 497-day operation of this pilot-scale HRAS demonstration plant aims to scrutinize the relationship between SOC and key factors, including influent COD concentration, DO concentration, and temperature, as well as to establish a link between oxygen consumption and the removal of COD, BOD_5, and sCOD.

An integral aspect of this research entails tracking the COD mass balance within the HRAS process. This balance is defined as the influent COD (COD_{IN}) equating to the effluent COD from the clarifier (COD_{OUT}), augmented by the COD harvested in the waste sludge (COD_W), and further augmented by the COD oxidized (COD_{OXID}). The fraction of COD_{OXID} is dependent on the SRT and HRT of the process.

Previous research has explored the relationship between COD_{OXID} and SRT. Haider et al. (2003) estimated that the COD_{OXID} accounted for a 12% at an STR of 0.1 days, while Miller et al. (2017) estimated suggested a value of 14% at an SRT of 1 day after primary sedimentation.

In contrast, Rahman et al. (2019) presented a lineal correlation between COD_{OXID} and COD_W, indicating that an increase in COD_{OXID} led to a decrease in COD_W. However, this study treated COD_{OXID} as an

independent variable determined solely by the operating conditions of the HRAS process, without considering potential influencing factors.

Interestingly, Jimenez et al. (2015) proposed the existence of an optimal SRT range for COD_W maximization, specifically between 0.25 and 0.4 days. Below this range, COD_{OXID} and COD_W showed a positive correlation, but beyond it, the correlation became negative. The current research aims to verify the COD_W levels at low COD_{OXID} (5-7%) and within the low SRT range (0.25-0.4 days) while identifying key factors that impact COD_W and COD_{OXID}.

Generally, the oxygen consumption in the CAS process ($g_{O2} \cdot d^{-1}$), without nitrification, is obtained from the $BOD_{5\ rem}$ and the endogenous respiration of the biomass, according to the following expression (Goodman and Englande, 1974):

$$\frac{gO_2}{d} = a \cdot \frac{gDBO_{5\ removed}}{d} + b \cdot MLSS \qquad \text{Equation 1.1}$$

Here, a-synthesis and b-endogenous respiration parameters are related to SRT, typically in the range of 4-40 days. However, applying Equation 1 directly to the HRAS process poses challenges due to its low SRT (0.2-0.8 days) and reduced endogenous respiration activity. Furthermore, it's worth noting that only 20-25% of the mixed liquor suspended solids (MLSS) in HRAS can be considered as active biomass, with the remaining 80% comprising influent suspended solids (SS) (Hauduc et al., 2019).

1.7 Microbial Ecology of HRAS

Early research on the microbial ecology of HRAS, such as the work by Böhnke et al (1997), observed that HRAS systems only supported the growth of the fastest-growing bacteria, while CAS systems harbored a diverse community of bacteria, protozoa, and metazoa.

Under the specified working conditions, the development of AHO (Accumulibacter, Competibacter, and other known phosphorus- and glycogen-accumulating organisms) rapid-growing microorganisms is preferred in HRAS (Hauduc et al., 2019). This preference helps avoid cell lysis, endogenous respiration, and consequently minimizes oxygen consumption. Due to the low SRT, HRAS retains only the fastest-growing organisms capable of utilizing rapidly degradable substrates such as Volatile Fatty Acids (VFA) and monomers.

The microbial ecology of HRAS and Low-Rate processes was investigated by Meerburg (2016), revealing that high-rate and low-rate communities differ distinctly in terms of richness, evenness, and composition. Both communities exhibit a similar degree of weekly dynamics, but high-rate system dynamics are more variable. High-rate communities are less influenced by deterministic factors, such as environmental and operational variables.

The high organic load and low SRT in the HRAS process justify the predominance of biological sludge consisting mainly of prokaryotic microorganisms, with minimal presence of eukaryotes and protozoa.

Prokaryotic microorganisms are characterized by a smaller diameter (around 1 micron), shorter cell division time, and a greater specific surface area. This larger surface area provides them with a higher rate of adsorption and absorption of organic matter, as reported by Böhnke et al (1992).

1.8 Settling Biomass Characteristics and SS Effluent Quality

The settling behavior of a suspension is determined by its concentration and flocculation tendency. In a primary clarifier (PC) fed with incoming wastewater containing a relatively low concentration of suspended solids (150-500 $mg \cdot L^{-1}$), the dominant settling regime is discrete flocculated or non-flocculated settling. In a secondary settling tank, such as the CAS process, with a high concentration of incoming suspended solids (2000-4000 $mg \cdot L^{-1}$), various settling regimes occur simultaneously at different locations throughout the tank: discrete flocculent settling in the upper part, hindered settling (particles settling collectively as a zone) in the incoming sludge, and compressive settling in the sludge blanket in the lower part (Figure 1.4). HRAS clarifiers have a concentration of incoming suspended solids (2000-3000 $mg \cdot L^{-1}$) similar to the CAS process and exhibit the same simultaneous settling regimes: discrete flocculent, hindered settling, and compressive settling.

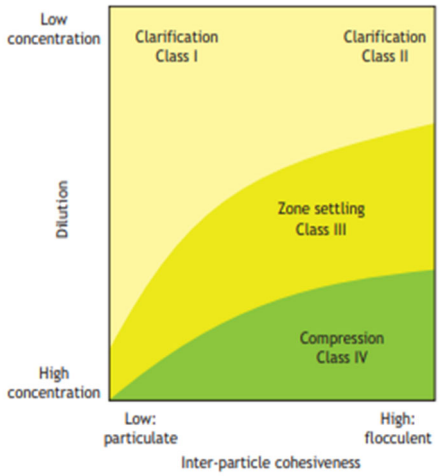

Figure 1.4 Settling regimes (Ekama et al 1997)

The four classes of settling involve different particle behaviors and, consequently, different controlling factors. Discrete settling (Class I) is influenced by the Overflow Rate (OFR). Flocculent settling (Class II) is affected by both OFR and depth. Zone settling (Class III) is influenced by Solids Loading (SL). Compression settling (Class IV) is influenced by Solids Retention Time and sludge depth (Clarifier Design WF-2010).

The HRAS process, like the CAS process, achieves the separation of biomass through settling. However, only 25-35% of the Mixed Liquor Suspended Solids (MLSS) in the HRAS reactor is biomass; the remainder is Primary Sludge flocculated with biomass, imparting different characteristics to this sludge compared to those presented by CAS and PC. Consequently, HRAS faces challenges related to the settling behavior of biological sludge and, consequently, carbon harvesting efficiency.

To quantify the settling behaviour of HRAS, five parameters have been used: i) sludge volume index (SVI), ii) Zone settling velocity (ZSV), iii) thickened concentration, iv) effluent suspended solids (SS), and v) threshold of flocculation (TOF).

i) Sludge Volume Index (SVI): HRAS has been reported to have low SVI in the range of 40-90 $mL \cdot g^{-1}$ (Böhnke et al., 1997), indicating good sludge settling characteristics. Studies comparing HRTs in HRAS have shown SVI values of 76 and 120 $mL \cdot g^{-1}$ for HRTs of 60 minutes and 8.45 hours, respectively (Meerburg et al., 2015). Additionally, Rahman et al. (2019) reported SVI values less than 100 $mL \cdot g^{-1}$ for a HRAS process with a SRT of 0.16-0.3 days, with no bulking problems observed even at a DO concentration of 0.5 $mg \cdot L^{-1}$. In a comparison between HRAS A-stage and HRAS-CS configurations for raw wastewater, both configurations exhibited good settleability with SVI values below 100 $mL \cdot g^{-1}$ (Rahman et al., 2019). However, HRAS A-stage showed better SVI results than HRAS-CS, achieved through low SRT of 0.16-0.3 days and high OLR, promoting good bioflocculation with a TOF less than 500 $mg_{TSS} \cdot L^{-1}$.

Some studies, such as those by Li and Yang (2007), Jimenez et al. (2015), and D. Rosso (2019), have indicated that conditions favoring maximum redirection of organic matter (minimum SRT, minimum oxidation) can make carbon harvesting difficult due to poor settling of biomass. While SVI is a good qualitative indicator of settling behavior, it does not provide quantitative information about effluent quality (Mancell-Egala et al., 2017).

ii) Zone Settling Velocity (ZSV): Torfs et al. (2016) reported ZSV values for a CAS process with MLSS concentrations of 2000-2500 $mg \cdot L^{-1}$ of 3.3-2.1 $m \cdot h^{-1}$, while Montornès HRAS pilot plant exhibited ZSV values of 5.1-4.1 $m \cdot h^{-1}$, indicating better settleability of HRAS sludges compared to CAS sludges.

iii) Thickened Concentration: Böhnke et al. (1997) stated that HRAS waste sludge can easily thicken by gravitational settling to 6-8% SS, higher than PC waste sludge (5-10% SS) but lower than CAS waste sludge (0.4-0.8% SS).

iv) Effluent Suspended Solids (SS): HRAS effluent has higher SS concentrations (60-150 $mg \cdot L^{-1}$) compared to CAS processes (15-30 $mg \cdot L^{-1}$), attributed to the low content of EPS (Mancell-Egala et al., 2017). This higher effluent SS concentration is explained by dispersed growth, where soluble substrate consumption for microbial growth results in the production of particulate and colloidal biomass. The low sludge ages in HRAS prevent the newly produced biomass from completely aggregating into settleable flocs, leading to lower Total Suspended Solids (TSS) removal efficiencies.

v) Threshold of Flocculation (TOF): TOF quantifies the minimum MLSS needed to form large flocs with significant settling. HRAS processes have been shown to have a higher effluent TSS concentration than CAS processes, likely due to poor biomass coagulation and flocculation (Liao et al., 2006). This limitation is attributed to impaired flocculation rather than coagulation. Bioaugmentation with sludge

from a biological nutrient removal reactor operating at long SRT has been suggested to overcome this limitation (Van Winckel et al., 2019).

1.9 Nitrogen removal in HRAS process

Conventional biological nutrient removal (BNR) processes result in the oxidation of a large fraction of organic carbon due to long solid retention time (SRTs), resulting in a reduction of sludge degradability, biogas production potential, and large demand of oxygen for nitrification and chemical oxygen demand (COD) for denitrification. Moreover, BNR processes entail high energy consumption, with energy consumption ranging from 0.3 to 0.8 $kWh \cdot m^{-3}$ for treating urban wastewater (Garrido et al., 2013). In this context, the High-rate activated sludge (HRAS) process is proposed as an innovative sustainable technology, replacing primary clarifiers (PCs), to enhance the energy efficiency of WWTP by redirecting carbon and nutrients to anaerobic digestion (Carrera et al., 2022).

The nitrogen content in domestic wastewater typically ranges from 20 to 70 $mg \cdot L^{-1}$ and is characterized as Total Kjeldahl Nitrogen (TKN), with 60-70% consisting of reduced forms as ammonium ($N\text{-}NH_4^+$). The rest is organic nitrogen (OrgN), both biodegradable and non-biodegradable fractions, bound to particulate, colloidal and soluble forms of COD.

The mechanism of $N\text{-}NH_4^+$ removal in HRAS process depends on the SRT: assimilation by microbial growth at 2-3 days and bio-adsorption at 0.5-1.0 days. At short SRTs, due to limited biomass growth, adsorption of $N\text{-}NH_4^+$ is dominant over assimilation (Ge et al., 2017). Accordingly, reported $N\text{-}NH_4^+$ removal values in HRAS literature increase with the SRT increase: 11% at 0.22 days, 8% at 0.5 days, 19% at 0.9 days, 10% at 1.2 days and 35% at 3 days (Ge et al., 2017; Miller et al., 2015; Rey-Martínez et al., 2021; Taboada-Santos et al., 2020). OrgN is primarily removed by being entrapped in settling solids and may be released by microorganisms either through metabolism or upon death and lysis. No nitrification has been reported for HRAS, it was only observed in the lab-scale HRAS pilots when the growth of a biofilm on the reactor walls was not prevented. Regarding TKN removal, reported values in HRAS depend on the SRT, ranging from 14±7% at 0.22 days (Miller et al., 2015), 18-38% at 0.3-0.6 days in full scale plant (De Graaff et al. 2016), 22% at 0.5 days and 49% at 3 days (Ge et al., 2017). These values are higher than the 10-16% TKN removal achieved in PCs (Seeley, 1992), reducing the energy demand of the subsequent nitrification-denitrification (N/DN) process.

1.10 COD/TKN Ratio in HRAS Effluent and Nitrogen Removal

HRAS effluent must undergo a subsequent nitrogen removal unit operation in order to fulfill the concentration limitations in WWTP discharges. The heterotrophic denitrification pathway in conventional N/DN process requires 4 – 8 $g_{COD} \cdot g_{N\text{-}NO3}$ for $N\text{-}NO_3$ reduction and biomass synthesis (Hertzier et al., 2010), depending on the value of the biomass yield associated with the specific available COD. Efficient nitrogen removal in the N/DN process, especially through heterotrophic denitrification,

necessitates a readily available carbon source. The mass ratio of COD to nitrate serves as a critical factor, with its balance determined by biomass synthesis yield (Y_H) (Hertzier et al., 2010). Notably, effective COD removal within HRAS is crucial, particularly since substrates with lower Y_H, such as volatile fatty acids, make more COD available for energy reactions, thereby necessitating lower COD/N mass ratios (Gori et al., 2011).

Moreover, strategies have been devised to reduce the COD demand in nitrogen removal processes. These modifications include:

i) The adoption of a short-cut nitrogen process in the mainstream, with nitrite oxidizing bacteria (NOB) out-selection to reduce COD demand for NO_2 reduction by 40%, compared to NO_3 reduction (Ge et al., 2015; Jiang et al., 2019; Pérez et al., 2014; Wang et al., 2019).

ii) Partial nitritation/Anammox (PN/A) in the mainstream, which attains a notable 66% nitrogen removal while maintaining a low biodegradable COD/N mass ratio (0.6-2.0 $g \cdot g^{-1}$) and a low BOD_5/N mass ratio (0.4-2.5 $g \cdot g^{-1}$) (Akaboci et al., 2018; Han et al., 2016; Hoekstra et al., 2019; Isanta et al., 2015; Jia et al., 2020; Laureni et al., 2016; Reino et al., 2018).

iii) Anammox process implemented in a sidestream configuration, yielding a 15-20% reduction in influent nitrogen load, and with successful deployment in around 100 full-scale plants (Daigger et al., 2011; Jenkins et al., 2003; Lackner et al., 2014; Siegrist et al., 2008; Wett et al., 2007). These strategies underscore the significance of optimizing nitrogen removal processes to achieve efficient treatment outcomes while minimizing the associated COD demand.

To fulfil the nitrogen effluent requirements, only ca. 25% of TKN_{in} can go to the effluent and waste streams (Rahman et al., 2019), so approximately 75% must be removed. The COD demand to remove the nitrogen can be calculated depending on the technology applied. For the conventional N/DN process, the COD demand is 6 $g_{COD} \cdot g_{TKNin}^{-1}$ (75% of 8 $g_{COD} \cdot g_{TKNin}^{-1}$) and for the short-cut N/DN it is 3.6 $g_{COD} \cdot g_{TKNin}^{-1}$ (75% of 4.8 $g_{COD} \cdot g_{TKNin}^{-1}$), and for the PN/A it is 1.5 $g_{COD} \cdot g_{TKNin}^{-1}$ (75% of 2.0 $g_{COD} \cdot g_{TKNin}^{-1}$). In the PN/A process with SBR in the PN, at most 70% of $N\text{-}NH_4^+{}_{in}$ is oxidized to $N\text{-}NO_2$, while the other 30% is oxidized by the Anammox (Liu et al, 2019; Magrí et al., 2021). Therefore, only 31% of $N\text{-}NH_4^+{}_{in}$ can be heterotrophically denitrified to maintain the $N\text{-}NO_2/N\text{-}NH_4^+$ mass ratio of 1.34$g \cdot g^{-1}$ in the influent of the Anammox process. Consequently, the organic material demand is only 1.5 $g_{sCOD} \cdot g_{N\text{-}NH4+in}^{-1}$ (31% of 4.8 $g_{sCOD} \cdot g_{N\text{-}NH4+in}^{-1}$ (Lemaire et al., 2014; Wan et al., 2016). Although this process requires a low COD concentration, it stabilizes the system due to the coexistence of heterotrophic denitrifiers and Anammox bacteria (Lackner et al., 2014; Pedrouso et al., 2017; Regmi et al., 2015, 2014; Yang et al., 2016).

In a PN/A process, several factors, such as the influent COD split, degradability, and load, play important roles in inducing and maintaining NOB suppression and AOB activity. The HRAS $sCOD_{out}$ is utilized by heterotrophic bacteria to reduce NO_2^- in the anoxic phase, but this reduces the NO_2^-

required for the subsequent Anammox process. The consumption of NO_2^- restricts its availability for NOB in the oxic phase. Moreover, an increase in organic loading in the HRAS effluent can negatively impact the system by creating competition for DO with heterotrophs (Hausherr et al., 2022). The key challenge is to strike a balance between the consumption of sCOD in the anoxic phase for NO_2^- reduction by heterotrophs while maintaining a high enough NO_2^- concentration for oxidizing $N\text{-}NH_4^+$ in the Anammox process. This process requires low sCOD concentration, but it stabilizes the system by allowing for the coexistence of heterotrophic denitrifiers and Anammox bacteria (Pedrouso et al., 2017; Yang et al., 2016).

1.11 Phosphorus removal in HRAS process

Phosphorus, characterized as total phosphorous (TP), is the other major nutrient in wastewater ranging from 6 to 8 $mg \cdot L^{-1}$ distributed in three forms: orthophosphate 50%, polyphosphates 30%, and organic phosphorous (OrgP) 20%. At time, OrgP, with biodegradable and non-biodegradable fractions, is found in soluble, colloidal, or particulate forms, and the last two are generally settled with the sludge.

Phosphorous is removed in the HRAS process by assimilating $P\text{-}PO_4^{3-}$ into biomass during microbial growth and entrapping it in particulate and colloidal OrgP in settling solids. Additionally, biological phosphorus removal was also demonstrated to be feasible at short SRTs in a HRAS with Sequencing Batch Reactor (SBR) process (Ge et al., 2015), indicating that phosphorus can be effectively captured and biologically concentrated in sludge stream concurrently with significant COD capture. Biomass growth was found a key factor for nutrients capture, and TP removal efficiencies were reported in a large range of SRT, from 3 to 0.22 days, with TP removal efficiencies from 15% to 53% (Böhnke et al., 1997; Ge et al., 2017; Miller et al., 2015). Ge et al. (2017) reported 5.1% removal of $P\text{-}PO_4^{3-}$ at SRT 0.5 days. Rey-Martínez et al. (2021) and Taboada-Santos et al. (2020) reported 9.5-12% and 13% at SRT 1.2-2.5 days and 0.9 days respectively.

Therefore, the HRAS process entails significant removal of nutrients from wastewater despite its main objective being the harvesting of COD to achieve zero energy consumption. Thus, HRAS involves the reduction of oxygen consumption for COD oxidation and nitrification, COD for denitrification and chemicals for phosphorus removal in the subsequent treatment steps of N/DN and phosphorus removal in the mainstream.

1.12 HRAS Control Process

The control variables in a HRAS process are similar to those in CAS process: DO, SRT, and sludge recirculation. However, the control objectives are different. In a CAS process, the effluent COD, TKN and TSS concentrations should be kept below their respective discharge limit. In comparison, there are no similar, strict limits for the HRAS effluent. The use of DO as control parameter is not proposed because no clear correlation between COD removal and DO was observed. The impact of DO on the

fate of organic carbon in the HRAS is not fully understood, as COD removal involves multiple mechanisms including absorption/adsorption, bio-assimilation as cells or extracellular polymeric substances, and mineralization. However, DO level affects sludge settleability and hence the effluent TSS. The use of SRT as control parameter need to control the MLSS, influent SS and effluent SS, due to the low inventory of biomass in the HRAS and the big affectation of SS_{IN} and SSO_{UT} in the SRT calculation, different from a CAS process, where SS_{IN} and SSO_{UT} can be neglected. The SRT controller therefore required not only an MLSS sensor in the bioreactor but also two additional SS sensor to measure the SS_{IN} and SSO_{UT}. This design failed as the controller was very sensitive to the accuracy of the influent SS sensors (Yaun Z, et al 2019). To keep the MLSS concentration in the HRAS bioreactor at a constant level could be a good solution due to the fact that the HRAS process is self-controlling, that means that an increase of influent COD load is matched with an increase of COD removal efficacy. This system will be implemented in our study. Finally, the control of recirculation sludge in HRAS is similar to CAS process, it is matched with influent flow.

Other challenges in the HRAS process are controlling the effectiveness of COD elimination to achieve a COD/TKN ratio within acceptable limits for subsequent denitrification. In a pilot plant study, Miller et al. (2017) implemented a control strategy based on DO, SRT and MLSS values. While the strategy demonstrated effectiveness in mitigating variations in COD performance, it did not consistently maintain the COD/TKN ratio at the desired values.

1.13 HRAS Modelling

HRAS process are a very dynamic system, as they are characterized by very low SRT and HRT. When the sludge is subjected to these very dynamic conditions, the microorganisms switch from a dominant growth model to a dominating storage model. Haider et al. (2003) found that working at a SRT shorter than one day produced a selection of fast-growing bacteria: A-Stage Heterotrophic Organisms (AHO) that use the sCOD only partially, in accordance with Böhnke et al (1997) who observed that HRAS systems only supported AHO, while CAS systems had a rich community of bacteria, protozoa and metazoans. Hauduc et al (2019) indicated that at SRTs lower than 3 days, AHOs are preferably developed, avoiding cell lysis and endogenous respiration, and consequently minimizing oxygen consumption. Due to the short SRT, the HRAS process retains only the AHO that can only use rapidly degradable substrates, for instance, volatile fatty acids (VFA) and monomers.

In the past years, modelling tools for HRAS process have been shown to be critical for improving system performance and designing new systems. Haider et al. (2003) proposed additional fractioning of sCOD to justify its incomplete degradation by AHO in the HRAS process. Their model described the removal of sCOD omitting COD adsorption. Later, Nogaj (2015) and Dynamita (2016) developed a model to describe the organic substrate transformation in the HRAS process, which included: dual soluble substrate utilization; production of extracellular polymeric substances (EPS); absorption of soluble substrate (storage); and adsorption of colloidal substrate.

There is an optimal SRT where carbon capture is maximized (0.25-0.4 days), while below ca. 0.2 days less COD is oxidized and only a small fraction is removed from the wastewater. SRT over 1 day leads to an increase of COD hydrolysis and oxidization, including a fraction of primary solids (Jia et al., 2020; Miller et al., 2015). Haider et al. (2003) also proposed a model that includes a readily biodegradable substrate, S_B, split into $S_{B,mono}$ and $S_{B,poly}$. In addition, the flocculation of suspended solids and colloids, which correlates closely with the total biomass concentration, is affected by the temperature and mixing intensity, represented in the model by a flocculation factor, f_r. A deflocculation process in the recirculation pumping is also considered. Figure 1.5 shows the biological processes added and modified for the removal and capture of organics in the modified model (Hauduc et al, 2019).

Finally, a topic of the utmost importance is the consideration of biological activity in the clarifier. (Rosso et al., 2019) highlighted that at the bottom of clarifier, in an anoxic condition, part of the carbon stored in the cells could be redissolved. This redissolution is greater in sludge with 0.3 d SRT than in sludge with 0.5 d SRT.

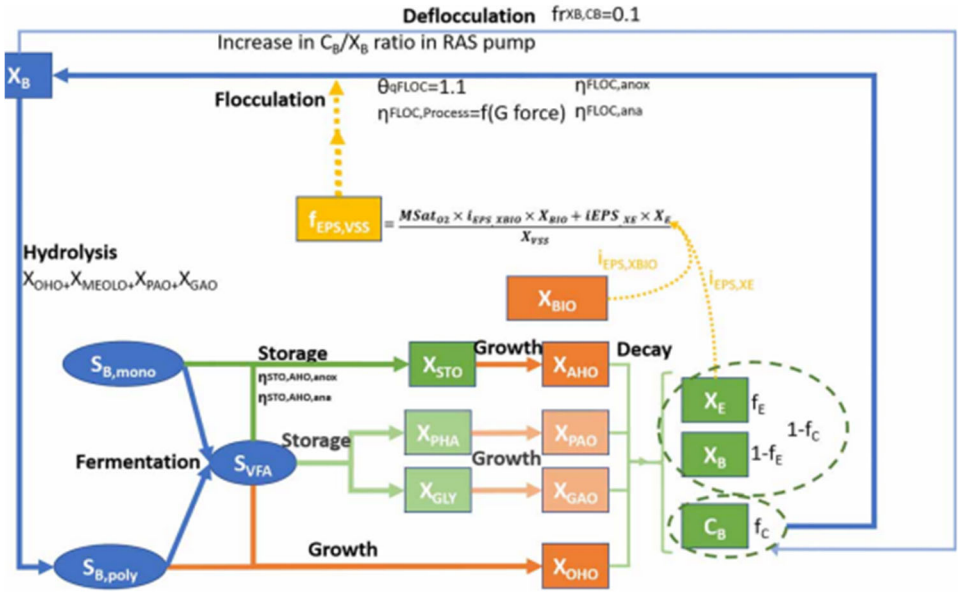

Figure 1.5 Biological processes added and modified for the removal and capture of organics in the modified model (Hauduc et al 2019)

1.14 Potential of HRAS for energy recovery from wastewater

Wastewater contains a significant amount of potential energy in the form of organic matter, which can be captured through anaerobic sludge digestion. For instance, a wastewater with a COD concentration of 500 $mg \cdot L^{-1}$ have a potential energy of 1.93 $kWh \cdot m^{-3}$ (3.86 $Kwh \cdot Kg_{COD}^{-1}$) (McCarty et al., 2011), surpasing the energy requirements for conventional wastewater treatment (0.3–0.8 $kWh \cdot m^{-3}$, 0.6–1.6 $Kwh \cdot Kg_{COD}^{-1}$) (Garrido et al., 2013). However, the conventional wastewater treatment methods like

PC, CAS and sludge anaerobic digestion recovers only around 33% of this potential energy (Wett et al., 2007, Wan et al 2016).

The implementation of HRAS instead of PC allows to send higher COD and TKN to anaerobic digestion. This not only significantly reduces the energy required for COD removal and nitrification in the mainstream treatment, but also increases the biogas production. HRAS achieve this by the concentration of wastewater organics thanks to the high OLR and short SRT and HRT. As a result, a high fraction of incoming COD recovered as sludge instead of being oxidized.

Furthermore, HRAS facilitates nitrogen management. The increase of TKN sent to anaerobic digestion allows for a higher volume of rich ammonia side-stream. Deammonication processes like partial nitrification (PN) and anaerobic ammonia oxidation by anaerobic autotrophic bacteria (Anammox) can be employed with low energy consumption. Likewise, primary sludge presents higher efficiency (65%) than the biological sludge (35%) to convert the COD of sludges to COD of CH4.

Several studies have demonstrated the energy-saving potential of HRAS. For example, Rahman et al., 2018 compare d the HRAS A-Stage with short-cut nitrogen removal to conventional PC with N/DN processes, reporting an energy production/ energy consumption (EP/EC) ratio of 0.98 and 0.54 for the two alternatives.

Meerburg (2016) also found a significant 44% total energy reduction comparing PC with conventional N/DN in the main-stream with HRAS with conventional N/DN in the main-stream and PN/A in the side-stream. De Graaff et al., (2016) reported for a two full HRAS a low energy consumption, 0. 1 $Kwh \cdot Kg_{COD}^{-1}$ with a 60%COD removed and a 0. 17 $Kwh \cdot Kg_{COD}^{-1}$ with a 74% COD removed but did not report the total energy consumption of each WWTP. Finally, Carrera et al (2022) reported an energy recovery higher than 100% for a HRAS treating a PC effluent and a PN/A nitrogen removal in the mainstream.

HRAS presents a promising alternative to PC as the initial treatment in wastewater treatment plants, offering substantial energy-saving opportunities and contributing to the goal of energy-neutral wastewater treatment.

1.15 Overview the Research Conducted on the HRAS Process

Table 1.1 provides a comprehensive overview of the research conducted on the HRAS process, covering key areas of investigation. The main topics explored in the literature include:

i) Process modeling (Ref 1,6-8)

ii) COD removal mechanisms (Ref 2-3).

iii) HRAS + PN/A availability process in the mainstream (Ref 4).

iv) SRT, HRT and DO on COD removal (Ref 5).

v) Control and process stability (Ref 7).

vi) Impact of HRAS on WWTP energy balance (Ref 9-10).

Based on pilot experience the conclusions of the HRAS main topics are:

i) A wide range of operational parameters make the comparation of HRAS efficiencies difficult.

ii) Recent research presents the SRT<0.5 days as the optimum to save energy.

iii) The influent CDO concentration appear as the main parameter to select the use of HRAS A-Stage for high COD concentration and HRAS-CS for low COD concentration.

iv) The HRAS applied as a substitute of PC allows higher energy savings than applied after PC.

v) The relation between nitrogen and phosphorus fractions removal with COD fractions removal are poorly understood.

vi) One of the limiting factors in the HRAS process efficiency is the settling facility of biological sludge.

vii) Process stability, specific oxygen consumption (SOC) and oxygen supply control under low SRT are not well studied.

viii) HRAS modelling has been investigated and validated.

ix) HRAS +PN/A in the mainstream appears as a new paradigm in biological nutrients removal.

Overall, the HRAS process is not a final treatment to guarantee a permanent effluent quality, it is a preliminary treatment whose main objective is to harvest the maximum COD to digestion with the minimum oxygen consumption. Therefore, there is not a unique operating condition that meets this objective. Its design depends on the influent wastewater characteristics, basically the COD fractionation, and the subsequent nitrification-denitrification process. Herein lies the complexity of the design and operation of the HRAS process.

Table 1.1 Objectives and conclusions of the most recent studies carried out by a HRAS process

Reference	WWTP	Pilot Plant	Feed ww	Reactor volume	SRT (days)	HRT (min)	Study main objective	Conclusions
Haider et al. (2003)	Vienne	2 stage CAS	effluent PC	4-14.5 m3	0.1 A-stage 10 B-stage		revision of ASM 1 model	sCOD must be split in fast sCOD degraded in A-stage and low sCOD degraded in B-stage
Jimenez et al. (2005)	Marrero	HRAS	raw WW		2-3 d	5-10-20-30-45-60	mechanisms study to cCOD and pCOD removal in a CAS process	floculation is the first step in cCOD and pCOD removal, fast for pCOD and slow for cCOD
Miller et al. (2013)	Hampton Roud	A/B process	raw WW	107 L	0.04-025d A-stage	30	COD removal study in the Astage	Astage allows a COD removal up to 50%
Regmi et al. (2014)	Hampton Roud	HRAS as a pretr. of PN/A plant	raw WW	510 L	0.25 d	30	availability of a PN/A fed with a HRAS effluent with a COD/TKN of 6.7±1.4	HRAS + PN/A in the main-stream could be a new paradigm in biological nutrients removal
Jiménez et al. (2015)	New Orleans	HRAS	raw WW	260 L	0.1-2.0 d	30-45	Effect of SRT, HRT and DO on the HRAS removal	COD removal 50%, SRT, HRT and DO low impact in sCOD removal max. cCOD removal at SRT>1.5d.HRT>45m max. pCOD removal at SRT>1.5d.HRT>30m
Nogaj et al. (2015)	Hampton Roud	HRAS	raw WW	107 L	0.2 d	30	HRAS model validation	sCOD must be split in fast sCOD and low sCOD Dual substrate model was more accurate than diauxic model for sCOD removal
Miller et al. (2017)	Hampton Roud	HRAS	raw WW	510 L	0.22 d	30	evaluate a cascade DO and MLSS control for COD removal and process stability	DO and MLSS controls COD removal variations but not the COD/TKN ratio variations
Hauduc et al. (2019)	New Orleans	HRAS	raw WW	510 L	0.3-2.0 d	30-66	a new HRAS model development	model validation for a HRAS process
Rahman et al. (2019)	Chesapeake Elizabeth	HRAS A-stage HRAS -CS	raw WW	510 L	0.1-0.3 d	30	Carbon redirection and harvesting understanding. Evaluate nutrients redirection	HRAS maximize energy recovery, carbon capture and nutrients redirection
Carrera et al. (2022)	Rubi-Valldoreix	HRAS	effluent PC	250 L	0.6 d	180	Carbon and nutrients harvesting in a HRAS fed with PC. Sludge settleability study. Impact of HRAS on full scale plant energy balance	51% COD recovery at SRT 0.6d. Correlation between sludge settleability and SRT.HRAS allows a two-thirds reduction of aeration requirements and one -third increase of biogas production

Chapter 2
OBJECTIVES

2.1 Problem definition

The conventional activated sludge (CAS) process, while effective in meeting effluent quality standards, poses significant energy consumption and environmental impact challenges. HRAS is proposed to improve the efficiency of the primary clarifier (PC) to remove more influent organic matter (measured as COD) and reducing overall electricity consumption in municipal wastewater treatment.

While many HRAS pilot plant studies have focused on SRT, HRT, and DO's impact on COD removal, several critical issues have been poorly analysed. There is a gap of knowledge to address on optimizing COD fractions removal, nutrient fractions removal, COD oxidation, and improving process stability in the HRAS process. Special attention has to be given to exploring HRAS effluent's COD/TKN and sCOD/N-NH_4^+ ratios and dissecting their implications on the suitability of different nitrogen removal strategies. Furthermore, the process performance should be validated through process simulation, a comparison that is often lacking in such studies.

2.2 Research objectives

The main motivation of this thesis is to study HRAS's removal efficiency and stability in a demonstration scale pilot plant at low SRT, HRT, and DO treating raw wastewater without PC and evaluate the energy savings. The objectives are divided into specific goals:

- To evaluate COD fractions removal and stability
- To study nutrient fractions removal, focusing on nitrogen and phosphorus removal
- To establish specific oxygen consumption SOC_{COD}, SOC_{sCOD}, and SOC_{BOD5} and control HRAS oxygen supply
- To evaluate the settleability and thickening ability of HRAS waste sludge

The attainment of these objectives has led to the following thesis outline:

Chapter 4 presents the results of COD fractions removal and process stability

Chapter 5 presents the results of the study of nitrogen and phosphorus fractions removal and HRAS's effect on subsequent nitrification-denitrification processes

Chapter 6 defines the mechanisms of oxygen measurement and control

Chapter 7 studies the clarifier characteristics of HRAS biomass.

Chapter 3
MATERIALS & METHODS

3.1 Pilot Plant Description

A pilot plant was designed to perform this research following the scheme presented in Figure 3.1. It was operated with pre-treated wastewater (grit and scum removal) from the WWTP of the municipality of Montornès del Vallès (Barcelona, NE Spain) serving a population of 95000 eq. inhabitants with significant load variations due to the industrial activity (30-40%). A screen system with a 5 mm mesh was installed to remove large solids from the influent. Figure 3.2 shows the pilot plant of 30 $m^3 \cdot d^{-1}$.

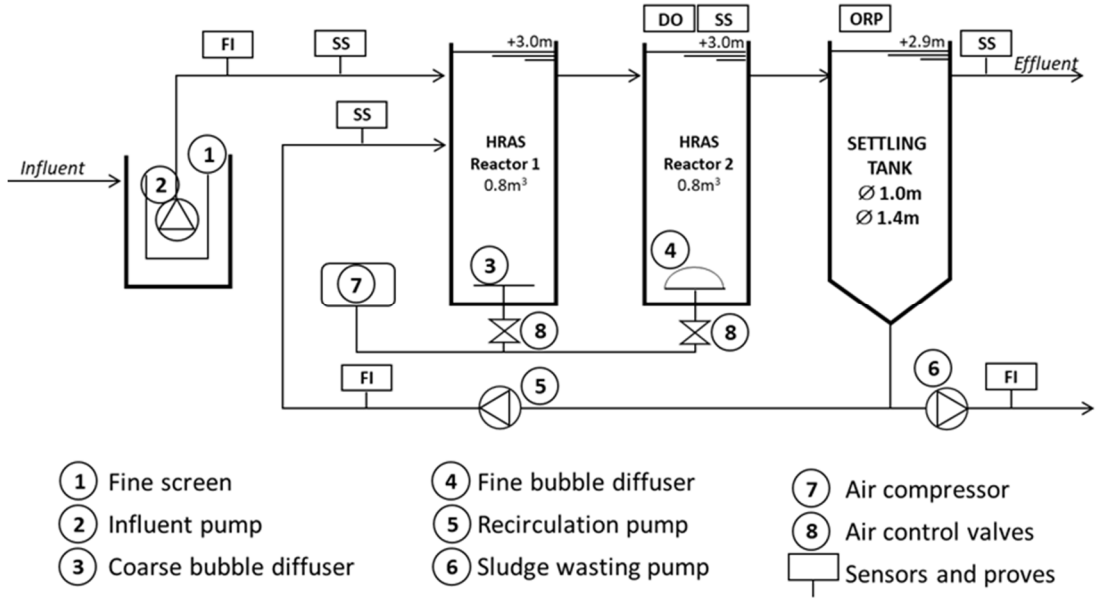

Figure 3.1. HRAS Pilot Plant Process Diagram.

Different operation periods were designed, where the flow rate was set constant or variable to mimic a real WWTP. The average daily flow range between 24.1 - 31.8 $m^3 \cdot day^{-1}$. The plant was composed by two 0.8 m^3 biological reactors (R1 and R2) with 2 $m^3 \cdot h^{-1}$ recirculation pump and 0.5 m3·h-1 wasting pump. The reactor R1 was installed before the aerobic reactor R2 to analyse the effect of flocculation over cCOD and pCOD removal.

The pilot plant was provided with two clarifiers (1.0 and 1.4 m diameter) that were operated alternatively and allowed to modify the OFR and SL without changing the HRT of the reactor, which constituted a singularity of the present study. The side water depth in the reactors and settling tanks was 3.0 m. Aeration in Reactor R2 was controlled using a DO sensor (Hach Lange) and a motorized valve with automatic PID control. The air supplied in reactor R1 was only to prevent the accumulation of MLSS at the bottom of the reactor, the overflow rate was 7.14 $m \cdot h^{-1}$, enough to keep the biomass in suspension.

Figure 3.2 Pilot plant 30 $m^3 \cdot d^{-1}$ at WWTP Montornes-Barcelona

3.2 Sampling and Analysis

The plant was equipped with two automatic samplers to collect and keep refrigerated at 5ºC 24-hour, influent and effluent integrated samples (Hach Lange). The analysis included COD (soluble, colloidal, and particulate), BOD_5, TSS, VSS, N-TKN, $N\text{-}NH_4^+$, TP and $P\text{-}PO_4^{3-}$ according to standard methods (Measurements, 1999). There were 92 days of representative results of the process. Days with extreme incidents in the influent were disregarded.

The COD fractions (particulate, soluble and colloidal) were calculated as follows: pCOD difference between total COD and filtered COD through 1,5µm; sCOD flocculated ($ZnSO_4$) and filtered through 0.45 µm (Mamais et al., 1993); cCOD difference between pCOD and sCOD. The BOD_5 analysis was performed with seed inoculum from a CAS plant, not from the HRAS reactor. Solid samples were collected twice a week from the reactors and recirculation and were analysed for TSS, VSS and COD, always following the recommendations prescribed in the standard methods (Measurements, 1999).

The pilot plant continuously monitored the following operational parameters: DO (reactor 2), ORP (bottom of clarifier), influent flow rate, recirculation flow rate and waste flow rate. The suspended solids in the influent, reactor R2, effluent and recirculation flow were continuously analysed by means of four digital sensors (Solitax sensor, Hach). Due to biofouling in the reactor, the DO sensor was equipped with an air blast-cleaning mechanism. The ORP sensor was installed in order to avoid anaerobic conditions in the bottom of clarifier.

3.3 Pilot Plant Influent Wastewater Characteristics

Table 3.1 summarizes the average characteristics of the influent, including raw wastewater and internal WWTP recirculation. The main potential for energy recovery and savings relies on capturing the colloidal and particulate fractions, which accounted for 75% of COD_{IN}, and limiting the oxidation of

the soluble fraction, which was 25% of COD_{IN} (Table 3.2). The pilot plant was operated in both dry and rainy weather, which impacted the influent COD, SS, TKN and TP concentrations.

Table 3.1. Pilot plant influent characteristics.

Parameter	Acronym	Average ± S.D.	Units
Chemical Oxygen Demand	COD_{IN}	686 ± 212	$mg \cdot L^{-1}$
Particulate Chemical Oxygen Demand	$pCOD_{IN}$	456 ± 201	$mg \cdot L^{-1}$
Colloidal Chemical Oxygen Demand	$cCOD_{IN}$	62 ± 24	$mg \cdot L^{-1}$
Soluble Chemical Oxygen Demand	$sCOD_{IN}$	171 ± 60	$mg \cdot L^{-1}$
Biochemical Oxygen Demand	BOD_{5IN}	254 ± 109	$mg \cdot L^{-1}$
Total Suspended Solids	TSS_{IN}	399 ± 175	$mg \cdot L^{-1}$
Volatile Suspended Solids	VSS_{IN}	297 ± 156	$mg \cdot L^{-1}$
Total Kjeldahl Nitrogen	$N\text{-}TKN_{IN}$	70 ± 15	$mg \cdot L^{-1}$
Ammonium Nitrogen	$N\text{-}NH_4^{+}{}_{IN}$	38 ± 9	$mg \cdot L^{-1}$
Total Phosphorous	TP_{IN}	8.7 ± 3.4	$mg \cdot L^{-1}$
Orthophosphates	$P\text{-}PO_4^{3-}{}_{IN}$	1.7 ± 0.8	$mg \cdot L^{-1}$
Reactor Temperature (*range*)	T	18-26	°C

The sewage collection system was by gravity, which meant that non-septic water conditions were present in the influent. The standard deviation (SD) of the averaged parameters is high as usual in a municipal wastewater with high industrial loadings.

Table 3.2 HRAS Influent ratios

Parameter	Ratio
pCOD/COD	0.66
sCOD/COD	0.25
cCOD/COD	0.09
COD/TKN	9.8
sCOD/N-NH4	4.5
COD/VSS	2.3
N/VSS	0.23
P/VSS	0.03

3.4 Pilot Plant Operating Conditions

The pilot plant was operated during 497 days, running over nine different operational periods, the main parameters and conditions of which are summarized in Table 3.3 and Table 3.4 Aside from the inherent variations in the influent water characteristics, the differences of operational parameters during the different periods were the flow rate: constant (CF) or variable (VF) according to the schedule in Table 3.5; the point of sludge wasting: from the reactor (R2) or from the clarifier (STL) and the settler diameter: 1.0 o 1.4 m. The HRT on the reactor R2 was 0.6 hours (Periods 1-9), while R1 was operated at HRT 0.6-0.8 hours during periods 1-6. The SRT was maintained under 0.5 days.

The SRT (0.2±0.05 days) was maintained practically constant in the low range during the whole operation to minimize sCOD oxidation. The SRT calculations (Equation 3.1) omitted the biomass in the clarifier, the suspended solids in the influent and the suspended solids in the anoxic reactor. This SRT was optimized to enhance sludge concentration, biomass yield and overall system efficiency

(Sancho et al., 2019). Hydraulic retention time (HRT) was calculated by Equation 3.2 without considering the recirculation flow. The HRT (<1 hour), which did not include the recirculation flow, was selected to strike a balance between allowing biomass development and biosorption, while still limiting COD mineralization.

Table 3.3 Pilot plant operating conditions in each experimental period.

Period [days]	Inflow [$m^3 \cdot d^{-1}$]	Inflow regime	Wasting point	Reactors in operation	Temperature R2 [ºC]	Clarifier Diameter [m]
1 (86d)	24.1	CF	R2	R1 + R2	18.5	1
2 (44d)	29.3	CF	STL	R1 + R2	22.1	1
3 (80d)	31.8	CF	STL	R1 + R2	25.6	1
4 (58d)	30.8	VF	STL	R1 + R2	26.3	1
5 (37d)	30.7	VF	STL	R1 + R2	22.8	1
6 (31d)	31.1	VF	STL	R1 + R2	19.3	1.4
7 (41d)	31.1	VF	STL	R2	18.9	1.4
8 (76d)	30.6	VF	STL	R2	23.2	1.4
9 (44d)	31.1	VF	STL	R2	20.1	1.4

CF: Constant; VF: Variable; R1: Reactor 1 optional; R2: Aerobic; and STL: Settler

The Solids Loading (SL) is the ratio between the amount of mixed liquor suspended solids (MLSS) coming into the settler and the settler surface (Equation 3.3). The overflow rate (OFR) is the ratio between the pilot plant inflow and the settler surface calculated by Equation 3.4. The sludge volume index (SVI) is the ratio between the solid volume after 30 minutes of settling (1 L sample) and the MLSS concentration of Reactor R2, calculated by Equation 3.5.

The organic loading rate (OLR) is the ratio between influent COD load and the inventory of the MLSS in R2 according to Equation 3.6. OLR was exceptionally high on Periods 3 due to the low MLSS and in Period 7 due to the high influent COD concentration.

$$SRT_{R2} = \frac{V_{reactor}R2 \cdot MLSS_{reactor}}{Q_{waste} \cdot MLSS_{waste} + Q_{effluent} \cdot MLSS_{effluent}} \quad \text{Equation 3.1}$$

$$HRT_{R1+R2} = \frac{Q_{in}}{V_{R1} + V_{R2}} \quad \text{Equation 3.2}$$

$$Solid\ load_{settler}(SL) = \frac{(Q_{in} + Q_r) \cdot MLSS_{reactor}}{Settler\ surface} \quad \text{Equation 3.3}$$

$$Overflow\ rate_{settler}(OFR) = \frac{Qin}{Settler\ surface} \quad \text{Equation 3.4}$$

$$Sludge\ volume\ index(SVI) = \frac{V_{30}}{MLSS\ concentration} \quad \text{Equation 3.5}$$

$$Organic\ Loading\ Rate\ (OLR) = \frac{Q_{in} \cdot COD_{in}}{V_{R2} \cdot MLSS_{R2}} \quad \text{Equation 3.6}$$

Coarse bubbles were used in Reactor R1 only to keep the biomass in suspension and prevent the accumulation of MLSS at the bottom of the reactor. The hydraulic overflow rate was 7.14 $m \cdot h^{-1}$. In turn in Reactor R2 fine bubbles were used for both aeration and mixing. The R2 DO set point was 0.5±0.2 $mg \cdot L^{-1}$ similar to the half-oxygen saturation. K_{O2} (0.5 $mg \cdot L^{-1}$) for AHO. The reactor temperature ranged between 18.5 and 26.3 °C without any correction. Sludge was wasted from Reactor R2 only during Period 1 and from the bottom of the settling tank during Periods 2-9.

Table 3.4 Reactors and settler operation parameters.

Period	MLSS R2 [$mg \cdot L^{-1}$]	HRT R1+R2 [hours]	SRT R2 [days]	DO R2 [$mg \cdot L^{-1}$]	External recycle	OLR-R2 [$kg_{COD} \cdot kg_{MLSS}^{-1} \cdot d^{-1}$]	OFR Q_{in} [$m \cdot h^{-1}$]	SL $Q_{in}+Q_R$ [$kg_{MLSS} \cdot m^{-2} \cdot d^{-1}$]	SVI_{30} [$mL \cdot g^{-1}$]	TSS (out) [$mL \cdot g^{-1}$]
1	3043	1.6	0.2	0.7	73 %	9.9	1.3	164	64	103
2	2577	1.3	0.3	0.4	60 %	8.8	1.6	155	51	92
3	1729	1.2	0.1	0.4	55 %	14.9	1.7	109	55	113
4	2555	1.2	0.2	0.4	54 %	8.5	1.6	156	67	119
5	2508	1.2	0.2	0.4	54 %	9.8	1.6	152	48	91
6	2290	1.2	0.2	0.5	70 %	9.3	0.8	79	55	66
7	2163	0.6	0.1	0.5	70 %	14.6	0.8	75	59	69
8	2010	0.6	0.2	0.5	62 %	10.4	0.8	65	49	65
9	1924	0.6	0.2	1.1	63 %	9.5	0.8	64	49	44
Mean	2311	1.1	0.2	0.5	62 %	10.6		113	55	85
S.D.	404.0	0.4	0.05	0.2	7 %	2.4		43	7	25

OLR: organic loading rate; OFR: over flow rate; SL: solids loading; SVI_{30}: sludge volume index 30 min.

Table 3.5 Hourly flow rate distribution according to the total daily flow of 24, 34 or 44 $m^3 \cdot day^{-1}$.

Time	Flow ($m^3 \cdot h^{-1}$)		
1:00	0.96	1.36	1.76
2:00	0.90	1.27	1.65
3:00	0.84	1.19	1.54
4:00	0.79	1.12	1.45
5:00	0.77	1.09	1.42
6:00	0.79	1.11	1.44
7:00	0.83	1.18	1.52
8:00	0.90	1.28	1.65
9:00	0.99	1.40	1.81
10:00	1.06	1.51	1.95
11:00	1.13	1.60	2.07
12:00	1.16	1.65	2.14
13:00	1.17	1.66	2.15
14:00	1.15	1.64	2.12
15:00	1.12	1.59	2.06
16:00	1.08	1.54	1.99
17:00	1.05	1.49	1.93
18:00	1.04	1.47	1.90
19:00	1.03	1.46	1.90
20:00	1.04	1.48	1.91
21:00	1.06	1.49	1.93
22:00	1.06	1.50	1.94
23:00	1.05	1.48	1.92
24:00	1.01	1.44	1.86
Daily flow	24.00	34.00	44.00

From period 7 onwards only the reactor R2 was operated to evaluate the performance in the absence of the anoxic reactor R1. From period 6 onwards the diameter of the clarifier was increased from 1m to 1.4 m to analyse the influence of overflow and sludge loads in the clarifier without changing the HRT in reactor R2. The pilot plant was operated at short SRT of 0.2 days at constant MLSS reactor concentration of 2000 ± 200 $mg \cdot L^{-1}$. The profile of the MLSS was monitored through the use of in situ on-line sensors. The waste was flowed by a helicoidal pump operated ON/OFF and controlled by the MLSS set point. Maintaining a constant and low MLSS reactor concentration prevented the washout of biomass minimized solid load in the settling tank and averted the formation of poorly settling sludge. The DO controlled by the PID varied in a narrow range around 0.6 $mgO_2 \cdot L^{-1}$. Likewise, to avoid the fermentation of the biomass at the bottom of the clarifier the recirculation flow rate was set at minimum 60% of the influent flow rate.

3.5 Process Simulation

The industrial-scale plant operation design and monitoring were based on prior simulations using the SUMO model (Hauduc et al., 2019). The SUMO model was selected because it considers the population of both OHO and AHO and the processes of adsorption and flocculation on readily biodegradable matter. i.e. volatile fatty acids (VFA), monomers, polymers, and colloidal matter. The process diagram adopted in SUMO simulations. and the main parameters for OHO and AHO growth are detailed in the Figure 3.3 and Table 3.6.

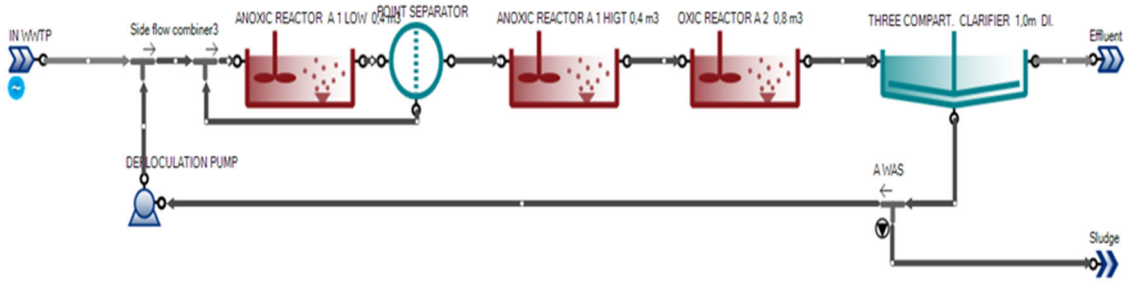

Figure 3.3 SUMO-Model Pilot Plant Process Diagram

Table 3.6 Main parameters for OHO and AHO growth.

	Units	OHO	AHO
Substrate		$sCOD_{(poly)}$	$sCOD_{(mono)}$ $sCOD_{(VFA)}$
Growth conditions		ox.anox.ana	ox
Maximum specific growth rate. µMax	d^{-1}	2	6
Half-saturation of readily biodegradable substrate K_s	$g_{COD} \cdot m^{-3}$	5	0.5
Half-saturation of O_2. K_{O2}	$g_{O2} \cdot m^{-3}$	0.05	0.5
Decay rate. b	d^{-1}	0.2	0.6
Yield	$g_{XBIO} \cdot g_{SB}^{-1}$	0.67	0.6

RESULTS

Chapter 4
RESULTS I

High-rate activated sludge at very short SRT: Key factors for process stability and performance of COD fractions removal

Redrafted from:

Canals, J., Cabrera-Codony, A., Carbó, O., Torán, J., Martín, M., Baldi, M., Gutiérrez, B., Poch, M., Ordóñez, A., & Monclús, H. (2023). High-rate activated sludge at very short SRT: Key factors for process stability and performance of COD fractions removal. Water Research, 231. https://doi.org/10.1016/j.watres.2023.119610

4.1 Overview

In HRAS processes, reducing the solid retention time (SRT) minimizes COD oxidation and allows to obtain the maximum energy recovery. The aim of this chapter is to study the automatic control strategy to assure the HRAS process stability and high COD fractions removal at very low SRT. The research includes the effects of temperature, influent concentration and MLSS reactor concentration over the sCOD, cCOD and pCOD removal. The Chapter studies the use of MLSS concentration to control the HRAS at a low SRT instead of the SRT itself. Low SVI values indicated the good settling properties of the biomass. With only low COD oxidation, a high organic matter removal was reached. The high removal efficiencies for pCOD compared to sCOD and cCOD also confirmed the importance of settling efficiency and stability in the HRAS. The direct correlation between COD influent and COD removal makes advisable to use the HRAS as a replacement of the primary clarifier. The HRAS acted efficiently as a filter for COD and pCOD peak loads and, in a lesser extent, for BOD_5, while sCOD peaks were not buffered. The adopted model presented a good fit for COD fractions except for pCOD when the temperature exceeds 23°C.

The objective of this chapter is to evaluate COD fractions removal and stability in HRAS process. In order to achieve this goal, the following sub-objectives have been established: i) Evaluating the removal efficiency of each COD fraction and BOD_5 and their correlations with key operational parameters, ii) Monitoring influent and effluent COD fractions and BOD_5 in long-term operation, iii) Evaluating COD oxidation, iv) Evaluating the OLR and ORR correlation, v) Comparing simulated COD fractions removal efficiency with pilot plant results.

4.2 Methodology

In order to evaluate the efficiency of the technology under different operational parameters, the HRAS-AS pilot plant was operated during 497 days over 9 different periods (Table 3.3 and Table 3.4) treating raw wastewater coming from grid and grease removal units, which constituted a significant step forward from the previous studies performed with the primary clarifiers (PC) effluent. During periods 1-3 the inflow regime was maintained constant $24 h \cdot d^{-1}$, in periods 4-9 it changed according to the time table provided in Table 3.5. From period 7 on, only the reactor R2 was operated to evaluate the performance in the absence of the anoxic reactor R1. Finally, from period 6 on, the clarifier was changed to increase the diameter from 1m to 1.4 m in order to analyse the influence of overflow and sludge loads in the clarifier without changing the HRT in the reactor R2.

The complexity of the HRAS technology lies in maintaining the process stability operating at such short specific SRT. In the conventional activated sludge (CAS) process, where the SRT ranges between 6 and 12 days, the reactor biomass is large enough to absorb the influent´s variations. However, the short

STR (<0.5 days) and HRT (R2 60 minutes) together with the lack of preliminary PC makes the HRAS process sensitive to the influent's variations.

Considering that there is a lack of automatic HRAS process control in previous studies, the control strategy appointed in this study was to maintain a constant MLSS reactor concentration of 2000 ± 200 $mg \cdot L^{-1}$. This low reactor MLSS concentration keeps from reactor biomass washout, lowering settling tank solid overload or prevent poor settling sludge, like in Period 3, MLSS below 1500 $mg \cdot L^{-1}$. Moreover, HRAS operates at a SRT approaching the washout SRT conditions based on the maximum growth rate of biomass (Nogaj et al. 2015).

Figure 4.1 shows the 24 h profile of the MLSS concentration and the waste sludge flow, both monitored through the use of in situ on-line sensors. Matching the waste sludge to the MLSS set point (2000 $mg \cdot L^{-1}$) ensured the consistency and process stability, even with low SRT and HRT values. Likewise, the recirculation flow rate was set at 60% of the influent flow rate to avoid the fermentation of the biomass at the bottom of the clarifier. The oxygen concentration in reactor R2 was monitored on-line to check the efficiency of the control system. The oxidation-reduction potential (ORP) was also monitored on-line to control the reduction conditions and avoid the CH_4 generation, which leads to COD loss and greenhouse gas generation. The values ranged between -150 and -300 mV. These results are valuable knowledge in the design of a full-scale plants.

The pilot plant was running both in dry and rain weather, which highly impacts the influent COD and SS concentration. In any conditions, the peak flow rates applied to the pilot plant were as maximum 1.3 times and as minimum 0.7 times the average of the dry flow rate. It was observed that in episodes of intense rain, the extreme dilution of COD and SS influent cause a decrease in the MLSS concentration in the reactor. However, due to the low STR, the process can recover the stability within few hours.

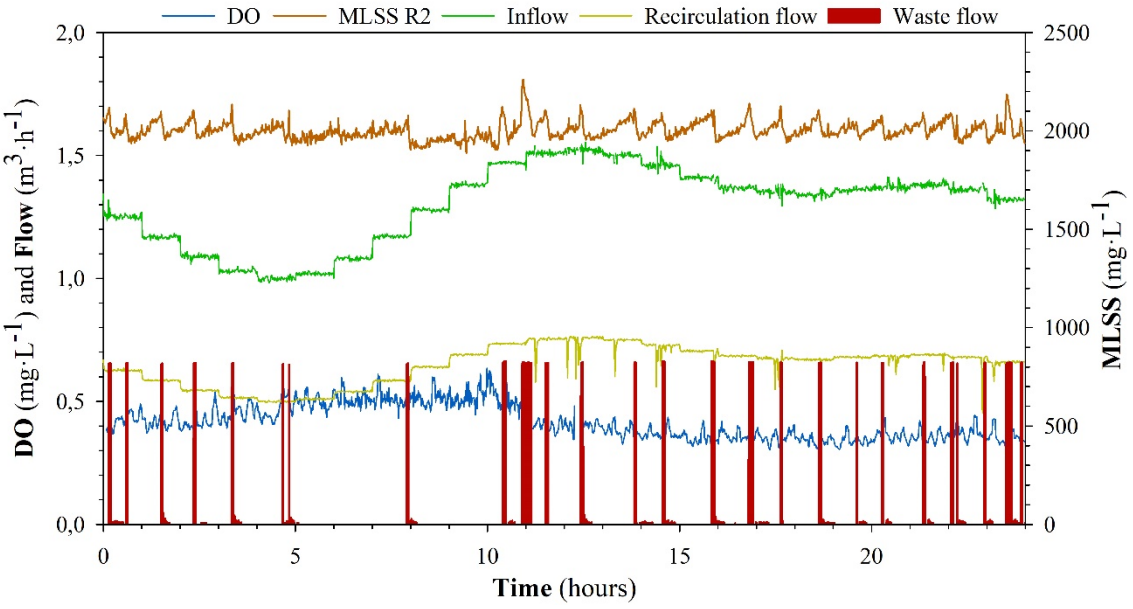

Figure 4.1 24h monitoring of the process control parameters: waste sludge flow rate and MLSS concentration in reactor R2, dissolved oxygen (DO) and recirculation flow rate.

4.3 Results and Discussion

4.3.1 Performance evaluation

For every experimental period, Table 4.1 gathers the average concentration and percentage of each COD fraction and BOD_5 in the influent together with the removal efficiency achieved. It should be noted that the removal efficiencies for each fraction indicate not only the effectiveness of the COD removal processes: adsorption, storage and oxidation but also the efficiency of the settling tank harvesting. The COD fractions and BOD_5 removal for each period is presented in Figure 4.2.

As further discussed in the following sections, the average COD removal for the entire operation of the pilot plant was 57 ± 9%. COD is the sum of each COD fraction, and their weight varies constantly during the day, and in greater proportion in seasonal changes. In general terms, the removal efficiencies obtained are significantly higher than those reported in primary clarifiers (35-40%) (Crites and Tchobanoglous, 1998) and in the same magnitude to those indicated by Böhnke et al. (1997) (55%) for a HRAS-AS process. On the other hand, Rahman et al. (Rahman et al., 2019) reported efficiencies of 67% applying similar operational conditions but operating at a constant temperature of 20 °C, while our pilot plant operated at variable temperatures (18.5 – 26.3 °C) and it had a negative linear correlation with COD removal (Figure 4.4B). The average BOD_5 removal for the entire operation of the pilot plant was 56 ± 10%, significantly higher than those reported in primary clarifiers (35-40%) (Crites and Tchobanoglous, 1998) and in the same magnitude to the 55% indicated by Versrille et al. (1985) for a HRAS-AS process.

Table 4.1 COD fraction concentration averages at influent and removal in each experimental period.

Period	$sCOD_{IN}$ [$mg \cdot L^{-1}$] (COD%)	sCOD (rem) [%]	$cCOD_{IN}$ [$mg \cdot L^{-1}$] (COD%)	cCOD (rem) [%]	$pCOD_{IN}$ [$mg \cdot L^{-1}$] (COD%)	pCOD (rem) [%]	Total COD_{IN} [$mg \cdot L^{-1}$]	COD (rem) [%]	BOD_{5IN} [$mg \cdot L^{-1}$]	BOD_5 (rem) [%]
1	180 (18%)	27 ± 12	61 (6%)	-4 ± 38	766 (76%)	81 ±7	990	66 ± 10	455	67 ± 14
2	183 (28%)	30 ± 13	61 (9%)	9 ± 25	419 (63%)	78 ± 10	658	57 ± 8	283	51 ± 13
3	187 (27%)	31 ± 11	59 (9%)	8 ± 36	438 (64%)	72 ± 8	684	55 ± 7	261	57 ± 8
4	161 (27%)	34 ± 9	69 (11%)	24 ± 20	372 (62%)	61 ± 9	602	50 ± 6	244	50 ± 12
5	222 (32%)	36 ± 9	60 (9%)	16 ± 32	401 (59%)	73 ± 8	680	56 ± 9	257	58 ± 5
6	168 (29%)	24± 12	50 (9%)	4 ± 33	372 (62%)	77 ± 8	585	55 ± 7	212	49 ± 7
7	200 (23%)	28 ± 5	83 (10%)	62 ± 11	570 (67%)	75 ± 13	853	63 ± 12	401	58 ± 3
8	138 (23%)	23 ± 11	69 (12%)	16 ± 47	381 (65%)	71 ± 13	588	53 ± 13	204	54 ± 11
9	102 (19%)	19 ± 13	54 (10%)	12 ± 32	359 (71%)	77 ± 6	515	59 ± 6	160	57 ± 13
Average	171 (25%)	29 ± 12	62 (9%)	12 ± 35	453 (66%)	74 ± 10	683	57 ± 9	254	56 ± 10

COD fraction percentage regarding total COD

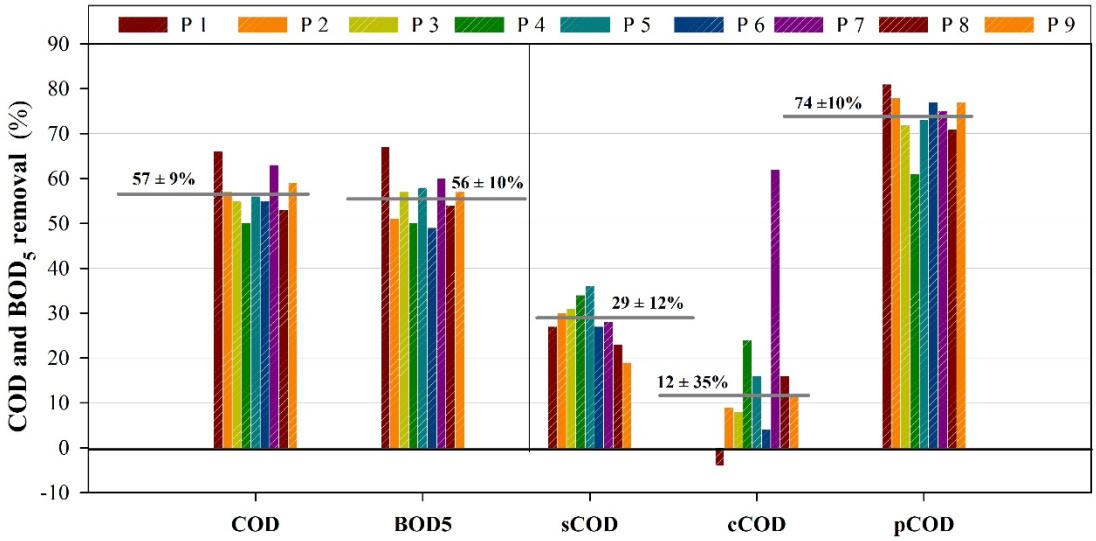

Figure 4.2. COD and BOD5 average removal efficiencies for each period. The horizontal line marks the average removal for the entire operation of the pilot plant and the associated standard deviation.

4.3.1.1 Soluble COD removal efficiency

The sCOD average concentration in the raw wastewater ranged from 102 to 222 mg·L^{-1} depending on the experimental period, which accounted for and average 29% of the influent COD (Table 4.1), reaching values up to 32% in the Period 5. sCOD includes the soluble inert COD, the readily biodegradable volatile fatty acids (VFA), the readily biodegradable monomers and polymers.

In turn, the collecting systems type: gravity, pumping, length and temperature have a determinant effect in COD fractions. According to (Wilén et al., 2006), the biological processes in the sewer system are predominantly aerobic in high flows and anaerobic in low flows, thus changing wastewater properties. Moreover, in an anaerobic sewer collection system, the temperature promotes an increase in fermentation rates and in turn increased the sCOD removal. Likewise, the temperature increases the VFA and monomers fraction stored by AHO organisms. Hauduc et al. (2019) reported that at 20 °C monomers fraction was ca. 60% of the sCOD, while at 15 °C monomers fraction was ca. 40% of the sCOD.

The sCOD removal efficiency achieved in the HRAS pilot plant had an average value of 29±12%, ranging between 19±13% and 36±9% depending on the experimental period. These results are in the same order than those indicated by (Miller et al., 2015), 33±12%, and by (De Graaff et al., 2016), 11 ± 61%. (J. Jimenez et al., 2015) achieved a sCOD removal of 50-60% working at a DO concentration of 1.0 mg·L^{-1} and higher SRT of 1 day.

In order to investigate the sCOD influent concentration effect over the sCOD removal efficiency, Figure 4.3 shows the relation between COD_{in} fractions and the COD removal at 20 °C corrected temperature (Θ=1.045) (Seeley, 1992) along the nine experimental periods considered. The good correlation

indicated that the sCOD removal was controlled by a biological oxidation-storage process according to Hauduc et al. (2019).

At time, Figure 5A shows, for each period, the sCOD removal, the temperature and $sCOD_{in}$ concentration. It can be highlighted that for the same $sCOD_{in}$ the temperature increase, promoted the increase of the sCOD removal: Periods 6 and 4 had similar $sCOD_{in}$ (168 $mg \cdot L^{-1}$) and a temperature difference of 7ºC, leading to an increase of 10% removal. However, periods 1 and 3, had similar $sCOD_{in}$ (180 $mg \cdot L^{-1}$) and a temperature difference of 7ºC, but the removal increase was only 4% probably due to the lower MLSS concentration in Period 3.

The relation between MLSS concentration in the R2 and the sCOD removal efficiency was investigated at 20 °C corrected temperature (Θ=1.045). The results for each operational period are shown in Figure 4.5, where it can be observed that periods 3, 2 and 1 with similar $sCOD_{in}$ and a MLSS concentration of 1729 $mg \cdot L^{-1}$, 2577 $mg \cdot L^{-1}$ and 3.000 $mg \cdot L^{-1}$ respectively, presented sCOD removal efficiencies of 24%, 27% and 29% respectively.

Finally, the elimination of the anoxic reactor R1 in periods 7, 8 and 9, confirmed the non-affectation of reactor R1 in sCOD removal.

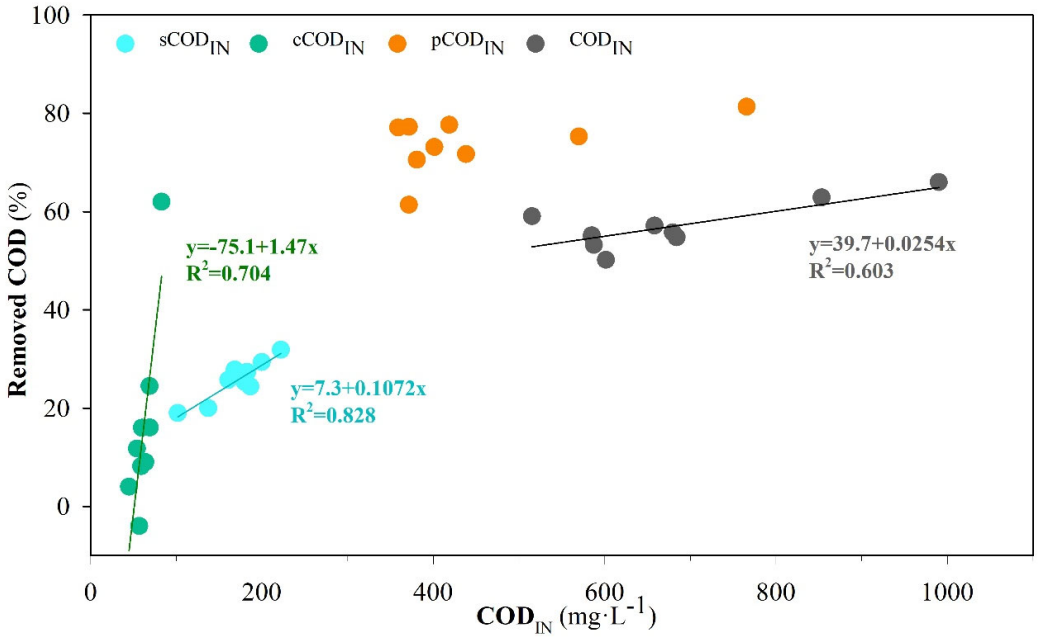

Figure 4.3. sCOD, cCOD, pCOD and COD removal percentage related to their influent concentration.

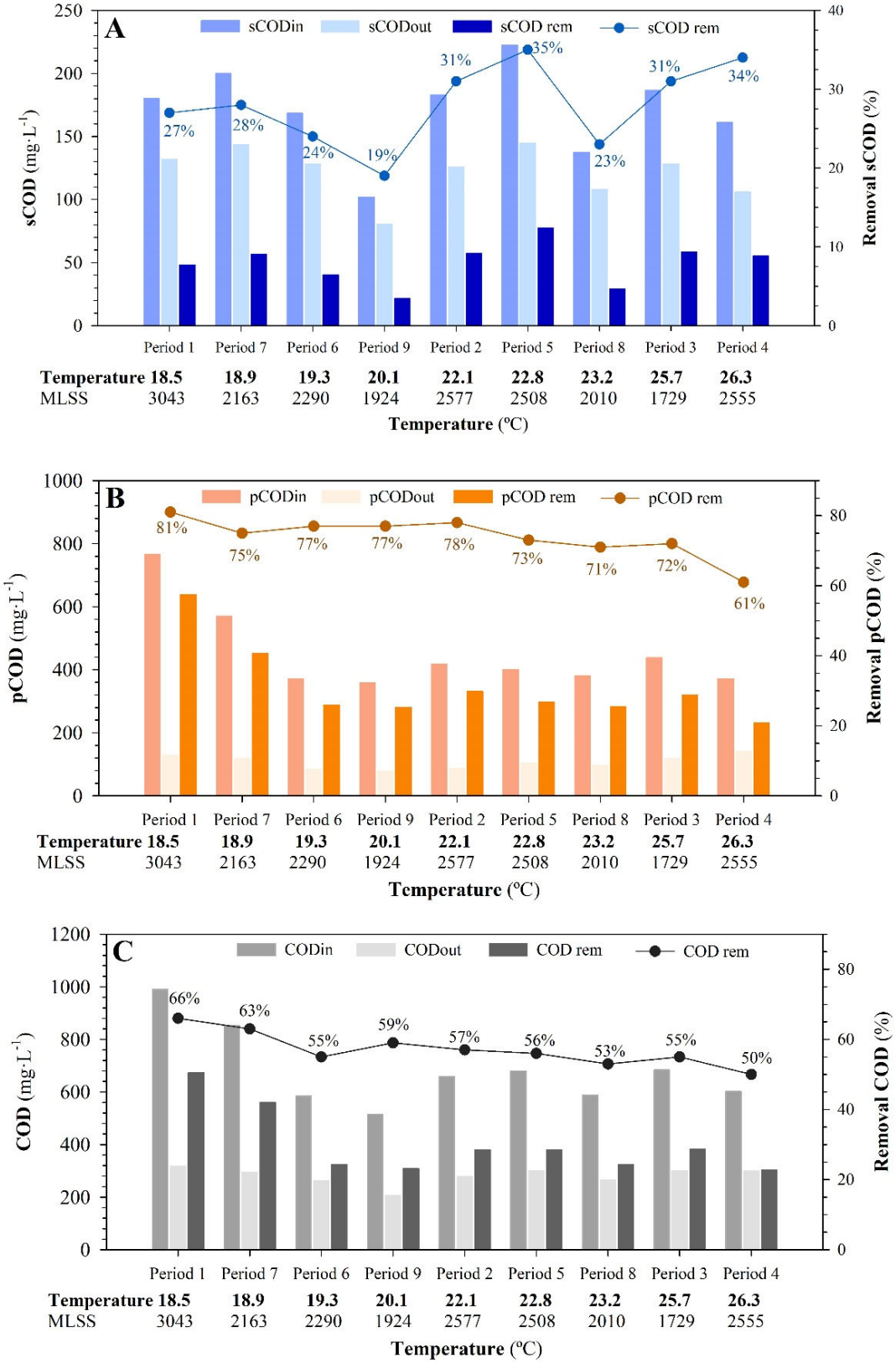

Figure 4.4. Influent, effluent and removal of COD fractions based on temperature. A) sCOD, B) pCOD and C) COD.

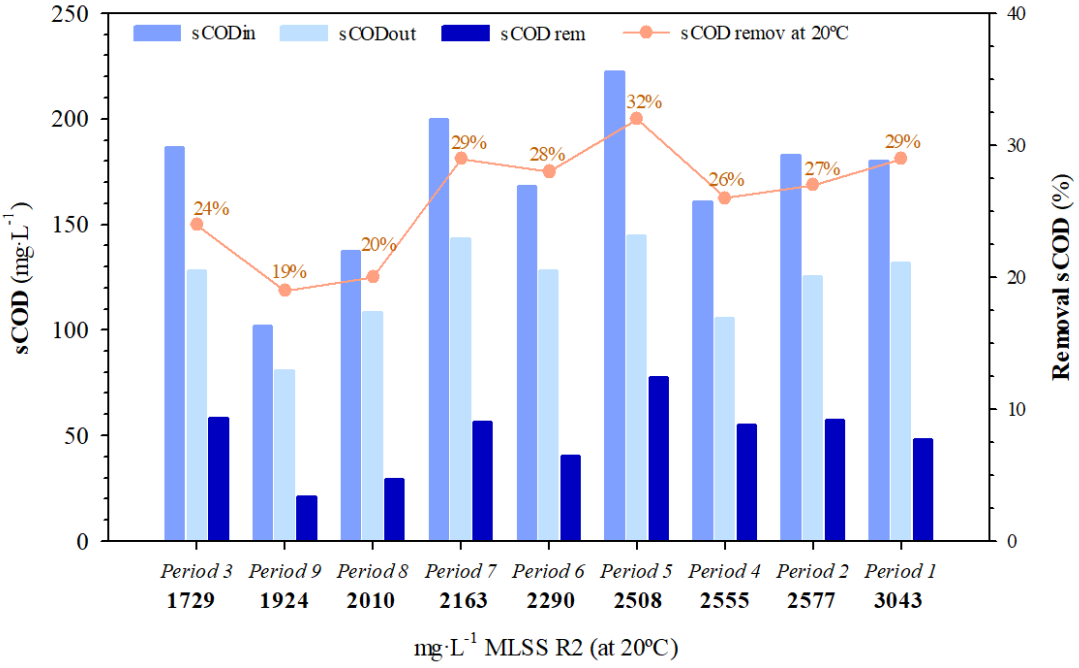

Figure 4.5: sCOD (influent, effluent and removal) and MLSS concentration in R2 at corrected temperature.

4.3.1.2 Colloidal COD removal efficiency

The cCOD average concentration in the raw wastewater ranged from 54 to 83 mg·L^{-1} depending on the experimental period, which accounted for and average 9% of the influent COD. In general terms, the removal of cCOD was between -4 and 24% (Table 4.1), with a noticeable increase during period 7 which corresponds to a significant increase in the inlet cCOD. The effect of the inlet cCOD with the removal efficiency was investigated, resulting a first-order kinetics shown in (Figure 4.4A) where the higher the inlet, the more removal efficiency, unlike that indicated by Bunch and Griffin (Bunch and Griffin Jr., 1987), who proposed zero-order kinetics.

It is important to highlight that during the first operational stage, the results led to negative cCOD removal due to the fact that the deflocculation produced by the high recirculation pumping was higher than the flocculation process to remove cCOD. In the design of the HRAS process equipment, such as pumps and agitators, the minimization of this deflocculation effect must be considered. Increased cCOD in the effluent was also reported by Miller et al. (2015), with negative removals of 28% due to the conversion of sCOD into non-flocculated colloidal biomass, and by Bisogni and Lawrence (1971) at short SRTs as a result of dispersed biomass growth. HRAS has been observed as bio-flocculation limited by low cCOD removal efficiency, which may potentially be due to lack of (EPS) production (Kinyua et al., 2017a). Likewise, decay processes and large clarifier hydraulic retention times can produce colloidal material (Hauduc et al., 2019).

4.3.1.3 Particulate COD removal efficiency

The pCOD constituted the major part of the inlet COD (66%), with an average influent concentration of 453 $mg \cdot L^{-1}$, ranging from 359 to 766 $mg \cdot L^{-1}$ depending on the experimental period (Table 4.1). The removal of the pCOD, which controls the overall COD removal because of its largest contribution, is associated with the adsorption onto biomass flocs by electrostatic interactions due to the biological activity. Moreover, the settling characteristics are determining in the HRAS process for the gravity separation of particulate matter.

The relationship between pCOD removal over the nine experimental periods and the following variables: solid loading (SL), overflow rate (OFR), $pCOD_{IN}$ concentration, MLSS and temperature are show in Figure 4.6. The solids loading (SL) did not affect pCOD removal due to the high sludge settling properties, low SVI30 (49-67 $mL \cdot g^{-1}$) (Table 3.4), compared to (110-180 $mL \cdot g^{-1}$) in CAS processes (Seeley, 1992) and similar to the values reported by Böhnke et al. (1997) (40-90 $mL \cdot g^{-1}$), Miller et al. (2015) (85±26 $mL \cdot g^{-1}$), Van Winckel et al. (2019) (88±81 $mL \cdot g^{-1}$) and Rahman et al (2019) (88±18 $mL \cdot g^{-1}$) in their HRAS pilot plant studies. Furthermore, the variation in the SL did affect the effluent suspended solid (SS) concentration (Figure 4.6A), although its impact was also linked to the variation in the overflow rate (OFR). At turn, OFR did not affect pCOD (Figure 4.6B) removal due to the high sludge settling properties. The variation of the OFR did, however, affect the effluent suspended solid SS_{OUT} concentration, although its impact was also linked to the variation in SL (Figure 4.6A).

The $pCOD_{IN}$ concentration had slight effect on the pCOD removal efficiency (Figure 4.3). Period 4, with an average pCOD removal efficiency of only 61%, corresponded mainly to August. The combination of both low $pCOD_{IN}$ load and the high temperature (26.3 °C) of this period explains the low efficiency achieved. pCOD removal remained at high values (70-80%), regardless of the $pCOD_{IN}$ concentration.

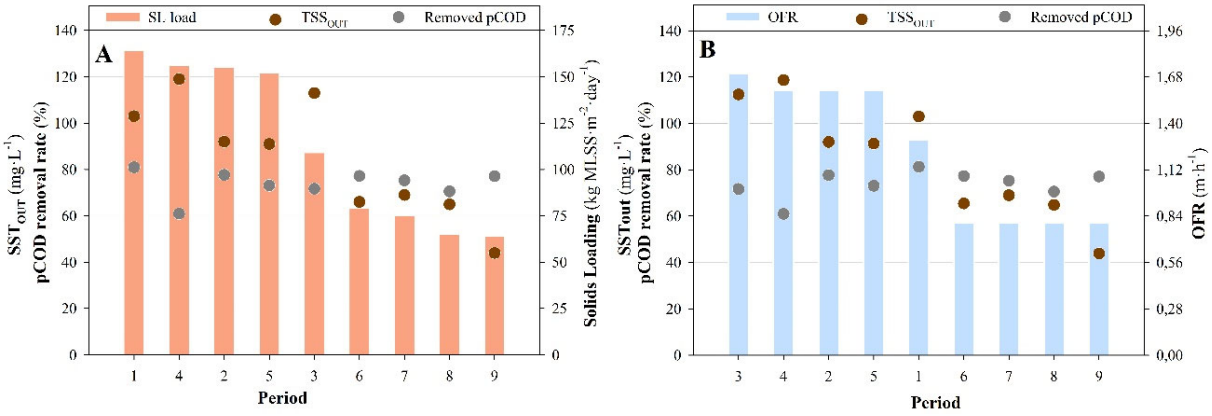

Figure 4.6. A) Relationship between solid loading, pCOD removal percentage and SS_{OUT}. B) Relationship between overflow rate and pCOD removal percentage and SS_{OUT}.

At time, Figure 4.4B shows, for each period, the pCOD removal, the temperature and the $pCOD_{in}$ concentration. It can be highlighted that for a given $pCOD_{in}$, the temperature increase promoted a decrease of the pCOD removal: Comparing Periods 6, 8 and 4, at similar $pCOD_{in}$ (372 $mg \cdot L^{-1}$) and MLSS concentration of 2290 $mg \cdot L^{-1}$, 2010 $mg \cdot L^{-1}$ and 2555 $mg \cdot L^{-1}$ respectively, and a temperature variation of 19.3ºC 23.2ºC and 26.3ºC resulted on a pCOD removal of 77%, 71% and 61% respectively suggesting that temperature has a negative contribution on pCOD removal.

On the one hand, as previously indicated by (Jorand et al., 1995), temperature does not affect the pCOD bioadsorption process; on the other hand, increasing the temperature leads to a decrease in the viscosity of the medium and should, consequently, cause better settling of the biological flocs. The behaviour observed may be related to the increased hydrolysis and decay process rate with temperature (Dynamita, 2016, Nogaj 2015), i.e. the redissolution of the pCOD into the settling tank. Another factor that produces an increase in hydrolysis is the continuous arrival of OHO heterotrophic organisms in the influent from the internal return line. However, here, other processes seem to be occurring. Most likely, the viscosity of the sludge decreases with increasing temperature, which results in less efficient particle capture in the settler.

The MLSS concentration in the reactor had a good correlation with the pCOD removal for all periods (Figure 4.7) since it promoted the flocculation and entrapment of particulate matter in biological flocs (Hauduc et al., 2019), e.g. pCOD removal efficiency was 6% higher in period 2 (MLSS 2577 $mg \cdot L^{-1}$) than in period 3 (MLSS 1729 $mg \cdot L^{-1}$). Nevertheless, the biomass activity in a HRAS process without primary clarifier, is not as constant as in a CAS process, and its characteristics are highly affected by the concentration and composition of the influent SS. For a MLSS concentration below 1500 $mg \cdot L^{-1}$ the settling began to worsen. The control system implemented in the pilot plant maintained MLSS at 2312 ± 404 $mg \cdot L^{-1}$, thus promoting pCOD removal efficiency.

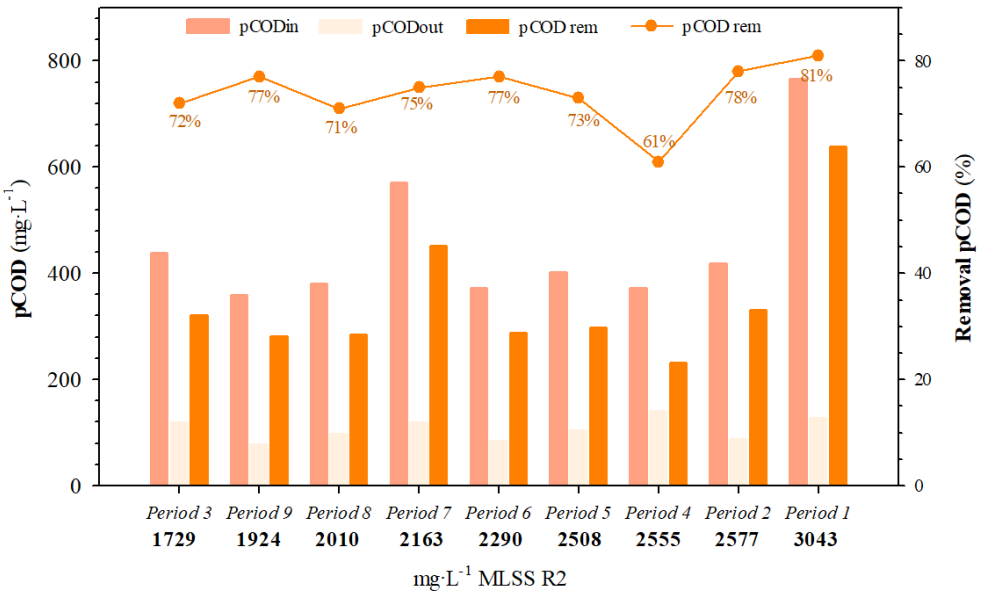

Figura 4.7: pCOD (influent, effluent and removal) and MLSS concentration in R2

Considering that the SRT values were practically constant during the whole operation and that the EPS content depends on the SRT applied (Rahman et al., 2016), the analysis of the EPS production and its effects were out of the scope in this study. Previous studies did not identified a significant influence of EPS on the bioflocculation and settling at short SRTs (Elliot, 2016; Kinyua et al., 2017a). Moreover, the HRAS removed the pCOD that would had been removed in a primary clarifier regardless of the biological activity.

In summary, the variables exerting the greatest effect on pCOD removal were the temperature, the $pCOD_{in}$ and the MLSS concentration in the aerobic reactor (R2). The OFR and SL in the settling tank had a minor impact on the pCOD removal. The pCOD removal efficiency was higher than a value of 65% reported by Jimenez et al. (2015) with a SRT of 0.5 days and DO of 0.5 $mg \cdot L^{-1}$ and was also higher than a value of 55% reported by Miller et al. (2013). The above confirms the robustness and success of the automatic control strategy, which maintained a fixed MLSS concentration in the reactor. This is to be noted, since this is the first study operated at a quite constant MLSS that achieved such high removal efficiencies.

4.3.1.4 Total COD

COD removal is the sum of each COD fraction's removal. The weight of each COD fraction changes constantly during the day and in greater proportion in seasonal periods. COD_{IN} concentration had a good correlation with COD removal (Figure 4.3). Temperature effect that on pCOD removal (Figure 4.4B), which was not offset by the positive effect on sCOD removal (Figure 4.4A) because the pCOD fraction was much higher than the sCOD fraction. The increase of biomass concentration in the reactor led to a slight increase of the pCOD and thus COD removal efficiency (Figure 4.8).

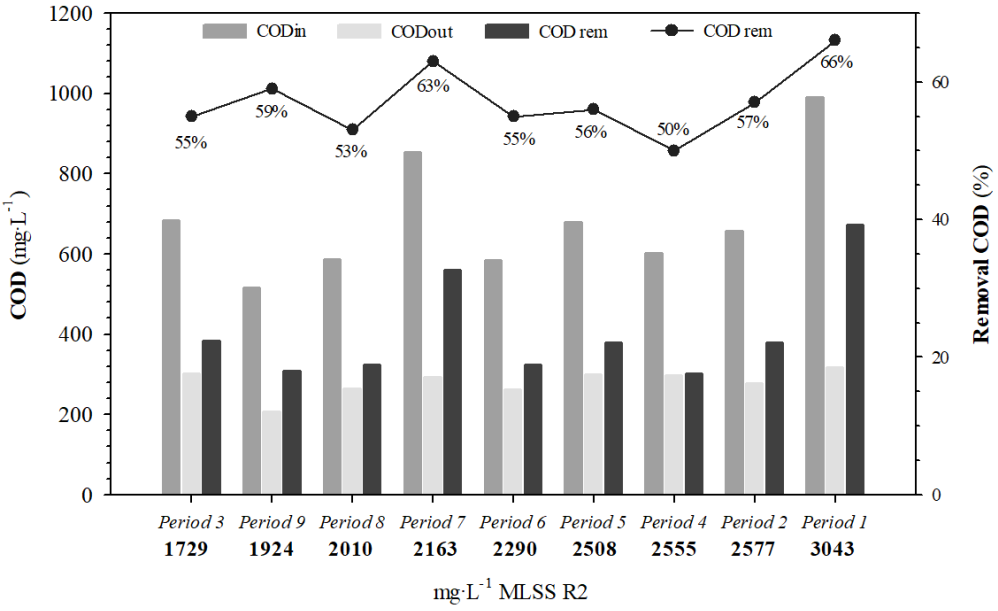

Figura 4.8: COD (influent, effluent and removal) and MLSS concentration in R2

As a summary, it is important to highlight the correlation between influent COD fractions and COD fractions removal. As shown in Figure 4.3, the cCOD removal presented highly dispersed values for a minimum variation in low influent concentrations (30-60 $mg \cdot L^{-1}$), the sCOD removal presents less dispersed values for a high range of influent concentrations (40-250 $mg \cdot L^{-1}$), and the pCOD removal present a minimal dispersion values for a high range of influent concentrations (350-800 $mg \cdot L^{-1}$). This highlights the importance of pCOD removal, like remarked by (Guven et al., 2019b) and, to a lesser extent of sCOD removal. The high dispersion of cCOD removal values and the low weight of cCOD in the total COD make this COD fraction the least important in the control of the HRAS process.

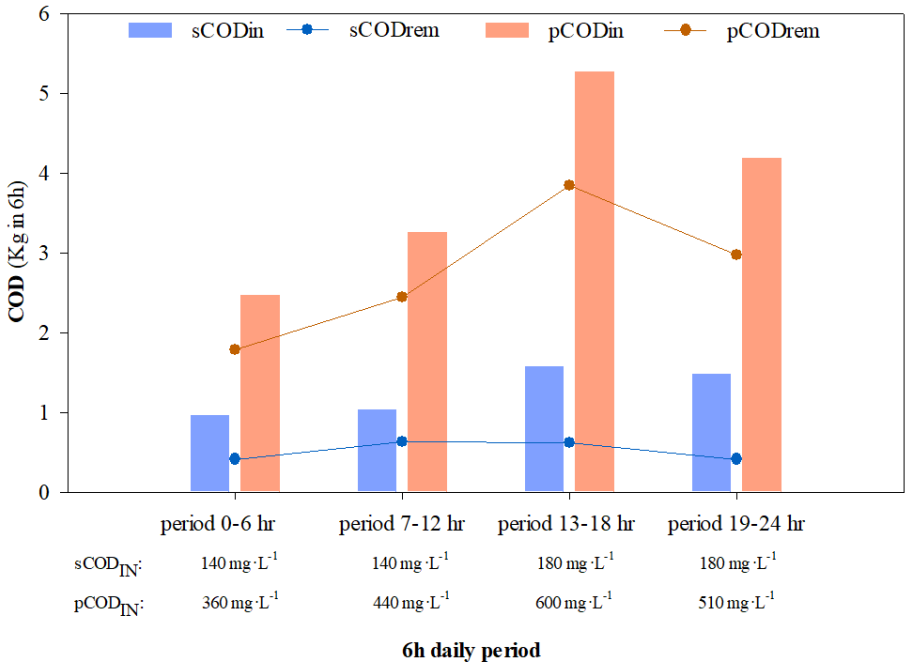

Figure 4.9: sCOD and pCOD influent and removal load in four six-hour periods per day.

From the standpoint of energy recovery, the key point is to harvest as much COD as possible (Guven et al., 2019a). Nevertheless, it is critical to differentiate the removal of each COD fraction given their importance in the subsequent nitrification–denitrification process. An increase of soluble COD in effluent HRAS would result in a quick removal during the aerobic cycle, thus decreasing the COD available for denitrification in the anoxic cycle (Regmi et al., 2014).

As a novelty of this study, the COD fractions removal analysis has been additionally carried out in periods of six hours. Figure 4.9 shows the sCOD and pCOD in the influent load and in the effluent for each 6-hour period, together with the amount removed. In periods 13h-18h and 19h-24h, the sCOD and pCOD load increased compared to periods 01h-06h and 07h-12h. While the sCOD remained constant during the day ca. 90 $g \cdot h^{-1}$, the pCOD removed increased with the pCOD load. More detailed hourly monitoring will be of interest in further development of the HRAS technology.

4.3.2 Effect of SRT over COD removal

The HRAS pilot plant was operated aiming at maintaining the MLSS constant as process control parameter. The SRT (0.1-0.4 days) resulting from the MLSS control was correlated with COD removal efficiency to evaluate the effect of the SRT on the system performance. Figure 4.10 shows the correlation between STR and each COD fraction removal during the whole operation time, with data divided into the different ranges of temperature conditions. It can be observed that there is no correlation in any case, indicating that SRT value was not a determining factor in COD fractions removal, at so low SRT, which is in agreement with the conclusions reported by Rahman et al. (2017).

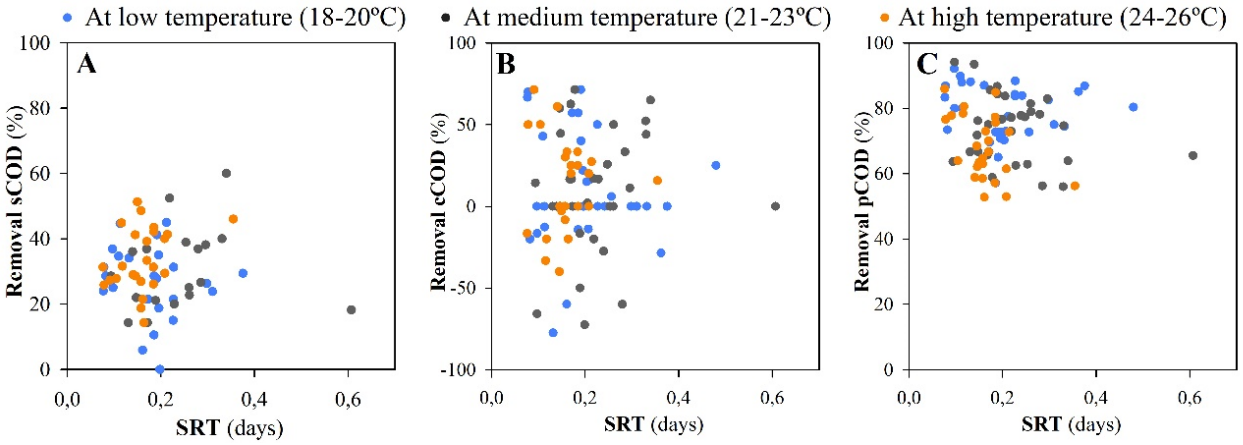

Figure 4.10. SRT and COD fractions removal at 18-20°C, 21-23°C and 24-26°C. A) sCOD, B) pCOD and C) COD

4.3.3 COD Mass Balance

The COD mass balance was calculated for each experimental period in order to investigate the efficiency of the process in terms of COD sent to digestion and COD oxidized. Figure 4.11 shows the results of the mass balance for each period. In general terms, the oxidation was low, under the values reported by Haider et al. (2003) (12% COD_{OXID} at STR 0.1 day), Miller et al (2017) (14% COD_{OXID} at STR 1 day) and Taboada-Santos et al. (2020) (16% COD_{OXID} at STR 0.9 days).

Thus, the HRAS working at low SRT (0.2 ± 0.05 days), low DO (0.5 ± 0.2 $mg \cdot L^{-1}$) and the already reported high variations in the influent load, permitt ed to send to digestion an average 55% of the influent COD, with a low average oxidation of 6.9±3.6% and maintaining the COD_{OUT} around 40% for almost every period.

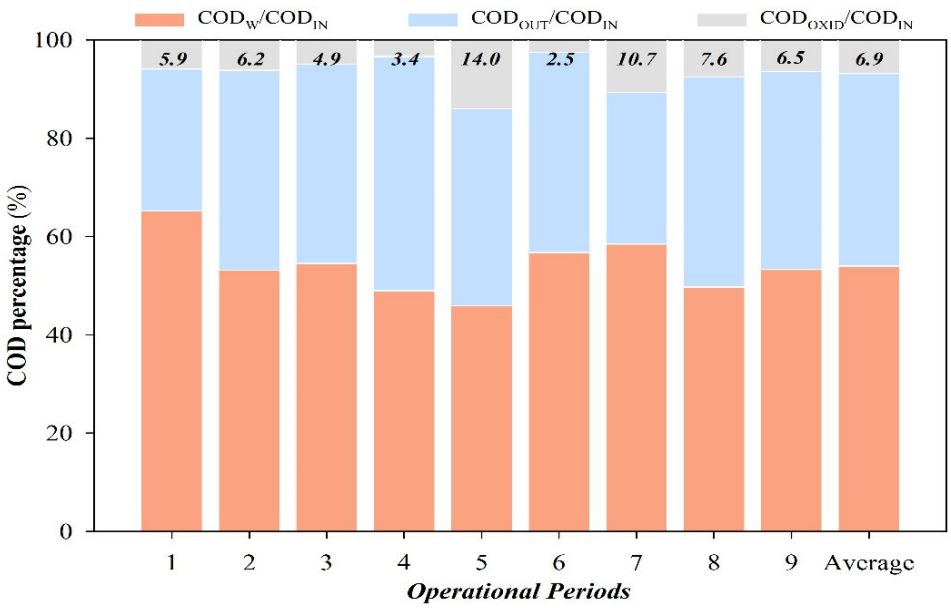

Figure 4.11. COD influent mass balance distribution: waste, out and oxidized.

4.3.4 BOD_5 removal

BOD_5 removal follows the same pattern than COD removal, presented in Figure 4.12. The COD and BOD_5 removal rates were similar: 57±9% and 56±10% respectively (Table 4.1). Figure 4.12B presents the correlation between COD and BOD_5 removed, approximately 38% of COD removed was BOD_5. Likewise, the BOD_5/COD ratios in the influent and effluent were the same, 40% and 40%, respectively, indicating no variation in water degradability features.

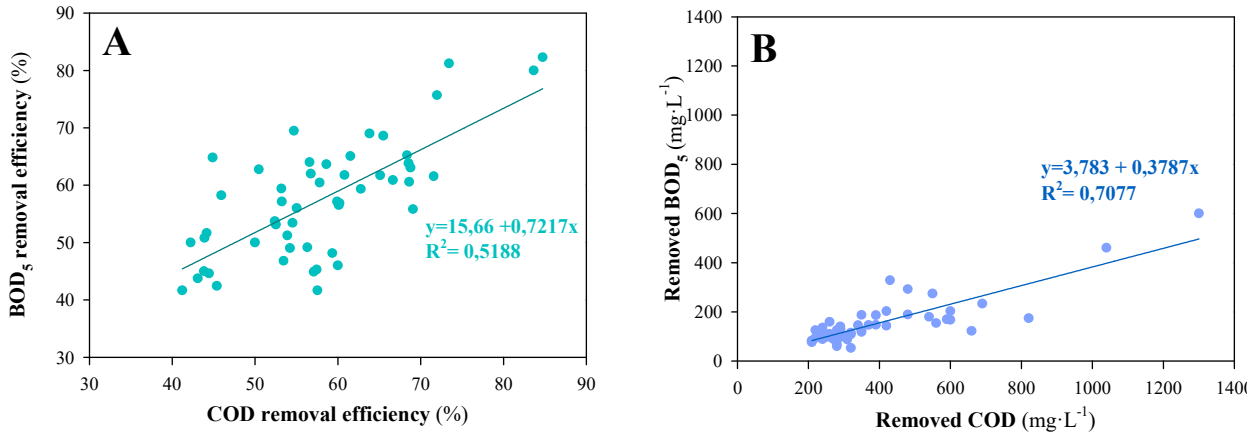

Figure 4.12: BOD_5 removal efficiency versus A) COD removal and B) removed COD

Overall, the HRAS influent and effluent concentrations of COD, COD fractions and BOD_5 for each period are presented in Figure 4.13. As it has been noted before (section 4.3) the BOD_5 removal efficiencies also include BOD_5-carbon redirection process (adsorption, storage and oxidation) and also

the BOD_5-carbon harvesting process (settling and waste). Figure 4.12 and 4.13 also indicate the high sCOD, pCOD, COD and BOD_5 removal and the buffering capacity of HRAS process.

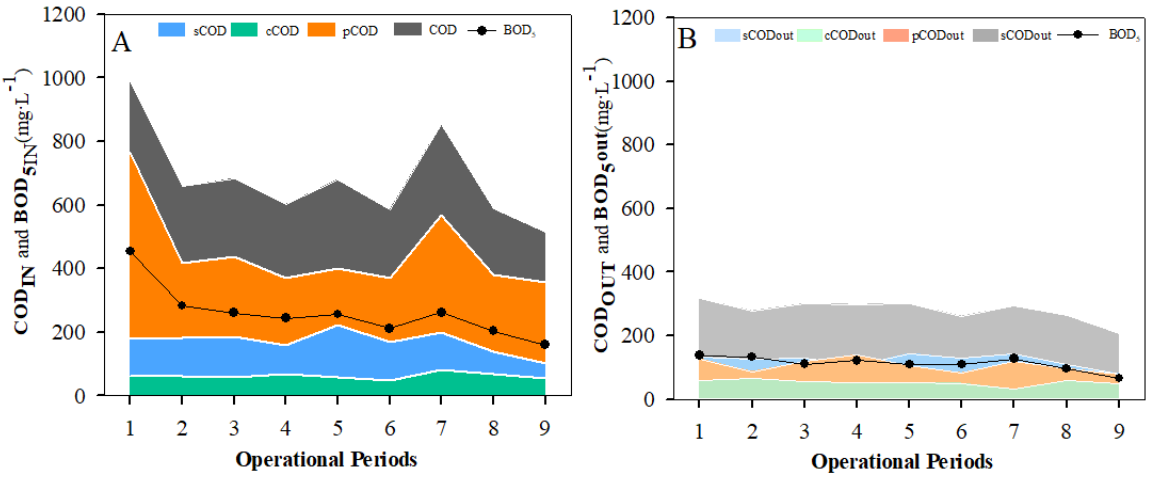

Figure 4.13: A) Raw water composition and B) Treated water composition in terms of COD, BOD5 and COD fractions over the nine experimental periods

4.3.5 Long-term stability evaluation

After analysing the average removal efficiencies of each period for the different COD fractions, Figure 4.14 and 4.15 show the daily evolution of COD_{IN} and COD_{OUT} throughout all the experimental time for each COD fraction and BOD5. It can be observed that the HRAS process did not act as a filter for $sCOD_{IN}$ peak loads (Figure 4.14A), as it did for pCOD (Figure 4.14B), since the high dispersion in $sCOD_{IN}$, 171±61 $mg \cdot L^{-1}$, was matched by a high dispersion in $sCOD_{OUT}$, 121±44 $mg \cdot L^{-1}$. On the contrary of pCOD (Figure 4.15B), there was not a clear correlation between the inlet concentration of sCOD and the removal efficiency (Figure 4.15A). The maximum sCOD removed was 140 mg/L, regardless of the influent concentration, since similar absolute removal value was achieved at inlet concentration of 230, 290 and 380 $mg \cdot L^{-1}$. Thus, the system presented a maximum sCOD removal capacity, as usual of biological processes.

However, the HRAS process acted as a filter for pCODin peak loads (Figure 4.14B), buffering the loads to the subsequent activated sludge process. Even with the high dispersion in pCODin (456±200 $mg \cdot L^{-1}$) the pCODout values presented a low dispersion (106±34 $mg \cdot L^{-1}$), and the maximum and average values of pCOD removal were 1,280 and 349±198 $mg \cdot L^{-1}$, respectively. The almost totally parallel relationship between the pCOD removal regression line and the line representing the total pCODin removal, dotted line (Figure 4.15B) indicates the presence of a non-settling pCOD that could not be removed and was independent of the pCODin concentration.

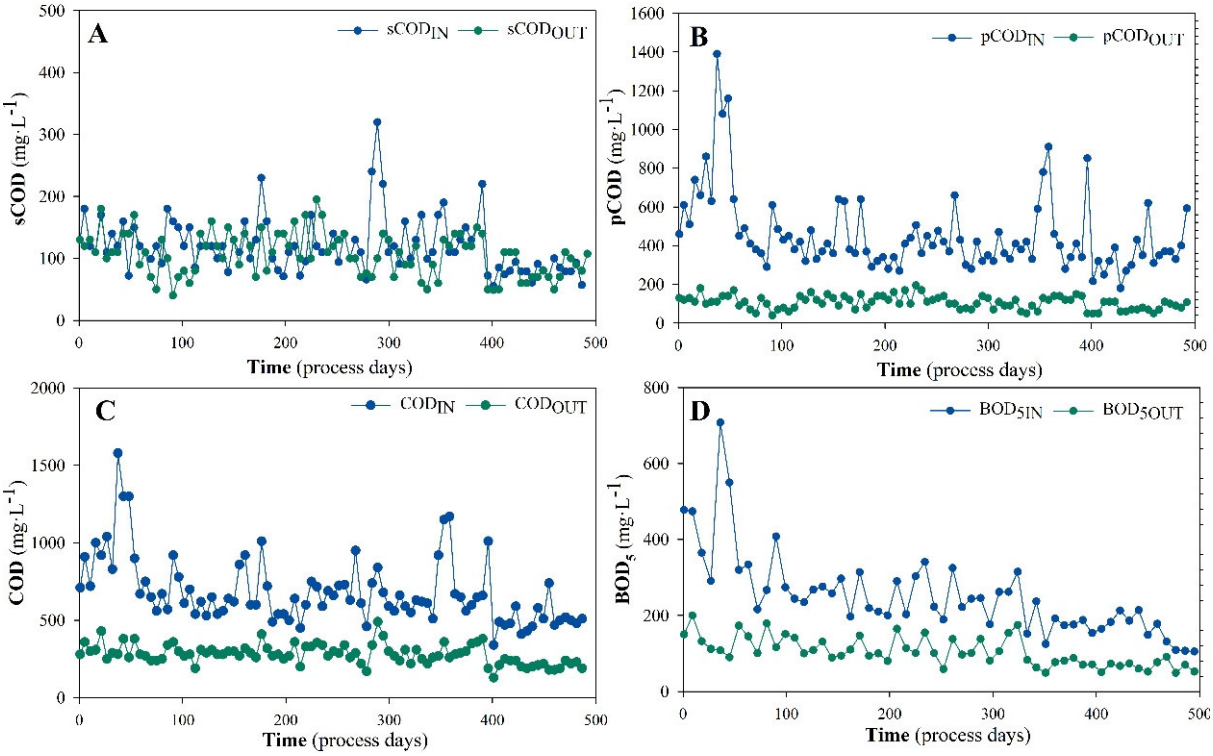

Figure 4.14. Daily variations of the influent and effluent concentrations of A) sCOD; B) pCOD; C) COD and D) BOD_5.

Accordingly, the HRAS process acted as a filter for CODin peak loads (Figure 4.14C), buffering the inlet loads to the subsequent activated sludge process. There was a high dispersion in CODin (683±214 $mg \cdot L^{-1}$) that was buffered in the process with a low dispersion in CODout (280±63 $mg \cdot L^{-1}$), thus, buffering the organic loads to the subsequent activated sludge process. The maximum and average COD removal values were 1300 and 403±195 $mg \cdot L^{-1}$, respectively. The almost total parallel relationship between the regression line of COD removal and the line representing total CODin removal, dotted line (Figure 4.15C) indicates that a constant amount of COD could not be removed and independently from the CODin concentration. This non-removable COD included non-settling pCOD, sCOD (poly) and non-flocculated cCOD under the pilot plant's operating conditions. Hence, the overall COD removal efficiency was lower due to the lower sCOD removal efficiency in comparison with the pCOD removal efficiency. Improvement on COD removal could only be achieved by either increasing sCOD oxidation, with the consequent energy consumption, or by improving the pCOD removal associated with improved settling.

Regarding the BOD_5 loading, the HRAS process acts as a filter for BOD_5 in peak loads (Figure 4.14D) and it buffers the organic loads to the subsequent activated sludge process. The high dispersion in the influent BOD_5 (253 ± 110 $mg \cdot L^{-1}$) is matched by a low dispersion in BOD_5out (112 ± 59 $mg \cdot L^{-1}$). The maximum and average values of BOD_5 removal were 600 and 154 ± 95 $mg \cdot L^{-1}$, respectively.

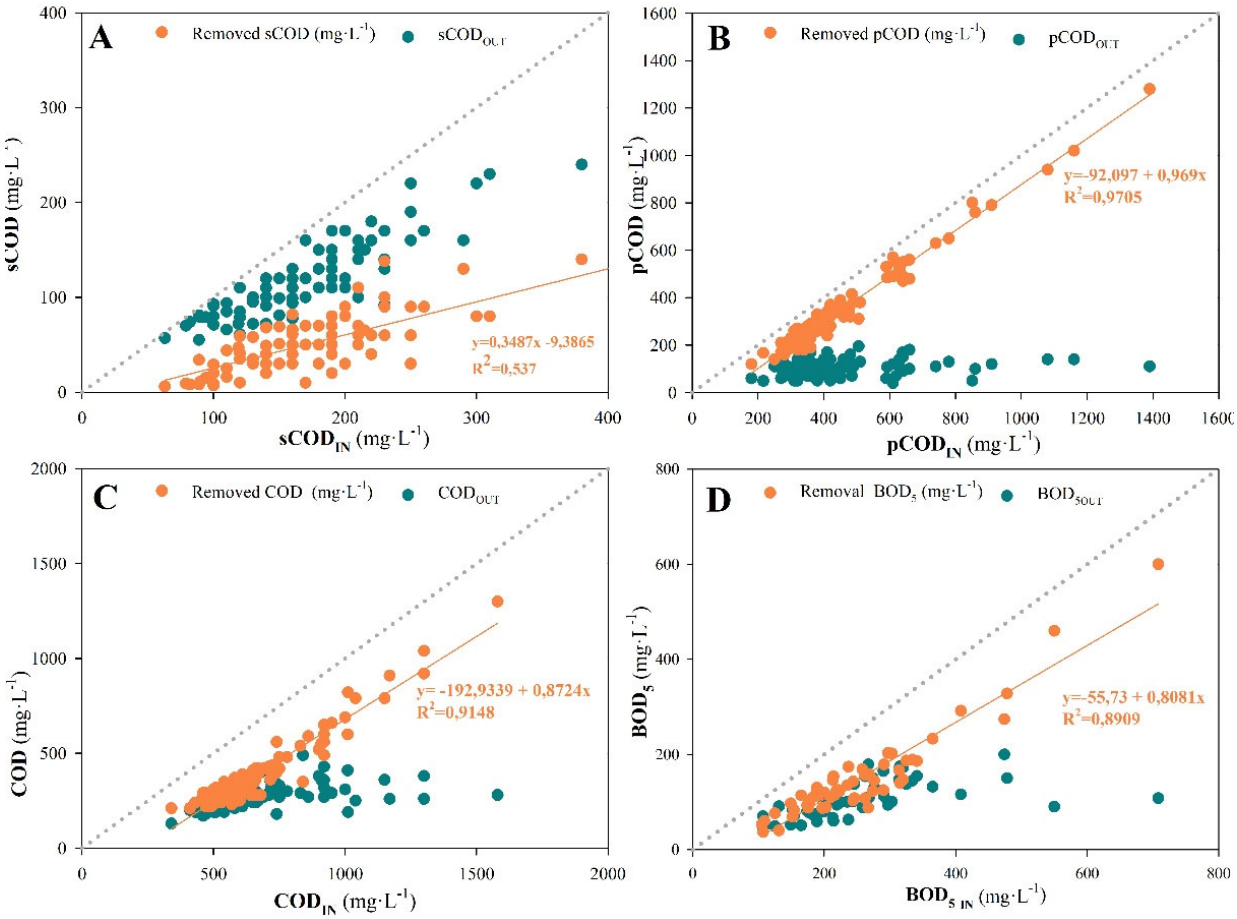

Figure 4.15. Relation between the removed, influent and effluent concentrations of A) sCOD, B) pCOD, C) COD and D) BOD_5.

The almost total parallel relationship between the regression line of BOD_5 removal and the line representing total BOD_5 removal, dotted line (Figure 4.15D) indicates the presence of a BOD_5 that could not be removed, which includes the non-settling BOD_5 and the nonbiodegradable BOD_5 at short HRT. Increased BOD_5 removal could be by achieved by increasing biodegradation, with the consequent energy consumption, or by improving the removal of particulate BOD_5, which is associated with improved settling, as indicated for COD.

Overall, the HRAS process made it possible not only to send larger amount of organic matter to anaerobic digestion (58-60% of the CODin and 49-67% of the BOD5in) compared to the 35-40% achieved with primary clarifier (Crites and Tchobanoglous, 1998) but also to laminate the influent load to the activated sludge unit, assuring its stability and reducing the size of the equipment to be installed in the unit to handle oxygen demand peaks.

4.3.6 Organic Removal Rate versus Organic Loading Rate

The present research analyses the correlation between Organic Loading Rate (OLR) and Organic Removal Rate (ORR) for COD, BOD_5 and sCOD, according to equations 3.16 - 3.21. Figure 4.16 shows

the good correlation between the OLR and ORR for COD, sCOD and BOD_5, referred to biomass in the oxic reactor R2. Additionally, it provides valuable insights into the MLSS activity, serving as a useful parameter for HRAS design, similar to its role in the design process of CAS systems. Finally, Table 4.2 presents the average, SD, and the range of each variable studied.

Table 4.2 OLR and ORR for COD, sCOD and BOD_5

	OLR_{COD}	ORR_{COD}	OLR_{sCOD}	ORR_{sCOD}	OLR_{BDO5}	ORR_{BDO5}
	[$Kg \cdot Kg_{MLSS}^{-1} \cdot d^{-1}$]		[$Kg \cdot Kg_{MLSS}^{-1} \cdot d^{-1}$]		[$Kg \cdot Kg_{MLSS}^{-1} \cdot d^{-1}$]	
Average ±SD	10.5 ± 3.5	6.1 ± 2.7	2.9 ± 1.2	1.0 ± 0.6	4.1 ± 1.5	2.2 ± 1.1
Range	5.7 - 22.3	3.2 - 15.7	0.9 - 7.3	0.2 - 3.2	1.9 - 8.4	0.7 - 6.7

The pilot plant operated at an COD OLR of 10.5 ± 3.5 $Kg_{COD} \cdot Kg_{MLSS}^{-1} \cdot d^{-1}$ (Table 4.2), which exceeds the reported range for HRAS process of 6.4 – 8.3 $Kg_{sCOD} \cdot Kg_{MLSS}^{-1} \cdot d^{-1}$ indicated by de Graaff et al (2016). Despite this higher COD OLR, the pilot plant achieved a satisfactory COD removal rate of 58%. Similarly, the BOD_5 in the pilot plant was 4.1 ± 1.5 $Kg_{BOD5} \cdot Kg_{MLSS}^{-1} \cdot d^{-1}$, surpassing the reported range for the CAS process (0.2 - 0.6 $Kg_{BOD5} \cdot Kg_{MLSS}^{-1} \cdot d^{-1}$ Crites and Tchobanoglous, 1998), with a corresponding BOD_5 removal rate of 54%. Finally, the pilot plant operated at 2.9 ± 1.2 $Kg_{sCOD} \cdot Kg_{MLSS}^{-1} \cdot d^{-1}$, resulting in an average sCOD removal rate of 34%.

Figure 4.16 shows that an increase in OLR, involves an increase in ORR, which consequently produces an increase of sludge generation. The process is self-controlled by increasing the waste flow rate in order to keep the reactor biomass concentration in the set point value of 2000 $mg_{MLSS} \cdot L^{-1}$.

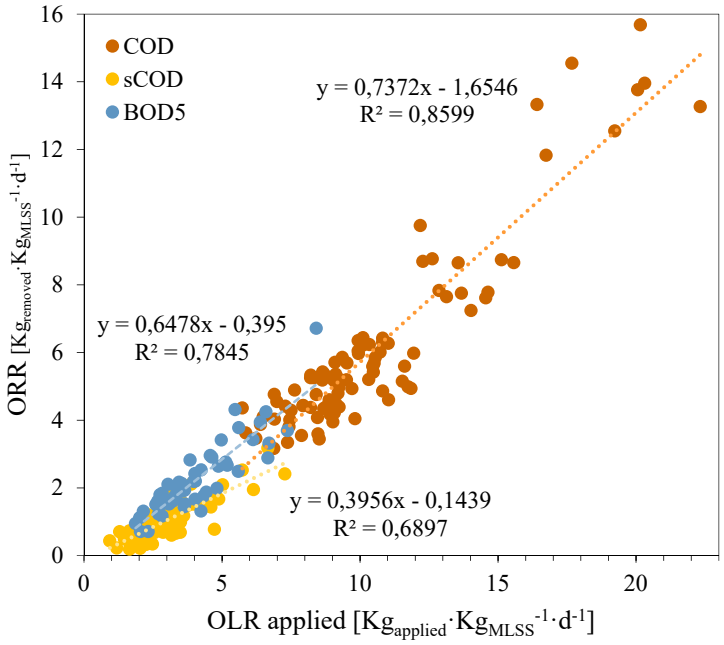

Figure 4.16 Relation between OLR and ORR for COD, sCOD and BOD_5.

4.3.7 Process simulation

Process simulations were carried out by means of Sumo-19 software, according to the model configuration detailed in the Figure 3.2 with the goal of testing its capability to predict the removal efficiency of the different COD fractions. The main parameters used in the model for the growth of ordinary heterotrophic organisms OHO) and A-stage fast-growing microorganisms AHO) are shown in the Table 3.6. The COD fractions used were determined according to the average values of the pilot plant for each period. The sCOD split and OHO and AHO fraction in the influent total COD were determined according to the default values of the model. No biological activity has considered in the clarifier.

In comparison with full scale facilities, the pilot plant has two specific characteristics: low flocculation in the reactor due to wall effects, and low deflocculation in the recirculation line due to the use of helicoidal pumps at low speed, instead of centrifugal pumps at higher speed. Thus the most sensitive parameters to be adjusted were the flocculation reduction factor in the reactor $\eta_{FLOC,Process}$ – to a value of 0.4 Reactor R1) and 0.2 Reactor R2) – and the deflocculation factor in the recirculation line to a value of 10%. The first parameter combines all hydrodynamic effects affecting the shear force on the flocs reactor geometry, type of aerators and mixers) that act on the residual colloids, and the second parameter refers to the deflocculation factor in the recirculation line (Hauduc et al., 2019). A reactive three-compartment clarifier with a 0.9 flocculation factor in the feed well and sludge blanket was used for the settling model.

Figure 4.17 presents the efficiencies obtained in the pilot plant versus the predicted with the model. sCOD, cCOD and pCOD removal efficiencies were closely predicted by the model as a function of their corresponding inlet concentrations with additional indication of the temperature.

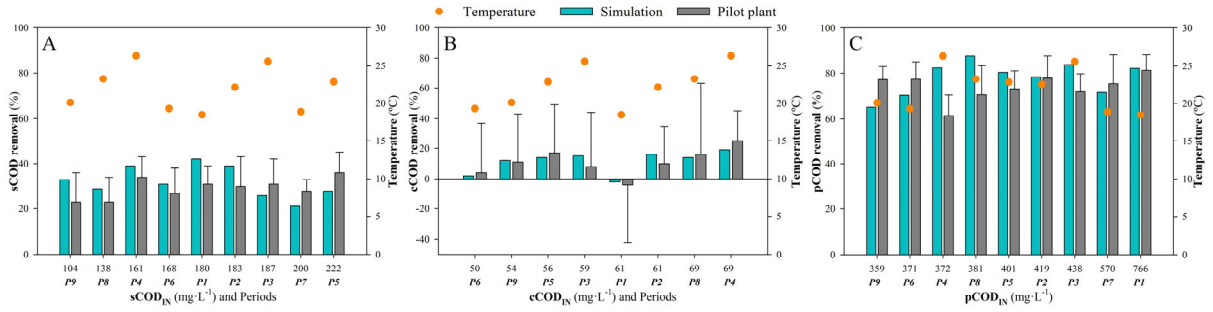

Figure 4.17. Removal efficiencies obtained by simulation and pilot plant: A) sCOD, B) cCOD and C) pCOD.

For $sCOD_{IN}$ values above 183 $mg \cdot L^{-1}$, the efficiency in the pilot plant was higher than that calculated in the model, and for values below 180 $mg \cdot L^{-1}$, the efficiency in the model was higher than that obtained in the pilot plant Figure 4.17A). A possible explanation for this is the fact that the saturation constant for the biodegradable organic substrate Ks used default constant in the model) was lower than the real

value. As shown in Figure 4.17B), the cCOD removal efficiencies were closely predicted by the model as function of the cCODin concentration. However, the large deviation in the experimental results of the cCOD data must be considered when analysing the model outcomes. Finally, for pCOD simulation, the model differs from the pilot plant results for temperatures above 23 °C Figure 4.17C), which is aligned with the reduction of pCOD removal efficiency observed in the pilot plant at highest temperatures Figure 4.4B).

In this study, the model was tested against HRAS-A stage pilot plant operation data and proven to match the COD fraction removal efficiency. Future research should supplement the current study with a thorough examination of nutrient removal efficiencies in both short- and long-term HRAS processes, as well as a COD balance and oxygen uptake rates.

4.4 Final remarks

Reducing SRT up to 0.2 days and HRT up to 0.6 hours, corresponding to one third of the usual values reported in HRAS operation, allows a high redirection and harvesting of organic matter 57±9%) for COD and 56±10%) for BOD_5, with a minimum 6.9% COD oxidation. The different COD fraction removal: 29±12%) sCOD, 12±35%) cCOD and 74±10%) pCOD, highlights the importance of settling efficiency and stability in the HRAS removal efficiencies.

Maintaining the biomass concentration in the reactor at 2000±200 $mg \cdot L^{-1}$ as process control strategy assured a very stable process even with the large variations in the influent. So, both in short- and long-term performance the best control parameter at very low SRT to ensure the process stability and minimize COD oxidation is not strictly the SRT but rather the MLSS concentration.

The biomass concentration was directly correlated with sCOD and pCOD removal, while reactor temperature hampered the pCOD removal but increased sCOD. The direct relation between influent COD concentration and COD removal makes it advisable to use the HRAS process as a replacement of the PC stage and not as a downstream treatment afterward.

Settling efficiency and stability showed a great importance in the HRAS performance. The low SVI_{30} values of 50-70 $ml \cdot g^{-1}$ shows the exceptional biomass settling properties, while the relatively high SS effluent concentration 50-120 $mg \cdot L^{-1}$ indicated a worse flocculation.

HRAS-AS process acts as a filter for the influent COD and pCOD peak loads and, albeit to a lesser extent, for BOD_5, buffering the influent load to the subsequent CAS process. The HRAS-AS process, on the other hand, does not act as a filter for sCOD peak loads, which is important regarding the subsequent denitrification process.

The HRAS, characterized by its high OLR ranging from 6 to 22 $Kg_{COD} \cdot Kg_{MLSS}^{-1} \cdot d^{-1}$, exhibits a ORR typically falling between 4 to 14 $Kg_{removed} \cdot Kg_{MLSS}^{-1} \cdot d^{-1}$. This OLR is notably higher, about 20 to 30 times, than that of the CAS process. Similarly, in terms of sCOD removal, HRAS with an OLR ranging

from 1 to 7 $Kg_{sCOD} \cdot Kg_{MLSS}^{-1} \cdot d^{-1}$ showcases an ORR of 0.5 to 3 $Kg_{removed} \cdot Kg_{MLSS}^{-1} \cdot d^{-1}$. Additionally, HRAS processes handling BOD_5 with an OLR between 2 to 8 $Kg_{BOD5} \cdot Kg_{MLSS}^{-1} \cdot d^{-1}$, again significantly higher than CAS, yield ORRs of 1 to 6 $Kg_{removed} \cdot Kg_{MLSS}^{-1} \cdot d^{-1}$.

The increase in OLR inherently leads to a rise in ORR, consequently resulting in higher sludge generation. However, HRAS exhibits a self-controlling mechanism by adjusting the waste flow rate to maintain the biomass concentration at the desired set point value of 2000 $mg_{MLSS} \cdot L^{-1}$. This self-regulation mechanism ensures the stability and efficiency of the HRAS process.

It's worth noting that the Sludge Exchange Rate SER) parameter may serve as a more representative indicator of HRAS process performance compared to the conventional SRT, reflecting the dynamic nature of organic matter removal and sludge generation in HRAS.

The simulation model adopted SUMO) resulted in a good fit for the sCOD. For pCOD, there was a good fit except for temperatures above 23 °C.

Chapter 5
RESULTS II

Nutrients removal by high-rate activated sludge and its effects on the mainstream wastewater treatment

Redrafted from:

Canals, J., Cabrera-Codony, A., Carbó, O., Baldi, M., Gutiérrez, B., Ordoñez, A., Martín, M. J., Poch, M., & Monclús, H. (2024). Nutrients removal by high-rate activated sludge and its effects on the mainstream wastewater treatment. Chemical Engineering Journal, 479. https://doi.org/10.1016/j.cej.2023.147871

5.1 Overview

The HRAS process entails significant removal of nutrients from wastewater despite its main objective being the harvesting of COD to achieve zero energy consumption. Thus, the HRAS involves the reduction of consumption of oxygen for COD oxidation and nitrification, COD for denitrification, and chemicals for phosphorus removal in the subsequent treatment steps of N/DN and phosphorus removal in the mainstream.

Until now, many HRAS pilot plant studies have been basically focused on describing the impact of SRT, HRT and DO on TKN, TP and COD removal. However, correlation between nitrogen and phosphorus fractions removal with COD fractions removal is poorly understood.

To guide this investigation, the central research question was to what extend the HRAS process removes nutrients, how does this relate to COD fractions removal and oxidation and to the settling working conditions. Subsequently, to explore what are the potential implications of the HRAS's effluent COD/TKN and sCOD/N-NH_4^+ ratios for the application of successive nitrogen removal technologies.

The primary objective was to evaluate nutrients the removal efficiency of the HRAS process, focusing on both nitrogen and phosphorus particulate and soluble fractions. Specifically, it will be necessary to i) evaluate TKN and TP fraction removal and their correlation with COD fraction removal and operating conditions, ii) evaluate the correlation between the COD oxidizion and N and P removal, iii) monitor TKN and TP fractions in long-term operation for ensuring HRAS process stability and iv) explore HRAS effluent's COD/TKN and sCOD/N-NH_4^+ ratios and dissecting their implications on the suitability of different nitrogen removal strategies.

The aim was to explore the dependence between nutrient removal and COD oxidation in a long-term analysis and discuss the most suitable nitrogen removal technology for the HRAS's effluent. By addressing these questions, the goal was to provide valuable insights into the effectiveness and application of HRAS in sustainable wastewater treatment.

5.2 Methodology

This study was conducted in a demo-scale pilot plant treating wastewater without PC with a substantial industrial component working at very low SRT (<0.5 d), HRT (< 1 h) and DO (<0.5 $mg \cdot L^{-1}$). TKN, N-NH_4^+, OrgN, TP, P-PO_4^{3-}, and OrgP were monitored over an extended 497-day operational period to evaluate the stability of the HRAS process and assess the removal efficiencies to examine their correlation with the COD fractions removal. Furthermore, the research delved into settler working conditions, including overflow rate (OFR), sludge volume index (SVI), and clarifier hydraulic retention time. Two alternative clarifiers were employed to manipulate OFR without altering the HRT in the reactor, allowing for an assessment of their impact on TKN and TP removal efficiency.

Two automatic samplers (Hach Lange) were used to collect and keep the integrated samples refrigerated at 5ºC for 24 hours, both from the influent and from the effluent. The analysis included TKN, $N\text{-}NH_4^+$, TP and $P\text{-}PO_4^{3-}$ according to standard methods ((APHA), 2005). The removal efficiency of each nutrient was calculated by mass balance. COD fractions (soluble, colloidal, and particulate), BOD_5, TSS, VSS were also analyzed from the samples every 4 days, and data with extreme incidents in the influent were disregarded. In total, there were 91 days of representative results of the process.

5.3 Results and Discussion

5.3.1 Performance evaluation

The HRAS pilot plant was operated for 497 days over nine operational periods, treating pretreated (grid and grease removed) raw wastewater. This was a significant step forward from previous studies that mostly used PCs' effluents. The nutrients' influent concentration and removal efficiency were monitored to evaluate the HRAS process's removal efficiency (Figure 5.1). As further discussed, it should be noted that the nutrient removal efficiencies indicate not only the effectiveness of the removal processes (biological assimilation and adsorption) but also the efficiency of the settling tank harvesting. No nitrification has been reported for HRAS at so low SRT.

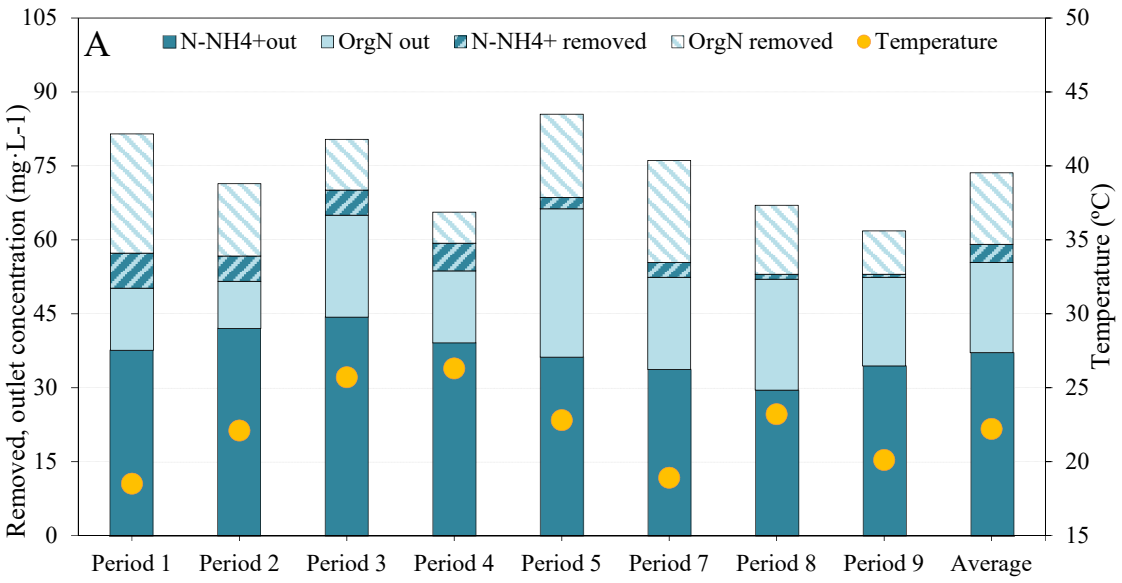

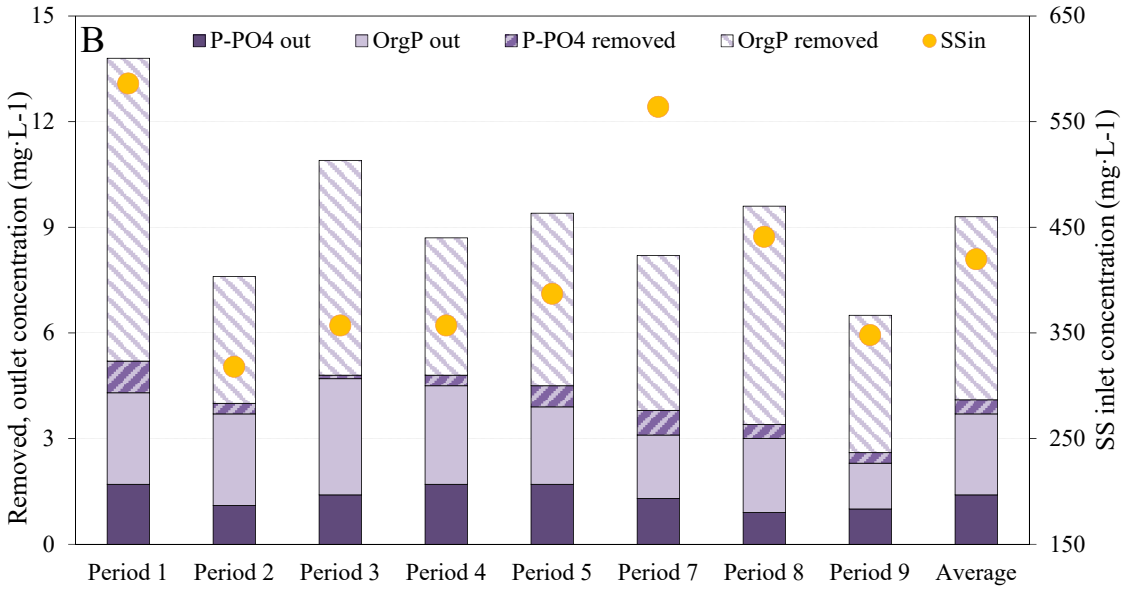

Figure 5.1. Nutrients fractions split between removal and effluent concentration of A) N-NH_4^+ and OrgN, and B) P-PO_4^{3-} and OrgP for the different experimental periods and average values. Temperature and SS influent concentration are plotted in dots.

5.3.2 Nitrogen removal: TKN, N-NH_4^+ and OrgN

For the nine experimental periods, the TKN removal efficiency had an average value of 23 ± 10% (Table 5.1), ranging between 17 and 35%, similar to previous reports of 14% and 23%, respectively (Miller et al., 2015; Rahman et al., 2019) and significantly higher than in PCs (10-16%). The primary distinction between PCs and HRAS lies in their operational mechanisms. PCs primarily removes settled particulate COD, nitrogen, and phosphorus through a discrete flocculant settling process (Torfs et al., 2016).

In contrast, HRAS operates as a biological process with a low SRT facilitating the adsorption of the soluble fraction in the biomass, the oxidation of the soluble fraction, the trapping of colloidal and particulate fractions in the biomass and hindered settling of biological flocs at a constant influent MLSS concentration of 2000 mg·L^{-1}, which enhances the flocculation (Torfs et al., 2016). The elevated sludge concentration in HRAS fosters more collisions between particulate materials, yielding better settling with larger flocs. Despite the low SRT of HRAS, it allows effective adsorption and trapping of colloidal and particulate fractions from the influent (Yetis and Tarlan, 2002).

The TKN_{in} split fractions were on average 54% for N-NH_4^+ and 46% for OrgN (Figure 5.2A, 2B). The OrgN removal efficiency achieved was 43 ± 21%, ranging between 32 and 65% depending on the experimental period (Table 5.1). This OrgN removal means that up to 85% of the TKN removal comes from OrgN, highlighting the importance of settling efficiency in nitrogen removal. However, the daily analysis shown in Figure 5.2B showed a high variability in $OrgN_{in}$ 34 ±13 mg·L^{-1} in the outlet concentration $OrgN_{out}$, 18±11 mg·L^{-1}, with maximum and average OrgN removals of 46.9 and 16 mg·L^{-1}, revealing that HRAS did not filter OrgN peak values. At this short SRT, the HRAS process had a low

impact on $N\text{-}NH_4^+$ removal, with an average efficiency achieved of 7.3 ± 7.5%, ranging between 2-14% depending on the experimental period (Table 5.1). These results align with literature findings: 11 ± 5% at 0.22 days SRT (Miller et al., 2015), 11% at 0.16 days SRT (Rahman et al., 2019), or 8% at 0.5 days SRT (Ge et al., 2015).

Table 5.1. TKN, $N\text{-}NH_4^+$, OrgN, influent concentration and removal in each experimental period

Period	TKN_{in} [$mg \cdot L^{-1}$]	TKN_{rem} [%]	$N\text{-}NH_4^+{}_{in}$ [$mg \cdot L^{-1}$]	$N\text{-}NH_4^+{}_{in}$ inlet [%]	$N\text{-}NH_4^+{}_{rem}$ [%]	$OrgN_{in}$ [$mg \cdot L^{-1}$]	$OrgN_{in}$ inlet [%]	$OrgN_{rem}$ [%]
1	81.5±19.3	35±9	44.7±10.8	55	14±12	36.8±14	45	65±11
2	64.5±4.2	19±8	47.1±11.4	73	10±6	17.4±13	37	42±33
3	80.0±11.3	17±7	49.4±3.3	61	8±8	31.0±6.9	39	33±21
4	65.6±23.5	19±10	44.7±14.6	68	12±11	20.9±12.5	32	41±34
5	85.5±14.4	25±9	38.5±11.1	45	5±4	47.0±15.9	55	38±22
7	76.0±13.6	33±11	36.7±6.5	48	8±5	39.3±16.8	52	48±19
8	67.0±8.8	18±7	30.5±6.4	46	3±1	36.5±10.2	54	38±18
9	61.8±43.9	19±7	35.0±3.7	57	2±2	26.8±4.5	43	32±9
Average	72.7±14.9	23±10	40.8±10.3	57	7.3±7.5	34.4±15	45	43±21

The considerable variability in $N\text{-}NH_4^+{}_{in}$ concentration, averaging 39.1 ± 8.8 $mg \cdot L^{-1}$, corresponded to a similarly variable $N\text{-}NH_4^+{}_{out}$ concentration of 37.8 ±7.1 $mg \cdot L^{-1}$, with a maximum $N\text{-}NH_4^+$ removal values achieved of 19.8 $mg \cdot L^{-1}$. Figure 5.2A shows negative removal values for $N\text{-}NH_4^+{}_{in}$ up to 35 $mg \cdot L^{-1}$, probably due to $N\text{-}NH_4^+$ formation by sludge fermentation in the bottom of the clarifier. The $N\text{-}NH_4^+$ formation was higher than that removed by biomass growth, and the same phenomenon applied to $P\text{-}PO_4^{3-}$ (Figure 5.2C). Above this value, the removal was positive, with an increasing percentage of removal. The pilot plant presented some sludge accumulation in the bottom of the clarifier, which is of utmost importance to consider in the recirculation pumping and clarifier design to avoid a high biomass inventory in the bottom of the clarifier. Overall, the HRAS process did not buffer the influent TKN peak values: the high dispersion of TKN_{in} was matched by a high dispersion in TKN_{out} (Figure 5.3). TKN_{out} was proportional to TKN_{in}, so the TKN removed increased with increasing TKN_{in} concentration (Figure 5.4). Given that the TKN includes soluble and particulate forms of nitrogen with different elimination mechanisms, its removal depends not only on each removal fraction but also on the inlet concentration of each form.

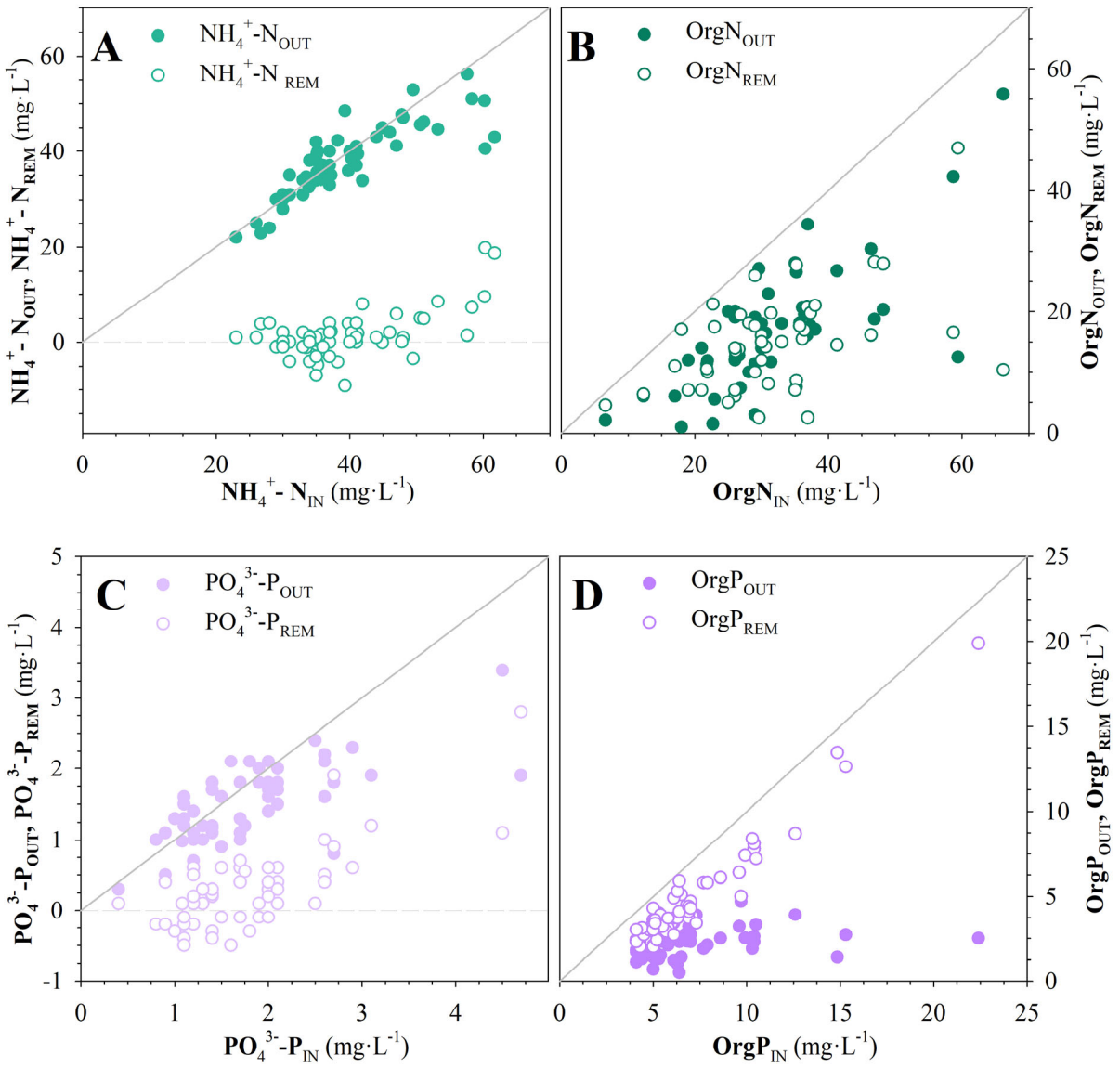

Figure 5.2 Nutrients removal and effluent concentration compared to the influent concentration for A) N-NH_4^+, B) OrgN, C) P-PO_4^{3-}, and D) OrgP during the whole HRAS pilot plant operation

5.3.3 Phosphorus removal: TP, P-PO_4^{3-} and OrgP

The TP removal efficiency achieved in the HRAS pilot plant had an average value of 56 ± 12%, ranging between 45 - 65 % depending on the experimental period as detailed in Table 5.2. These results are higher than the 30-40% usually achieved in PCs, similar to the 53% indicated by (Böhnke et al., 1997), and higher than the reported by Rahman et al. (2019) treating pre-treated wastewater and Ge et al. (2017) treating sewer biofilm effluent: 35% and 15% working at SRT of 0.16 days and 0.5 days respectively.

The achieved P-PO_4^{3-} removal efficiency had an average value of 23 ± 17%, with a range of 9-32% across different experimental periods. These results are higher than in PCs, and higher than the values reported in the literature (Ge et al., 2017; Miller et al., 2015; Rey-Martínez et al., 2021; Taboada-Santos et al., 2020). The OrgP removal efficiency had an average value of 66 ± 12%, ranging from 57% to

75% for each experimental period. Given that the influent TP composition in the pilot plant was 81% $OrgP_{in}$ and 19% $P\text{-}PO_4^{3-}{}_{in}$ (Table 5.2), the noteworthy OrgP removal efficiency highlights the importance of settling efficiency in phosphorus removal. As much as 95% of TP removal can be attributed to the removal of OrgP.

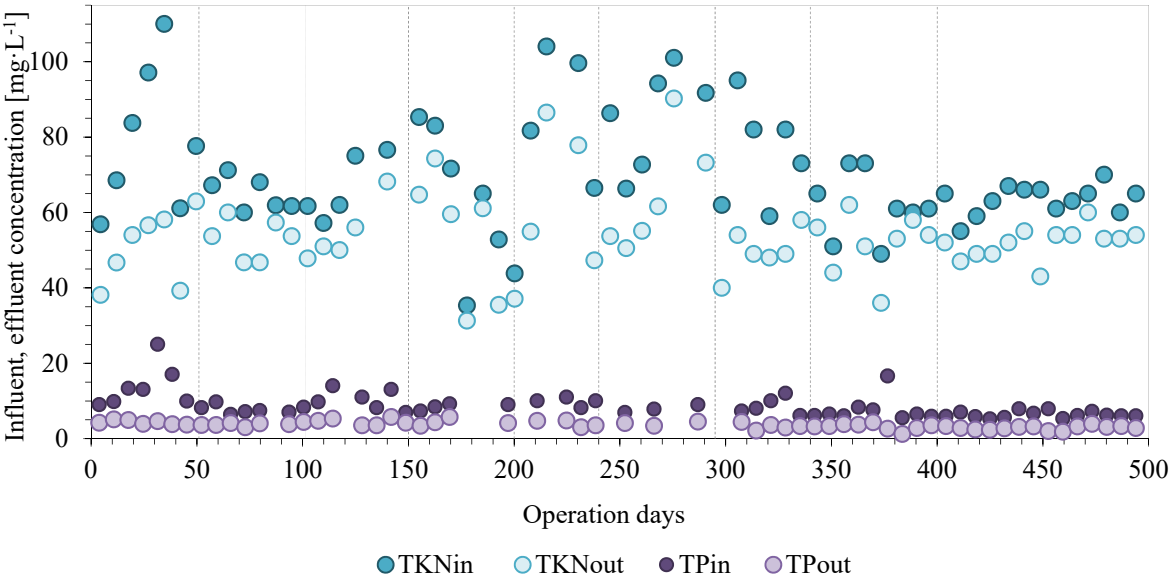

Figure 5.3 TKN and TP inlet and outlet concentration during the pilot plant operation

Table 5.2 TP, $P\text{-}PO_4^{3-}$, OrgP, influent concentration and removal in each experimental period

Period	TP_{in} [mg·L^{-1}]	TP_{rem} [%]	$P\text{-}PO_4^{3-}{}_{in}$ [mg·L^{-1}]	$P\text{-}PO_4^{3-}{}_{in}$ inlet [%]	$P\text{-}PO_4^{3-}{}_{rem}$ [%]	$OrgP_{in}$ [mg·L^{-1}]	$OrgP_{in}$ inlet [%]	$OrgP_{rem}$ [%]
1	13.8±5.6	65±12	2.6±1.1	19	31±17	11.2±5.9	81	71±15
2	7.7±1.2	51±10	1.5±0.3	19	22±19	6.2±0.9	81	57±15
3	11.0±2.6	54±10	1.6±0.6	15	9±7	9.4±2.2	85	64±9
4	8.7±0.9	49±8	2.0±0.5	23	13±6	6.7±0.6	77	58±9
5	9.4±1.6	56±9	2.3±1.4	24	25±9	7.1±1.4	76	70±9
7	8.1±2.4	59±14	2.0±0.4	25	32±23	6.1±2.5	75	68±10
8	7.8±3.7	55±18	1.3±0.3	17	24±17	6.5±4.5	83	71±22
9	6.5±0.9	56±8	1.3±0.4	20	27±20	5.2±1.1	80	75±12
Average	9.1±3.5	56±12	1.8±0.8	20	23±17	7.3±3.5	80	66±12

The correlation between influent, effluent, and removed concentrations of $P\text{-}PO_4^{3-}$ and OrgP are shown in Figures 5.2 C and 5.2D. The HRAS process acted as a filter for TP_{in} peak values, as the high dispersion of the influent concentration (8.3 ± 2.7 mg·L^{-1}) was attenuated in the TP_{out} (3.5 ± 0.9 mg·L^{-1}), with maximum and average removals of 14 and 4.7 mg·L^{-1}. Regarding TP (Figure 5.5), the almost parallelism of the TP removal regression line and the line representing the complete TP removal, plotted as a dotted line, indicates the presence of a certain amount of TP that was not removed. This non-removable fraction is independent of the TP_{in} concentration. By increasing the TP_{in} concentration, there was an increase in the TP removal, but with great dispersion for low TP_{in} values, considering that TP includes soluble and particulate forms of phosphorus with different elimination mechanisms. Accordingly, the $OrgP_{in}$ range (6.94 ± 3.22 mg·L^{-1}) was also attenuated by the HRAS, achieving an average $OrgP_{out}$ of 2.20 ± 0.83 mg·L^{-1}, and maximum and average removal of 19.9 and 4.78 mg·L^{-1}.

Figure 5.2D shows the similar parallelism, indicating that only a small fraction of the $OrgP_{in}$ concentration cannot be removed. This non-removable OrgP included the non-settling particulate and colloidal TP at the pilot plant's operating conditions. Consequently, HRAS acts as a filter for OrgP.

Regarding the $P\text{-}PO_4^{3-}$ there was significant variability in both the influent and effluent concentrations, averaging 1.7 ± 0.8 $mg \cdot L^{-1}$ and 1.4 ± 0.5 $mg \cdot L^{-1}$ respectively. Figure 5.2C shows negative removal efficiencies calculated when $P\text{-}PO_4^{3-}{}_{in}$ was below 2 $mg \cdot L^{-1}$, possibly due to $P\text{-}PO_4^{3-}$ formation in the bottom of the clarifier by sludge fermentation. Therefore, $P\text{-}PO_4^{3-}{}_{out}$ was higher than the amount eliminated by biomass growth, as was observed for $N\text{-}NH_4^+$ (Figure 5.2A). When employing HRAS, the TKN and TP removal efficiencies exceed those achieved by conventional PCs, which removes 10-16% and 30-40% respectively (Metcalf and Eddy, 2003) . This achievement is discussed in section 3.4 to evaluate the subsequent mainstream processes after HRAS.

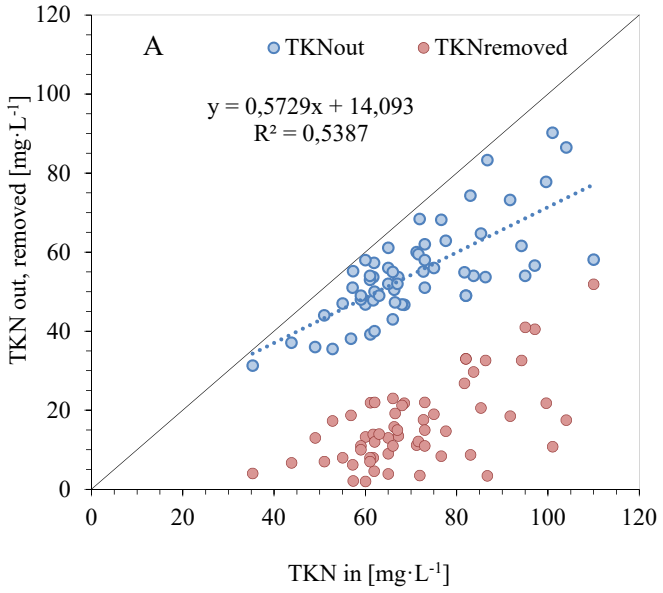

Figure 5.4 TKN removal and outlet concentration compared to the influent concentration during the whole HRAS pilot plant operation.

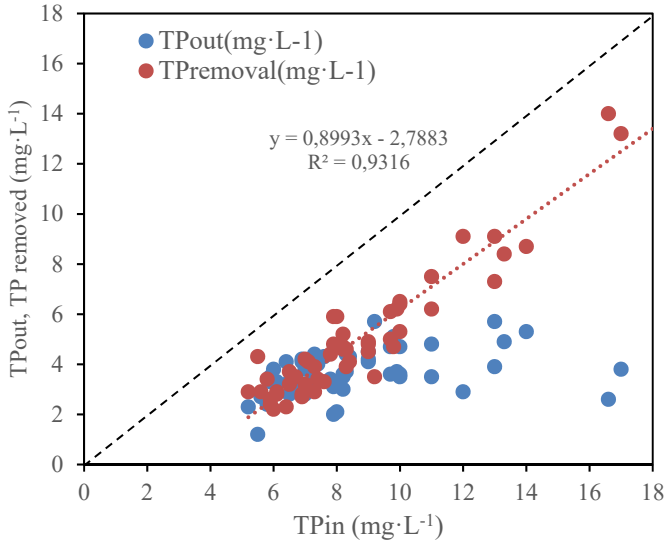

Figure 5.5 TP removal and outlet concentration compared to the influent concentration during the whole HRAS pilot plant operation.

5.3.4 Operating Parameters and Nutrients Removal

The type of wastewater collection system, whether it is gravity or pumping, the length of the system, and the temperature all have a significant impact on the removal of soluble TKN and TP fractions (Puig et al., 2010). In high-flow sewer systems, biological processes are predominantly aerobic, while in low-flow systems, they are anaerobic. The temperature in low-flow systems promotes higher fermentation rates and consequently, higher removal of the soluble fractions. Since the influence of HRAS operating parameters cannot be isolated and correlated with nutrient removal efficiency, Figure 5.1 presents the results classified in operating periods to study the overall effect of temperature, suspended solids, and nutrient inlet concentration. At such low SRT (0.2±0.5d), the SRT does not a significantly influence the removal of nutrient fractions, a trend consistent with findings regarding COD fractions (Chapter 4).

The highest TKN and TP removal efficiencies were achieved in Periods 1 (TKN 35 ± 9%, TP 65 ± 12%) and Period 7 (33 ± 11%, 59 ± 14%), both of which were operated at similar temperature (ca. 18.7ºC, the lowest) and SS_{in} concentration (ca. 575 $mg \cdot L^{-1}$, the highest) (Tables 5.1, 5.2 and 5.3). However, the low temperature in Period 9 (20.1 ºC) did not improve the 19% performance of TKN removal compared to Period 4 (26.3 ºC), which had similar SS_{in} (ca. 352 $mg \cdot L^{-1}$) and similar TKN_{in} (ca. 64 $mg \cdot L^{-1}$). Therefore, temperature does not have a significant impact on improving the TKN removal efficiency compared to the SS_{in} and TKN_{in} concentrations.

Equal analysis was done for the rest of nutrients. The $N\text{-}NH_4^+$ removal increased with an increase in influent concentration. Periods 1 and 4 had the same $N\text{-}NH_4^+{}_{in}$ concentration of 41.7 $mg \cdot L^{-1}$ and a temperature difference from 18.5 to 26.3 ºC did not promote a rise of $N\text{-}NH_4^+$ removal efficiency. On the other hand, Periods 7 and 1, had the same temperature of 18.5 ºC and the same SS_{in} concentration of 570 $mg \cdot L^{-1}$, but the $N\text{-}NH_4^+{}_{in}$ concentration increased from 36.7 to 41.7 $mg \cdot L^{-1}$, and the removal efficiency from 5% to 12%. Thus, $N\text{-}NH_4^+{}_{in}$ concentration has a higher effect on $N\text{-}NH_4^+$ removal than temperature and SS_{in} concentration (Figure 5.1A).

Table 5.3. SS inlet concentration, removal efficiency, clarifier diameter, OFR and temperature of the reactor in each operation period.

Period	SS_{in} [$mg \cdot L^{-1}$]	Removed [%]	Clarifier Diameter [m]	OFR Q_{in} [$m \cdot h^{-1}$]	Temperature R2 [ºC]
1	586	81 ± 6	1.0	1.3	18.5
2	318	71 ± 10	1.0	1.6	22.1
3	357	68 ± 12	1.0	1.7	25.6
4	357	64 ± 18	1.0	1.6	26.3
5	387	77 ± 9	1.0	1.6	22.8
7	564	85 ± 7	1.4	0.8	18.9
8	411	81 ± 11	1.4	0.8	23.2
9	348	87 ± 5	1.4	0.8	20.1
Average	406.7	76 ± 12	-	-	21.87

The SS_{in} concentration affected de TP removal slightly, with 62% removed in Periods 1 and compared to 53% in the other periods (Figure 5.1B). Likewise, the TP removal was constant 56 ± 5%, apparently unaffected by temperature and SS_{in}. Period 1, with a high TP_{in} concentration of 13.9 $mg \cdot L^{-1}$, presented

the highest TP removal of 65% compared to the other Periods (54 ± 3%). As a result, TP_{in} has a greater effect on TP removal than temperature or SS_{in}. Finally, the removal efficiency of $P\text{-}PO_4^{3-}$ presented a high dispersion of 23 ± 8 % due to the outlet concentration being close to the detection limit. Ultimately, the HRAS process yields superior results for wastewater rich in particulate fractions of TKN, TP, and COD but may not be as effective for wastewater with high proportions of soluble fractions.

Two different clarifiers were used during the different operational periods to evaluate the effectiveness of OFR on the nutrient's removal. In Chapter 4 we analysed the effect of OFR on the COD fractions removal, concluding that it did not affect pCOD removal due to the good settling properties reflected in the low SVI_{30} values. The SVI_{30} observed during the nine operational periods in the HRAS pilot plant ranged from 49 to 67 $mL \cdot g^{-1}$. These values are notably lower than the range of 110-180 $mL \cdot g^{-1}$ typically found in CAS processes (Seeley, 1992), and align closely with values reported in other HRAS studies, such as 40-90 $mL \cdot g^{-1}$ (Böhnke et al., 1997), 85 ± 26 $mL \cdot g^{-1}$ (Miller et al., 2015), and 88 ± 18 $mL \cdot g^{-1}$ (Rahman et al., 2019). However, the variation of the OFR did affect the SS_{OUT} concentration, although its impact was also linked to the variation in solids loading (SL). Here, the OFR clarifier did not affect the TKN or TP removal efficiencies: Periods 7, 8 and 9 with an OFR of 0.8 $m \cdot h^{-1}$ significantly lower than the other periods, did not lead to a consistent improvement in TKN and TP removal efficiencies, as it did for SS removal and SS effluent concentration (Table 5.3, and Figure 5.6).

Thus, the minimal impact of temperature and clarifier OFR on nutrient removal in HRAS can be attributed to effective biomass settling, reflected in low SVI30 values. HRAS's reliance on mechanisms like adsorption and entrapment, less sensitive to temperature, and its short SRT contribute to its resilience to temperature variations and OFR changes, showcasing its stability.

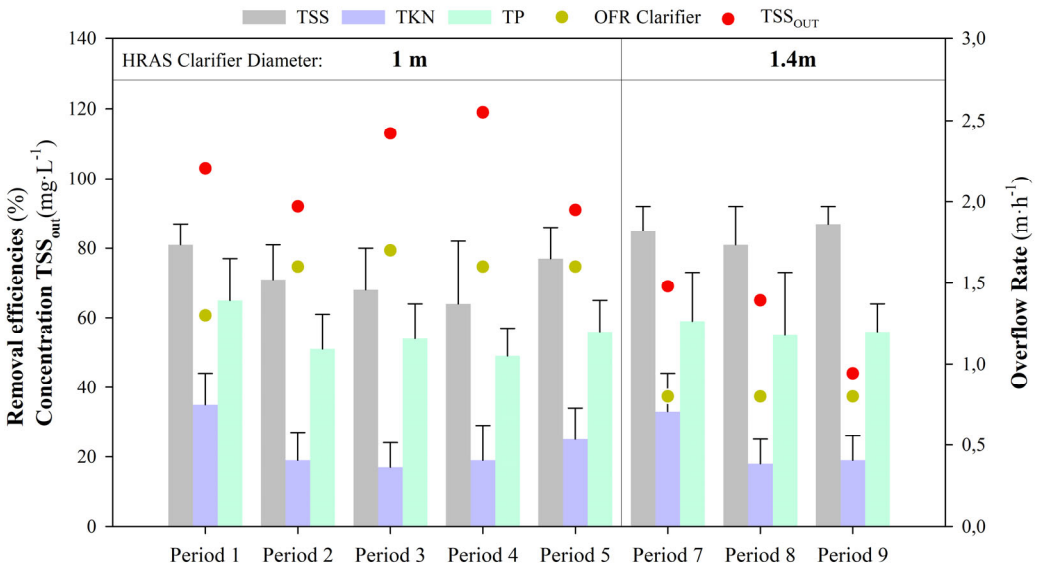

Figure 5.6 TP, TKN and TSS removal efficiencies with OFR and TSS_{out} of each operation period.

5.3.5 Organic Matter and Nutrients Removal

One of the objectives of this study was to establish criteria for maximizing TKN and TP removal while minimizing COD oxidation to send it to anaerobic digestion. Table 4.1. gathers the sCOD, cCOD, pCOD and COD concentrations, both the influent concentration and the removal efficiency average (Chapter 4). Figure 5.7 illustrates the relationship between the COD removal and the TKN and TP removal efficiency. The removal of nutrients and COD associated with particulate material was investigated, and correlations were found between their removal behaviour, as shown in Figure 5.8. HRAS at low SRT confirms the non-dependence between oxidized COD and wasted TKN and TP (Table 5.1, 5.2) as it does for wasted COD (Chapter 4). Thus, the nitrogen and phosphorus removal processes remained low dependent of COD oxidized.

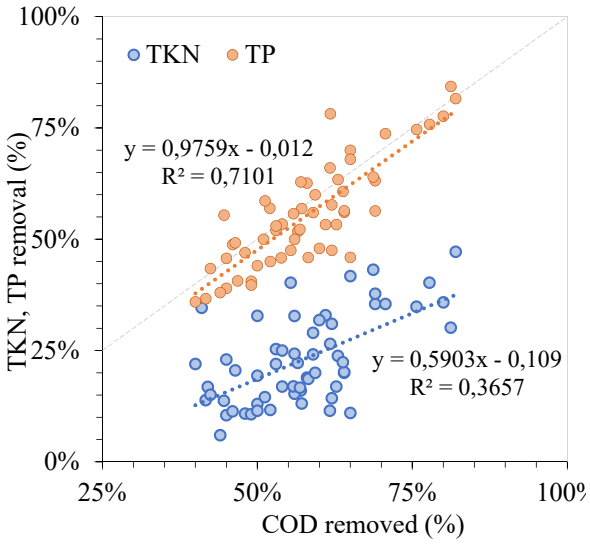

Figure 5.7 TKN and TP removal efficiencies compared to COD removal efficiency during the 497 days HRAS pilot plant operation.

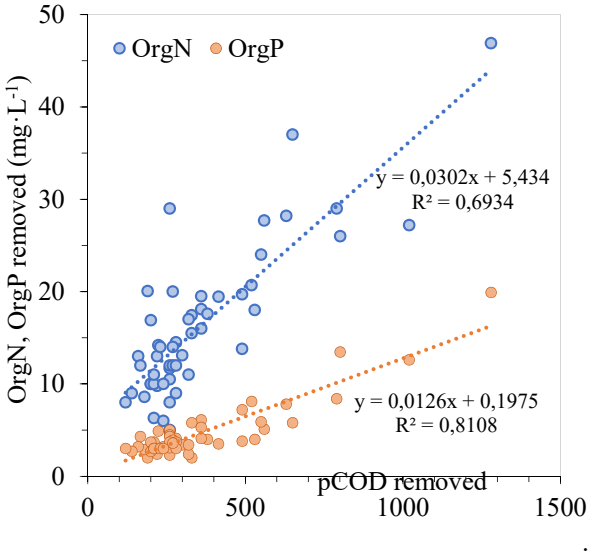

Figure 5.8 Relation between the particulate COD (pCOD) removed and the organic nutrients (OrgN. OrgP) removed during the 497 days HRAS pilot plant operation.

The removal of N-NH_4^+ and P-PO_4^{3-} mainly occurs through assimilation (Rahman et al., 2019), while sCOD removal can occur through bioaccumulation trough intercellular storage, microbial growth and carbon oxidation (Miller et al., 2015). However, this study could not establish any relationship between sCOD, N-NH_4^+, and P-PO_4^{3-} removal. Regarding soluble nitrogen and sCOD removal, the average results over the nine operational periods indicated that 50 mg·L^{-1} of sCOD and 3 mg·L^{-1} of N-NH_4^+ were removed, resulting in a sCOD/N-NH_4^+ mass ratio of 16.6 g·g^{-1}. This COD/N mass ratio is higher than the 11.5 g·g^{-1} estimated from biomass formula $C_5H_7O_2N$ (Henze et al., 2015), suggesting a possible intracellular storage of sCOD. The HRAS process shows promise for sCOD removal through aerobic storage preserving VFAs as polymers (Nogaj et al., 2015). While this mechanism depends on electron acceptors, exceptions like PAOs and GAOs exist. PHB formation aids sCOD storage during the high-

rate biodegradable COD phase, although it contributes only partially to the total removal and oxygen uptake ratio. Intracellular storage is more common in activated sludge systems with feast/famine conditions. The HRAS, like CAS, operates under non-steady dynamics, prompting a varied microbial response that extends beyond biomass growth, involving sorption, accumulation, and storage mechanisms (Carucci et al., 2001; Nogaj et al., 2015). Alternatively, the biomass may have a different nitrogen content under the high load working conditions (Takács and Vanrolleghem, 2006).

To characterize the HRAS waste, we compared the OrgN/VSS, OrgP/VSS and pCOD/VSS ratios in the influent to the effluent lines (Table 5.4). The average ratios increased from 0.11 $g_{orgN} \cdot g_{VSS}^{-1}$ (influent) to 0.26 $g_{OrgN} \cdot g_{VSS}^{-1}$ (effluent) and the 0.02 $g_{orgP} \cdot g_{VSS}^{-1}$ (influent) to 0.03 $g_{OrgP} \cdot g_{VSS}^{-1}$ (effluent) due to the derivation of settling material with low N and P content. Similar increments were also observed in PCs (Puig et al, 2010, Takács and Vanrolleghem, 2006). Additionally, the average pCOD/TSS rose from 1.15 $g_{pCOD} \cdot g_{TSS}^{-1}$ (influent) to 1.46 $g_{pCOD} \cdot g_{TSS}^{-1}$ (effluent) and the average pCOD/VSS ratio raised from 1.47 $g_{pCOD} \cdot g_{VSS}^{-1}$ (influent) to 1.62 $g_{pCOD} \cdot g_{VSS}^{-1}$ (effluent) due to the derivation of settling inorganic TSS and organic pCOD (particulated carbohydrates). Removing the inorganic TSS results in an increase in the active fraction of the MLSS in the subsequent biological N/DN process. Similarly, diverting organic pCOD with a low COD/VSS ratio to anaerobic digestion instead of to the aerobic process enhances the methane production and reduces the oxygen demand in the second stage treatment. Figure 5.9 depicts the strong correlation between COD and TSS, as well as between COD and VSS, in the waste line.

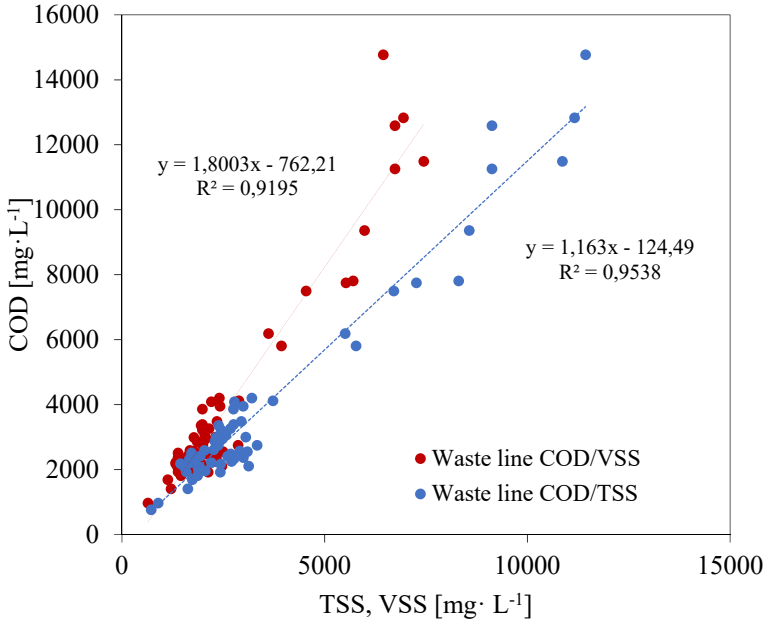

Figure 5.9 COD of biomass in the waste line COD/TSS and COD/VSS

The HRAS process not only removes COD but also modifies the distributions of the COD fractions from the influent to the effluent. In municipal wastewater, pCOD represents a significant portion of the total wastewater COD, and part of it could be converted to sCOD during biological processing. This conversion, as suggested by Regmi et al (2015) is more suitable for nitrification processes. In our study,

we observed an increase in the cCOD fraction from 9% to 19%, while the sCOD fraction increased from 25% to 43%.

Figure 5.10 illustrates the daily pilot plant variations of COD/TKN_{out}, COD_{out} and TKN_{out}. Since TKN_{out} was almost constant compared to COD_{out}, the oxidation of the sCOD fraction, despite the increase in energy consumption, is the only suitable strategy to control the ratio COD/TKN_{out}. One of the limitations of HRAS is its ability to meet the stringent COD/N ratio for subsequent N/DN processes and to avoid fluctuations in the COD/TKN_{out} that affect the stability and performance of the nitrogen removal process. The COD/TKN_{out} ratio (5.3 ± 0.8 $g_{COD} \cdot g_{TKN}^{-1}$) is not only controlled by COD and TKN removal but also by the COD/ TKN_{in} ratio (9.8 ± 1.4 $g_{COD} \cdot g_{TKN}^{-1}$). Similar values were reported by Miller et al (2015) and Nogaj et al (2015), both studies working at the SRT of 0.3 days.

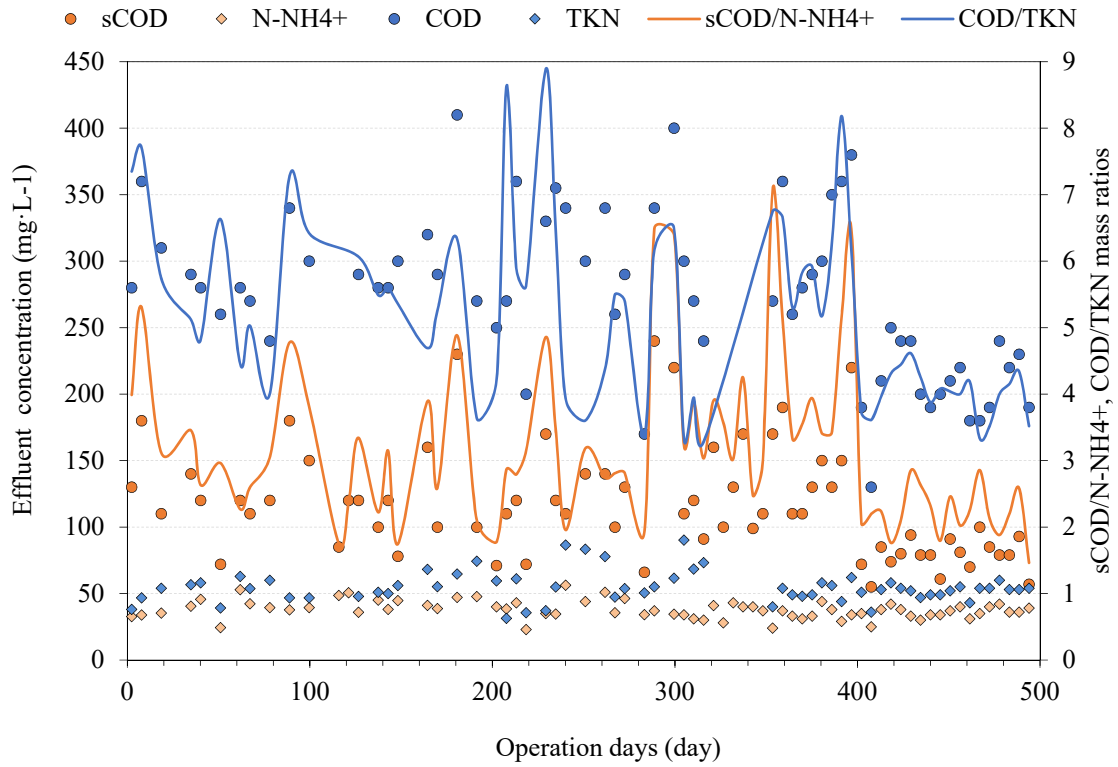

Figure 5.10 Daily evolution of the COD, sCOD, TKN and N-NH_4^+ effluent concentrations, and the corresponding COD/TKN and sCOD/ N-NH_4^+ mass ratios.

However, the COD/N ratio might not be the most suitable metric for assessing N/DN technologies. The soluble ratio sCOD/N-NH_4^+ offers an alternative (Liu et al., 2019b) that could serve for evaluating technologies like the PN/A. PN/A involves an initial SBR reactor for partial nitritation followed by a separated reactor for the Anammox process. Figure 5.10 includes the daily variations of $sCOD/TKN_{out}$ (3.2 ± 1.2 $g_{sCOD} \cdot g_{N\text{-}NH4+in}^{-1}$), $sCOD_{out}$ (117 ± 42 $mg \cdot L^{-1}$) and N-NH_4^+ effluent concentration (38 ± 7 $mg \cdot L^{-1}$). The experimental results indicated that the variation in the sCOD/N-NH_4^+ ratio was due to a higher variation in the sCOD concentration than the N-NH_4^+ concentration, with sCOD removal being

the most effective way to control the sCOD/N-NH_4^+ ratio, with a correlation between influent and effluent ratios illustrated in Figure 5.11.

Table 5.4. Overflow rate, influent and effluent pCOD, OrgN and OrgP with VSS ratios and pCOD and VSS with TSS ratios in each experimental period

Period	OFR clarifier	pCOD/VSS $g_{pCOD} \cdot g_{VSS}^{-1}$		orgN/VSS $g_{orgN} \cdot g_{VSS}^{-1}$		orgP/VSS $g_{orgP} \cdot g_{VSS}^{-1}$		pCOD/TSS $g_{pCOD} \cdot g_{TSS}^{-1}$		VSS/TSS $g_{VSS} \cdot g_{TSS}^{-1}$	
	$m \cdot h^{-1}$	in	out	in	out	in	out	in	out	in	out
1	1.3	1.50	1.23	0.08	0.14	0.02	0.03	1.32	1.19	0.88	0.97
2	1.6	1.61	1.00	0.12	0.13	0.03	0.03	1.42	0.98	0.88	0.98
3	1.7	1.75	1.67	0.10	0.19	0.03	0.03	1.23	1.25	0.70	0.75
4	1.6	1.59	1.73	0.11	0.16	0.03	0.02	1.08	1.54	0.68	0.89
5	1.6	1.76	1.80	0.21	0.48	0.03	0.04	1.07	1.39	0.61	0.77
7	0.8	1.22	1.84	0.09	0.26	0.01	0.03	1.05	1.80	0.86	0.98
8	0.8	1.15	1.77	0.10	0.36	0.02	0.04	0.99	1.72	0.86	0.97
9	0.8	1.15	1.90	0.10	0.39	0.02	0.03	1.07	1.80	0.93	0.95
Average		1.47	1.62	0.11	0.26	0.02	0.03	1.15	1.46	0.80	0.91

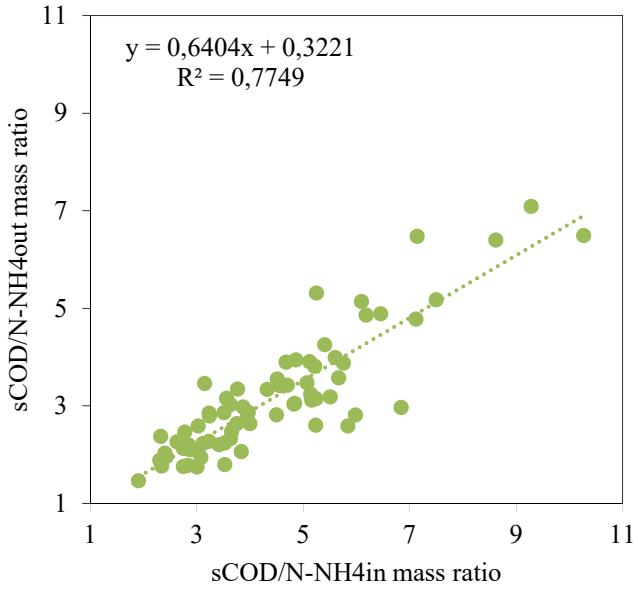

Figure 5.11 Daily sCOD/N-$NH_4^+{}_{in}$ compared to sCOD/N-$NH_4^+{}_{out}$. Experimental values

5.3.6 Suitability of Subsequent Technologies

HRAS effluent must undergo a subsequent nitrogen removal unit operation in order to fulfill the concentration limitations in WWTP discharges. Understanding the nature of the COD/TKN ratio is crucial information for designing optimized subsequent treatment processes for nitrogen removal. The analysis informs the potential for considering the application of different advanced nitrogen removal processes in the wastewater treatment.

The heterotrophic denitrification pathway in conventional N/DN process requires 4 – 8 $g_{COD} \cdot g_{N\text{-}NO3}$ for N-NO_3 reduction and biomass synthesis (Hertzier et al., 2010), depending on the value of the biomass

yield associated with the specific available COD. However, there are alternative technologies with a lower COD demand, such as the Short-cut N/DN process with NOB out-selection consuming 2.4 - 4.8 $g_{COD} \cdot g_{N\text{-}NO2}^{-1}$ (Hertzier et al., 2010), and the PN/A consuming 0.6 – 2.0 $g_{COD} \cdot g_{N\text{-}NO2}^{-1}$ (Akaboci et al., 2018; Han et al., 2016; Hoekstra et al., 2019; Isanta et al., 2015; Jia et al., 2020; Laureni et al., 2016; Reino et al., 2018). In this section we discuss the nitrogen removal technologies according to the HRAS effluents COD/TKN and sCOD/N-NH_4^+ effluent's ratio.

To fulfill the nitrogen effluent requirements, only ca. 25% of TKN_{in} can go to the effluent and waste streams (Rahman et al., 2019), so approximately 75% must be removed. The COD demand to remove the nitrogen can be calculated depending on the technology applied. For the conventional N/DN process, the COD demand is 6 $g_{COD} \cdot g_{TKNin}^{-1}$ (75% of 8 $g_{COD} \cdot g_{TKNin}^{-1}$) and for the short-cut N/DN it is 3.6 $g_{COD} \cdot g_{TKNin}^{-1}$ (75% of 4.8 $g_{COD} \cdot g_{TKNin}^{-1}$), and for the PN/A it is 1.5 $g_{COD} \cdot g_{TKNin}^{-1}$ (75% of 2.0 $g_{COD} \cdot g_{TKNin}^{-1}$). In the PN/A process with SBR in the PN, at most 70% of N-$NH_4^+{}_{in}$ is oxidized to N-NO_2, while the other 30% is oxidized by the Anammox (Liu et al, 2019; Magrí et al, 2019). Therefore, only 31% of N-$NH_4^+{}_{in}$ can be heterotrophically denitrified to maintain the N-NO_2/N-NH_4^+ mass ratio of 1.34$g \cdot g^{-1}$ in the influent of the Anammox process. Consequently, the organic material demand is only 1.5 $g_{sCOD} \cdot g_{N\text{-}NH4+in}^{-1}$ (31% of 4.8 $g_{sCOD} \cdot g_{N\text{-}NH4+in}^{-1}$) (Lemaire et al., 2014; Wan et al., 2016). Although this process requires a low COD concentration, it stabilizes the system due to the coexistence of heterotrophic denitrifiers and Anammox bacteria (Lackner et al., 2014; Pedrouso et al., 2017; Regmi et al., 2015, 2014; Yang et al., 2016).

To increase the COD/TKN_{out} ratio, employing Anammox in the return line from the digested sludge dewatering, i.e. the sidestream, can reduce the nitrogen load to the HRAS up to 15% (Lackner et al., 2014). To assess this outcome over our pilot plant, Figure 5.12 shows in blue dots the COD/TKN_{out} experimental results, and in red dots the COD/TKN_{out} calculated outcomes considering there was an Anammox process in the sidestream, which reduced up to 15% the TKN_{in} load. The thresholds 6.0 for N/DN; 3.6 for Short-cut N/DN and 1.5 for PN/A process are marked in dotted lines. Results showed that regardless the COD/TKN_{in} ratio, the COD/TKN_{out} permitted that the direct implementation of the PN/A process in the mainstream since the values where over the 1.5 threshold.

For the use of the nitrogen short-curt N/DN, a COD/TKN_{out} threshold of 3.6 is required, which was compromised for low COD/TKN_{in} values. However, implementing the sidestream Anammox ensured reaching the 3.6 nitrogen short-curt N/DN threshold even for cases with lower COD/TKN_{in}. Even with the sidestream Anammox process, the conventional N/DN (6.0 threshold) can be applied only to very high COD/TKN_{in} wastewater. Thus, most appropriated process according to the COD/TKN ratio is the short-cut N/DN process in the mainstream with an Anammox process in the sidestream. Short-cut N/DN process has been reported as a mature technology with the potential to become an energy neutral wastewater treatment plant (Rahman et al., 2019; Wu et al., 2023).

In a PN/A process, several factors, such as the influent COD split, degradability, and load, play important roles in inducing and maintaining NOB suppression and AOB activity. The HRAS $sCOD_{out}$ is utilized by heterotrophic bacteria to reduce NO_2^- in the anoxic phase, but this reduces the NO_2^- required for the subsequent Anammox process. The consumption of NO_2^- restricts its availability for NOB in the oxic phase. Moreover, an increase in organic loading in the HRAS effluent can negatively impact the system by creating competition for DO with heterotrophs (Hausherr et al., 2022). The key challenge is to strike a balance between the consumption of sCOD in the anoxic phase for NO_2^- reduction by heterotrophs while maintaining a high enough NO_2^- concentration for oxidizing $N\text{-}NH_4^+$ in the Anammox process. This process requires low sCOD concentration, but it stabilizes the system by allowing for the coexistence of heterotrophic denitrifiers and Anammox bacteria (Pedrouso et al., 2017; Yang et al., 2016).

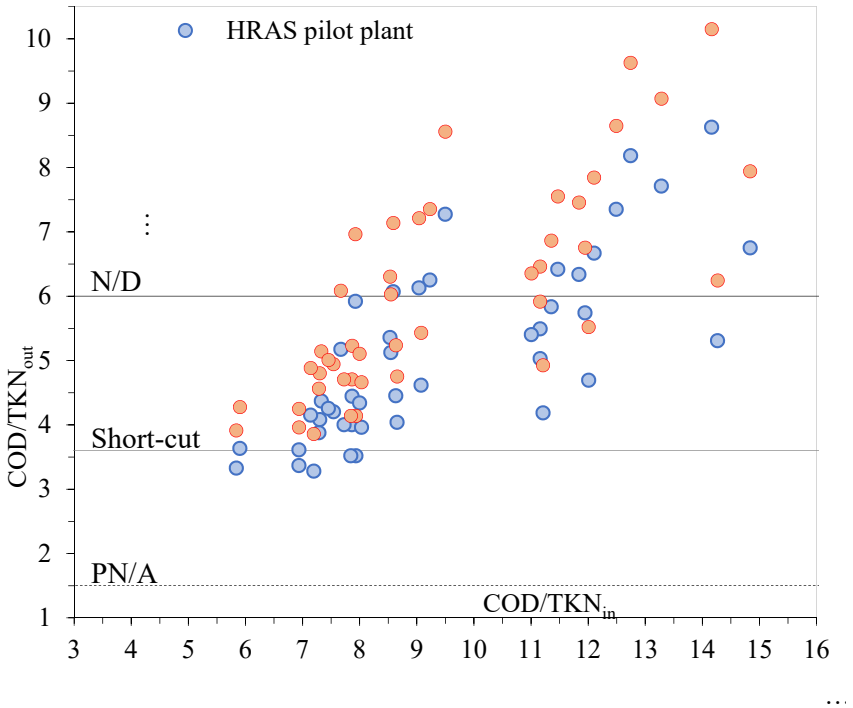

Figure 5.12 Daily COD/TKNout mass ratio compared to the COD/ TKN_{in}. Experimental values in blue dots. Red dots corresponding to calculated values with a side stream Anammox reducing the TKN influed load up to a 15%. The COD/TKN thresholds are plotted for PN/A (1.5), short-cut (3.6) and N/DN (6.0).

The HRAS process can effectively remove significant portions of carbon and, to a lesser extent, nitrogen. However, it is important to highlight the wide compositional variation of urban wastewater over time. The influent quality is affected by site-specific conditions, such as the nature of discharged compounds, in sewer microbial transformation, sewer length and its residence time, gas-transfers in sewers, water, and ambient temperatures (Gori et al., 2011). Wastewater temperature and HRT in the sewer network affect the influent sCOD/COD and pCOD/VSS ratios due to the rate of substrate hydrolysis at warmer temperatures and longer residence times (Guisasola et al., 2008) and the release of ammonia from organic nitrogen. In colder wastewaters and shorter sewer lines, the organic nitrogen keeps embedded in the solids and it is sent to digestion instead of secondary nitrification/denitrification.

Throughout the 497-day operation of the pilot plant in a Mediterranean climate, significant variation in the influent quality of urban wastewater were observed. In February and March, which were the coldest months with a lowest temperature of 18.5ºC, the influent contained 20% of the COD_{in} as sCOD and 54% of the TKN_{in} as $N\text{-}NH_4^+$. However, in July and August, which were the hottest months with a temperature of 26.1ºC, the influent contained 27% of COD_{in} as sCOD and 69% of TKN_{in} as $N\text{-}NH_4^+$. The seasonal variation of temperature resulted in a 30% increase in $N\text{-}NH_4^+$ and a 35% increase in sCOD fractions when the temperature increased by 8ºC. Therefore, it is crucial to conduct a detailed study of seasonal variations in parameters such as sCOD, pCOD, TKN, $N\text{-}NH_4^+$, TP, temperature, and alkalinity to ensure the appropriate application of the HRAS process A-Stage and the selection of the N/DN as a B-Stage process. This approach should consider the process performance, stability, energy recovery, energy consumption, and sludge production. Hence, it is essential to optimize the design and operation of the integrated A-Stage for energy recovery and B-Stage for nitrogen removal processes in a holistic manner.

5.4 Final remarks

The HRAS pilot plant operating with an SRT of 0.2 days, HRT of 0.5-1 hour, and a DO concentration of 0.5 $mg \cdot L^{-1}$ achieved nutrient removal efficiencies surpassing conventional primary clarifiers, although they do not reach remarkable levels for high nutrient removal. Removal rates were significantly correlated with influent nutrient concentrations, highlighting HRAS as a more suitable primary clarifier replacement than a downstream treatment. TKN and TP removal showed a positive correlation with COD and pCOD, emphasizing the significance of adsorption and entrapment processes.

The particulate influent fraction and concentration played a substantial role in nutrient removal efficiency, while temperature and OFR in settling tanks had minimal effects due to excellent biomass settling properties. Interestingly, the nitrogen and phosphorus removal processes were independent of COD oxidation, and the surplus sCOD removal may be attributed to intracellular storage or the high nitrogen content in biomass in a heavily loaded HRAS process.

A long-term analysis of the COD/TKN ratio indicates that a short-cut nitrogen process, complemented by Anammox in the sidestream, represents a highly suitable option for subsequent nitrogen removal. Further research is needed to understand the role of aerobic storage in HRAS, and optimizing HRAS nutrient and COD removal with minimal energy consumption should be considered.

Chapter 6
RESULTS III

Specific Oxygen Consumption in HRAS process

6.1 Overview

This Chapter focuses on the oxygen consumption and Specific Oxygen Consumption (SOC) of the HRAS process. The chapter delves into relationships between organic matter removal and oxygen consumption. Until now, the most used way to quantify the oxygen consumption has been the COD_{OXID} Taboada -Santos et al 2020, Jimenez et al 2015, Miller et al 2017, Rahman et al 2018, and Haider et al 2003.

This chapter addresses the research to discusses the experimental determination of Oxygen Uptake Rate (OUR) and the Specific Oxygen Consumption (SOC), but not only for COD, such the works of De Graaff et al (2016), Demoulin et al (1998) and Jetten et al (1997), but also for BOD_5 and sCOD. The study accounts for the unique aspects of treating wastewater without a primary clarifier, showcasing an increase in oxygen transfer efficiency using HRAS as an initial step. The study also analyses the main factors that affect the SOC values: influent COD concentration, COD removal and influent wastewater biodegradability.

In the HRAS process, the objective is not to supply air based on oxygen demand along the bioreactor length, as in conventional CAS processes. Instead, the focus is on minimizing oxygen supply while maintaining DO concentrations within the range of 0.2-0.5 $mg \cdot L^{-1}$. This approach aims to prevent deteriorating biomass settling characteristics and avoid anaerobic conditions in the settler.

This Chapter concludes by emphasizing the importance of SOC_{COD} trends, daily monitoring of OUR, and process modelling using SUMO software to compare the real pilot plant SOC with model predictions. The insights gained contribute to optimizing energy consumption and ensuring the stability of the subsequent wastewater treatment.

The main objective was to establish specific oxygen consumption and to control HRAS oxygen supply. In order to achieve this goal, the following sub-objectives were established. i) Determination of the oxygen uptake rate (OUR) preceding kLa experimental determination, ii) Evaluating SOC_{COD}, SOC_{sCOD}, and SOC_{BOD5} with influent COD concentration, DO concentration, and temperature, iii) Analyzing the correlation between COD_{OXID}, COD_W, and SOC, iv) Identifying factors significantly affecting CODW and CODOXID, v) Comparing model-derived predictions with data from an industrial-scale pilot plant and, vi) Assessing the most effective method for controlling oxygen supply.

6.2 Methodology

6.2.1 k_La and OUR determinations

HRAS oxygen consumption was obtained from the continuous calculation of the oxygen uptake rate (OUR) in R2 reactor. Previously, the mass transfer coefficient (k_La) was determined in clean water as

function of the percentage of opening air valve (OAV). k_La depends on both the temperature and the intensity of the mixing, and hence on the type of the aeration devise used and the geometry of reactor.

The determination of the k_La has been carried out in the 0.84 m^3 R2 reactor, 3.0 m side water depth, one fine bubble diffuser SULCER 9¨, giving a superficial diffuser density of 18%, filled with clean water, previous displacing oxygen with nitrogen until it reaches an oxygen concentration close to zero. DO was monitored at 1.5 m water depth. To different opening positions of the air supply valve the oxygen concentration has been brought to saturation, taking oxygen concentration time readings.

A oxygen mass balance is applied to determine Kla in batch test according to (Dolp et al. 2001 and Meetcalf and Eddy 2003):

$$\frac{dDO}{dt} = k_L a \cdot (DO_{sat} - DO) \qquad \text{Equation 6.1}$$

$$k_L a = ln \frac{DO_{sat(T)} - DO_T(t_0)}{DO_{sat(T)}(t) - DO_T(t)} \cdot \frac{1}{t} \qquad \text{Equation 6.2}$$

Where k_La is the volumetric oxygen mass transfer coefficient in clean water [h^{-1}] at the working temperature (T), in the reactor (VT basis). $DO_{sat(T)}$ is the saturation dissolved oxygen (DO) at temperature T and field atmospheric pressure. $DO_T(t)$ is the DO in the reactor [$mgO_2 \cdot L^{-1}$] at a time t [h] at temperature T. $DO_T(t_0)$ is the DO in the reactor [mg $O_2 \cdot L^{-1}$] at the initial time t_0 at T. t is the interval calculation time used. We have assumed that VT (volume of water + volume of bubble) is equal to V_L (volume of water) (Dolp et al. 2001).

The effect of temperature on oxygen transfer is establish by using the following function:

$$k_L a_T = k_L a_{20^oC} \cdot \theta^{T-20} \qquad \text{Equation 6.3}$$

Where k_La_T [h^{-1}] is oxygen mass transfer coefficient at temperature T [ºC], and $k_La_{20^oC}$ is oxygen mass transfer coefficient at temperature 20ºC . The Θ value for fine bubble diffuser is 1.024.

Oxygen uptake rate (OUR) represents the rate at which the oxygen is being utilized by bacteria per unit of time and reactor volume. K_La value was used to calculated OUR according to the DO mass balance in the liquid phase:

$$OUR_t = \alpha \cdot k_L a_T \cdot [\beta \cdot DO_{sat(T)} - DO_{(T)}(t)] - \frac{dDO}{dt} \qquad \text{Equation 6.4}$$

Where OUR is the oxygen uptake rate [$mg_{O2} \cdot L^{-1} \cdot h^{-1}$], $\frac{dDO}{dt}$ is the derivative of oxygen concentration in time, and α and ß are the parameters defined as (Meetcalf and Eddy 2003):

$$\alpha = \frac{k_L a_{(wastewater)}}{k_L a_{(cleanwater)}} \qquad \text{Equation 6.5}$$

$$\beta = \frac{DO_{sat(wastewater)}}{DO_{sat(cleanwater)}} \qquad \text{Equation 6.6}$$

Schwarz, M, et al (2021), proposed and average and maximum α-factor for HRAS of 0.45 and 0.54 respectively. The study has assumed and average α-factor of 0.48. No fouling factor have considered due to the low pilot plant running time.

Constant monitoring of DO reactor concentration and OAV was conducted in pilot plant to calculate OUR, using equation 6.4. Data was recorded in 5-seconds intervals by online sensors and summarized as 1-minute averages. A minimum 32% opening air valve position was fixed, to avoid reactor sludge settling. The oxygen sensor was installed at half the height of the water sheet.

6.2.2 Specific Oxygen Consumption (SOC) calculations

To relate oxygen consumption with the organic matter removed, the following three parameters were established:

Specific Oxygen Consumption for COD

$$SOC_{COD} = \frac{Kg\ O_{2\ consumed}}{KgCOD_{IN} - KgCOD_{OUT}} \qquad \text{Equation 6.7}$$

Specific Oxygen Consumption for sCOD

$$SOC_{sCOD} = \frac{Kg\ O_{2\ consumed}}{Kg\ sCOD_{IN} - Kg\ sCOD_{OUT}} \qquad \text{Equation 6.8}$$

Specific Oxygen Consumption for BOD_5

$$SOC_{BOD_5} = \frac{Kg\ O_{2\ consumed}}{Kg\ BOD_{5\ IN} - Kg\ BOD_{5\ OUT}} \qquad \text{Equation 6.9}$$

Where $KgCOD_{IN}$, $KgsCOD_{IN}$ and $KgBOD_{5IN}$ are the daily influent flow rate multiplied by the average concentrations of COD_{IN}, $sCOD_{IN}$ and BOD_{5IN} respectively, and $KgCOD_{OUT}$, $KgsCOD_{OUT}$, $KgBOD_{5OUT}$ are the daily effluent flow rate multiplied by the average concentrations of COD_{OUT}, $sCOD_{OUT}$ and BOD_{5OUT} respectively. The Kg O_2 consumption is the daily oxygen consumption from OUR.

6.3 Results and Discussion

6.3.1 SOC Assessment from COD Mass Balance

A first calculation of SOC_{COD} could be obtained from each operational pilot plant periods in accordance with COD mass balances (Figure 4.11) and the SOC_{COD} expression, (Equation 6.7). There is a lineal correlation between the SOC_{COD} obtained and the COD_{OXID} for the nine periods Figure 6.1. It's noteworthy that the SOC_{COD}, calculated as COD_{OXID} divided by COD_{rem} (COD_{IN} - COD_{OUT}) from the COD balance, follows a similar pattern as COD_{OXID} itself. In other words, the lower the $\%COD_{OXID}$, the higher the energy efficiency measured as SOC_{COD}. Take in mind that an increase of COD_{OXID}, could

be due to a reduction of COD_W and consequently an increase of SOC_{COD}, i.e. a decrease in the energy efficiency of the process.

HRAS process, operating under extreme conditions (SRT 0.2 ± 0.05 d, DO 0.5 ± 0.2 2 $mg \cdot L^{-1}$) and subject to high influent load variations, demonstrated the ability to harvest an average of 54% of the COD_{IN}, with a low COD_{OXID} of 6.9% that correspond a SOC_{COD} of 0.11 $Kg_{O2} \cdot Kg_{CODremoved}^{-1}$ (Figure 6.1) .The average COD_{OXID} in the pilot plant is lower than those reported by Haider et al. (2003) (12%), Miller et al. (2015) (14%), and Jimenez (2015) (22%). Similarly, the average COD_{OXID} for the entire operational period, 6.9 ± 3.6%, aligns with the optimal COD_W range of 6-7% for energy save, as indicated by Wett et al, (2020). Moreover, the average COD_{OXID} obtained for the entire operational period, 6.9 ± 3.6%, closely corresponds to the average percentage of sCOD removed in relation to COD_{IN} (7.2%), 25% of COD_{IN} as sCOD and 29% sCOD removed (Table 4.1).

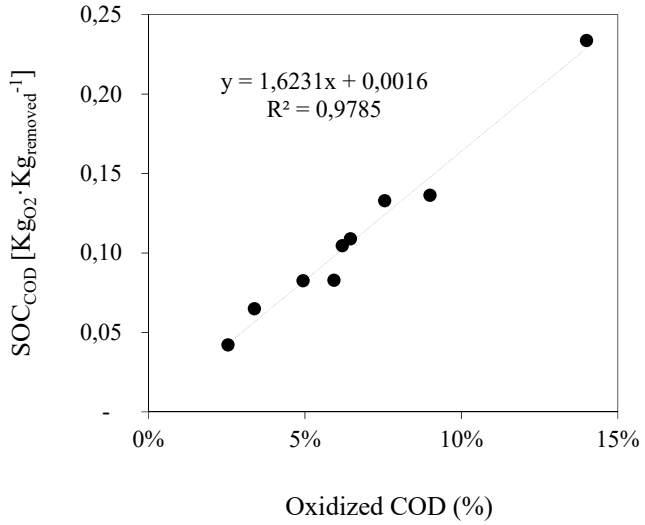

Figure 6.1 Correlation between the SOC_{COD} and the COD_{OXID} for the nine periods.

6.3.2 SOC determination from OUR

One of the main objectives of this study was the experimental determination of the SOC related to the organic matter removal. Thus, the first steep was the k_La experimental determination under various position of the OAV, according to section 6.2.1 description. The results are presented in Figure 6.2, along with the corresponding logarithmic adjustments. Subsequently, the calculation of the oxygen consumption as OUR was performed for six days period during operational period 9. On these days the pilot plant operated exclusively the reactor R2, allowing a precise calculation of oxygen consumption.

It is important to note that this HRAS study treats wastewater without the use of PC. Therefore, raw wastewater with a high content of surfactants enters directly to the reactor, leading to reduced oxygen transfer efficiency and consequently reducing the α-factor value, which has a great importance in the

OUR calculation (Equation 6.4). In this study, an average α-factor of 0.45 was assumed, which is lower than the 0.6 typically used in CAS processes with a PC. Surfactants are affectively removed in the HRAS process, compensating for the lower α-factor in the (first stage) HRAS with a higher α-factor of 0.8 in the (second stage) CAS. Furthermore, the α-factor in the second stage exhibits a more consistent diurnal pattern (Schwarz et al 2021). In two stage process, only 6% of required oxygen is supplied in the first stage (α-factor 0.45), while 92% is supplied in the second stage (α-factor 0.8), in contrast to CAS processes, which provides the 100% of the oxygen under an α-factor of 0.6. This indicates an 29.8 % increase in the oxygen transfer efficiency using HRAS as an initial step.

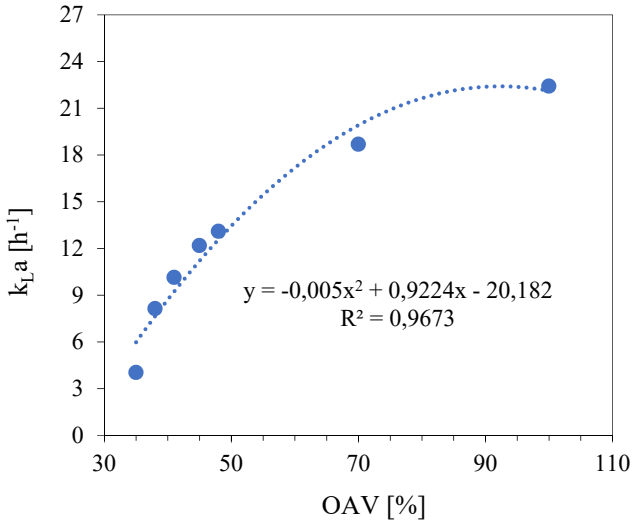

Figure 6.2 Experimental results and logarithmic adjust of k_La depending on the % of opening air valve (OAV) at 20º C in clean water.

The second steep was the determination of OUR according the Equation 6.4. A detail study was run for the OUR determination during six days of period 9, working only reactor R2. The average OUR at 20ºC obtained is presented in Table 6.1 and range from 31 to 54 $mg_{O2}·L^{-1}·h^{-1}$, with an average of 42±8 $mg_{O2}·L^{-1}·h^{-1}$.

And finally, the thirst steep was the calculation of the different SOC at 20ºC using Equations 6.7 (SOC_{COD}), 6.8 (SOC_{sCOD}), and 6.9 (SOC_{BOD5}). It's crucial to emphasize that the term $KgCOD_{IN}$ - $KgCOD_{OUT}$ employed in these equations represents the COD removed from the water line, excluding the COD harvested for digestion (COD_W).

The SOC_{COD} values, outlined in Table 6.1, range from 0.08 to 0.18 $KgO_2·KgCOD_{rem}^{-1}$, with an average of 0.11 $KgO_2·KgCOD_{rem}^{-1}$. These findings align with values reported in previous studies such as those by De Graaff et al. (2016) (0.13-0.21 $KgO_2·KgCOD_{rem}^{-1}$), Demoulin et, al. (1998) (0.17 $KgO_2·KgCOD_{rem}^{-1}$), Jetten et al. (1997) (0.21 $KgO_2·KgCOD_{rem}^{-1}$ and Taboada-Santos et al. (2020) (0.19 $KgO_2·KgCOD_{rem}^{-1}$). Also, it is noteworthy that these SOC_{COD} values are slightly lower than those

reported by Jimenez (2015) (0.2-0.38 $KgO_2 \cdot KgCOD_{rem}^{-1}$) and Böhnke et al. (1997) (0.23-0.33 $KgO_2 \cdot KgCOD_{rem}^{-1}$).

To gain deeper insights into the SOC_{COD}, we examine the relationships between SOC_{COD} and COD removed. Figure 6.3A reveals a negative correlation between SOC_{COD} and the COD_{rem}. A higher the CODrem, lower the SOC_{COD} ratio. The correlation, however, is not too high, that means that SOC_{COD} could not be the best ratio to analyse the specific oxygen consumption.

The SOC_{BOD5} obtained in the Pilot Plant (Table 6.1) ranges from 0.23 to 0.53 $KgO_2 \cdot KgsBOD_{5rem}^{-1}$, with an average of 0.37 $KgO_2 \cdot KgBOD_{5rem}^{-1}$ consistent with values reported by Constantine et al. (2012) and Versprille et al. (1985). The relationship between SOC_{BOD5} and BOD_{5rem} is further detailed in Figure 6.3B, that also reveals a negative correlation between $SOC_{BOD5}$and the BOD_5remo. An increase of BOD_5rem, promote a reduction of SOC_{BOD5} ratio. The correlation, in this case is higher, that means that SOC_{BOD5} could be a good ratio to analyse the specific oxygen consumption.

The SOC linked to SOC_{sCOD} exhibits notable dispersion, ranging from 0.53 to 1.60 $KgO_2 \cdot KgsCOD_{rem}^{-1}$ with an average value of 0.90 $KgO_2 \cdot KgsCOD_{rem}^{-1}$ (excluding days with very low $sCOD_{IN}$ $\leq 100 mg \cdot L^{-1}$). Figure 6.3C visually reveals a negative correlation between SOC_{sCOD} and the $sCOD_{rem}$. An increase of $sCOD_{rem}$, promote a reduction of SOC_{sCOD} ratio. The good correlation, in this case, highlight that that SOC_{sCOD} could be the best ratio to analyse the specific oxygen consumption.

It's crucial to note that SOC, in relation to sCOD, COD and BOD_5 is not a stoichiometric parameter like the oxygen demand for nitrification. Instead, it represents a global oxygen demand influenced by operational conditions, such as influent concentration, leading to its wide range of variation.

Table 6.1 Operating parameters of sampling days considered for the study of OUR and SOC, average and standard deviation.

Parameter	Units	Sampling date						Av	S.D.
		03/11/20	05/11/20	10/11/20	12/11/20	16/12/20	17/12/20		
OAV (average)	%	46	51	40	42	35	38	42.0	5.8
Flow rate	$m^3 \cdot d^{-1}$	31.2	30.8	31.2	31	32.4	30.8	31.2	0.6
Temperature	ºC	23.1	22.1	21.7	22.1	18.3	19.2	21.1	1.9
OLR	$Kg_{COD} \cdot Kg_{MLSS}^{-1} \cdot d^{-1}$	10.8	7.4	7.9	8.4	9.2	9.1	8.8	1.2
COD_{IN}	$mg \cdot L^{-1}$	590	410	430	460	480	510	480	64.5
COD_{rem}	%	59%	51%	56%	57%	52%	63%	56%	4%
$sCOD_{IN}$	$mg \cdot L^{-1}$	110	120	120	120	100	63	105.5	22.3
$sCOD_{rem}$	%	15%	34%	34%	49%	7%	10%	25%	17%
BOD_{5IN}	$mg \cdot L^{-1}$	188	154	165	183	107	105	150.3	36.5
BOD_{5rem}	%	63%	54%	69%	60%	35%	50%	55%	12%
BOD_5/COD	-	0.32	0.37	0.38	0.40	0.22	0.20	0.32	0.08
DO	$mg \cdot L^{-1}$	1	1	1.3	1.1	1	1	1.1	0.1
MLSS (R2)	$g \cdot L^{-1}$	2.00	2.00	1.99	1.99	1.99	2.03	2.00	0.02
SRT	d	0.1	0.1	0.2	0.2	0.3	0.1	0.2	0.1
OUR 20ºC	$mg_{O2} \cdot L^{-1} \cdot h^{-1}$	55	59	40	49	30	38	45	11.1
$O_{2\ consum}$ 20ºC	$Kg_{O2} \cdot day^{-1}$	1.10	1.21	0.83	1.01	0.67	0.84	0.90	0.20
SOC_{COD} 20ºC	$Kg_{O2} \cdot Kg_{COD}^{-1}$	0.10	0.18	0.11	0.12	0.08	0.08	0.11	0.04
SOC_{sCOD} 20ºC	$Kg_{O2} \cdot Kgs_{COD}^{-1}$	1.60	0.86	0.61	0.53	2.00	2.34	1.32	0.77
SOC_{BOD5} 20ºC	$Kg_{O2} \cdot Kg_{BOD5}^{-1}$	0.29	0.45	0.23	0.29	0.53	0.47	0.37	0.12

***OAV**: opening air valve; **OLR**: organic loading rate; **SRT**: solids retention time; **OUR**: Oxygen uptake rate; **SOC_{COD}**: Specific oxygen consumption versus COD; **SOC_{sCOD}**: Specific oxygen consumption versus sCOD; **SOC_{BOD5}**: Specific oxygen consumption versus BOD_5*

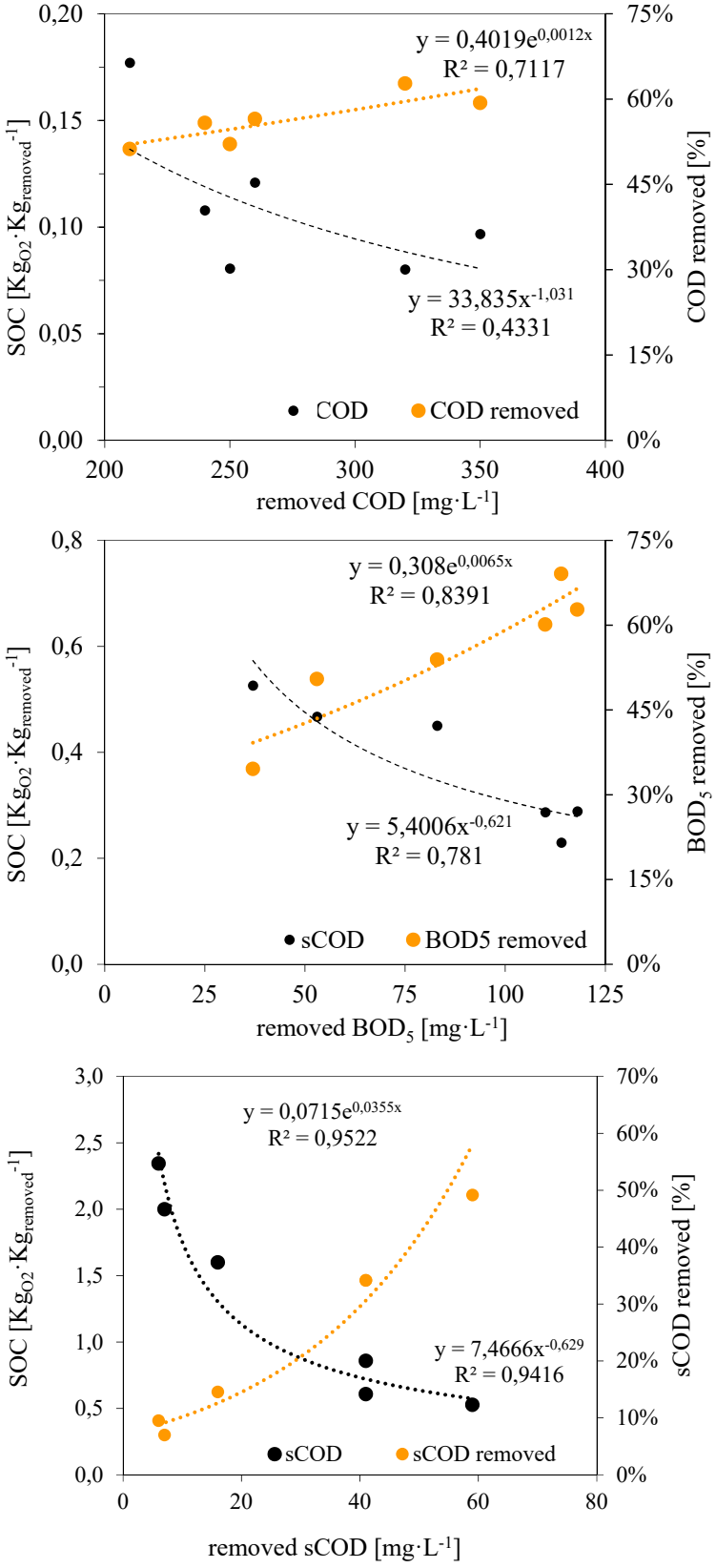

Figure 6.3 A) SOC_{COD} and % COD_{rem} versus COD_{remo}; B) SOC_{BOD5} and % BOD_{5rem} versus BOD_{5remo}, C) SOC_{sCOD} and % $sCOD_{rem}$ versus $sCOD_{rem}$ at 20º C, SRT 0.2±0.1 days, DO 1.1±0.1 $mg \cdot L^{-1}$.

6.3.3 SOC determination from OUR and from COD balance

To further evaluate the importance of the SOC_{COD} trend, Figure 6.4 presents the calculated values of $SOC_{COD,}$ for each period, from the COD mass balance (Section 6.3.1) and the SOC_{COD} based in the experimental OUR estimation (Section 6.3.2).

The disparity between the two SOC_{COD} values obtained for each period stems from the fact that the SOC from the COD balance involve the oxygen consumption derived from the difference between the COD_{IN}-COD_{OUT}-COD_W, which reflects the way in which the pilot plant has been operated, basically the COD_W, whereas the SOC from the OUR correspond to applying the expression experimentally obtained to the average COD_{rem} values for each period (Figure 6.3.A), which represents a more accurate operation form. Periods 5 and 7 serve as clear examples of inaccurate oxygen control, attributed to high $sCOD_{IN}$ levels (>200 $mg \cdot L^{-1}$) in both periods (Table 4.1) and an additional low COD_W (46%) in period 5 (Figure 4.11).

Furthermore, Figure 6.5 highlights the noteworthy negative correlation between the BOD_{IN}/COD_{IN} ratio and the SOC_{COD} and SOC_{BOD5}. A higher BOD_{IN}/COD_{IN} ratio, indicative of more easily biodegradable wastewater, results in lower SOC. This implies that not only do COD_{rem} (Figure 6.3A) and BOD_{rem} (Figure 6.3B) affect the SOC, but also the biodegradability of influent wastewater plays a significant role.

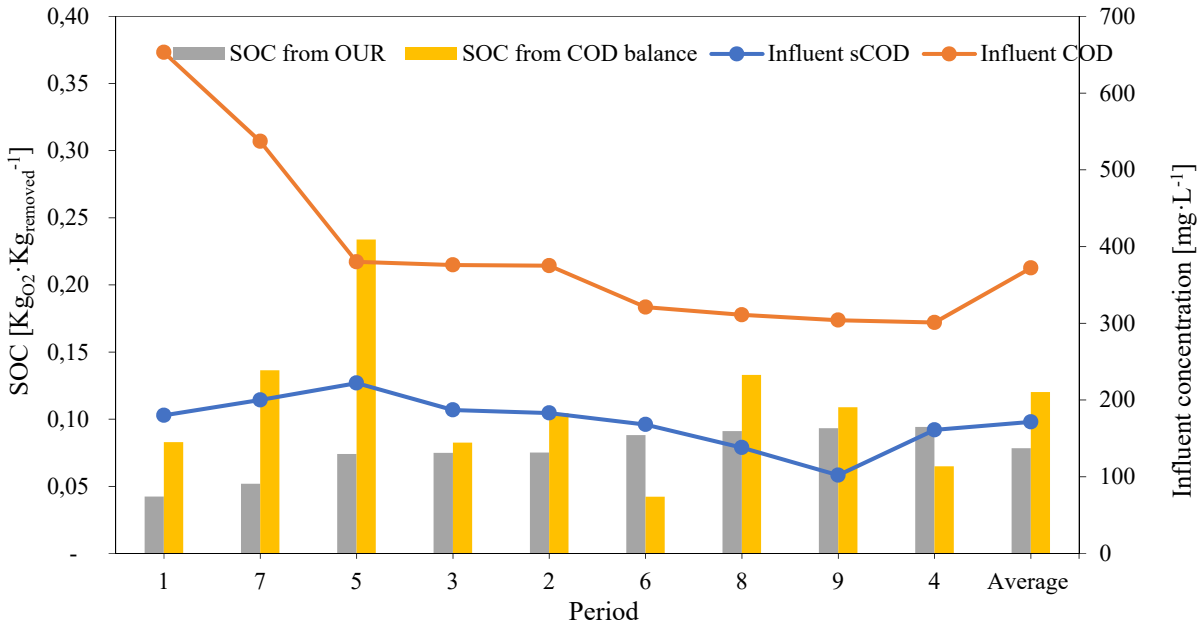

Figure 6.4. SOC_{COD} ($Kg_{O2cons} \cdot Kg_{CODremoved}^{-1}$) from OUR and COD balance for each period, and COD_{IN} and $sCOD_{IN}$ concentration.

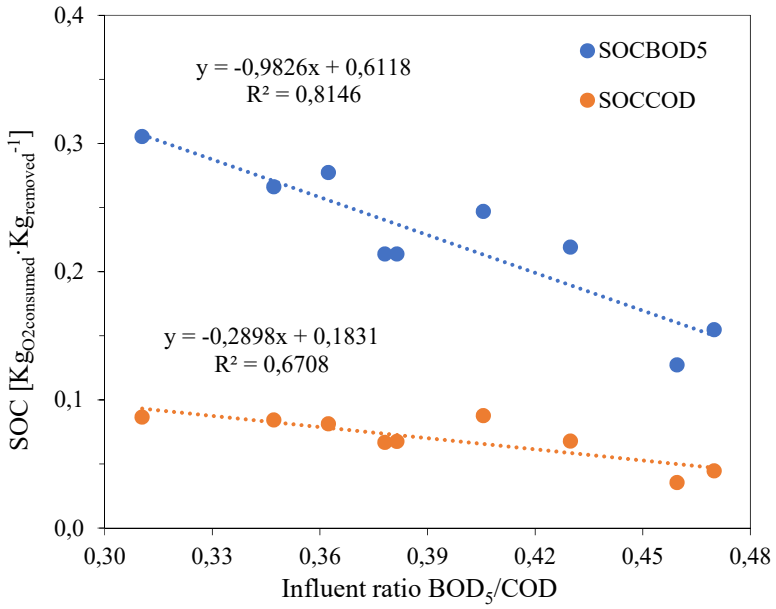

Figure 6.5 Correlation between SOC_{BOD5} and SOC_{COD} with $BOD5_{IN}/COD_{IN}$ ratio

6.3.4 Daily Monitoring OUR

In the pilot plant reactor, daily 24-hour monitoring of MLSS, DO, and %OAV was conducted, allowing for the calculation and monitoring of associated K_{La} (Figure 6.2) and OUR Equation 6.4 values. The primary operational conditions of the pilot plant included a variable flow rate (Figure 4.1), the use of raw wastewater influent, the control of waste sludge through an MLSS set point of 2000 ± 200 $mg \cdot L^{-1}$ in the reactor, and a minimum 32% OAV to prevent biomass settling in the reactor. Figure 6.6 A shows that for average daily organic loads, the monitored variables align with the flow influent flow pattern. The implemented control system, which maintains constant DO and MLSS set point of 2000 ± 200 $mg \cdot L^{-1}$ in the reactor, enabled matching the oxygen supply with the oxygen demand. Similarly, Figure 6.6 B demonstrated that for low and constant organic loads, the control system effectively balanced the oxygen supply and demand. However, Figure 6.6 C reveals that during periods of low organic influent load, characterized by minimum oxygen demand, the minimum required mixing air (32% OAV) exceeds the oxygen process demand, resulting in an increase in oxygen concentration and an excessive energy consumption. To address this issue, an additional mixing system could be installed to help achieve complete mixing during periods of minimum influent load and avoid excessive energy consumption.

Additionally, the HRAS reactor's low HRT (40-60 minutes) does not allow for influent load dilution, as in CAS processes with 9-16 hours of HRT. This lack of dilution leads to high OUR peak values. Therefore, the oxygen supply system must be capable of covering a range from half to twice the average OUR value (Table 6.2). The different OUR patterns observed (study of six days of period 9), for the first four days compared to the last two days, with average OUR values of 46 and 34 $mgO_2 \cdot L^{-1} \cdot h^{-1}$ and maximum OUR values of 76 and 46 $mgO_2 \cdot L^{-1} \cdot h^{-1}$, respectively, are related to the average $sCOD_{rem}$

values of 39 and 7 mg $sCOD_{rem} \cdot L^{-1}$ (Table 6.2). This confirms the direct association between oxygen demand and sCOD removal, as previously discussed by Hauduc et al. (2019).

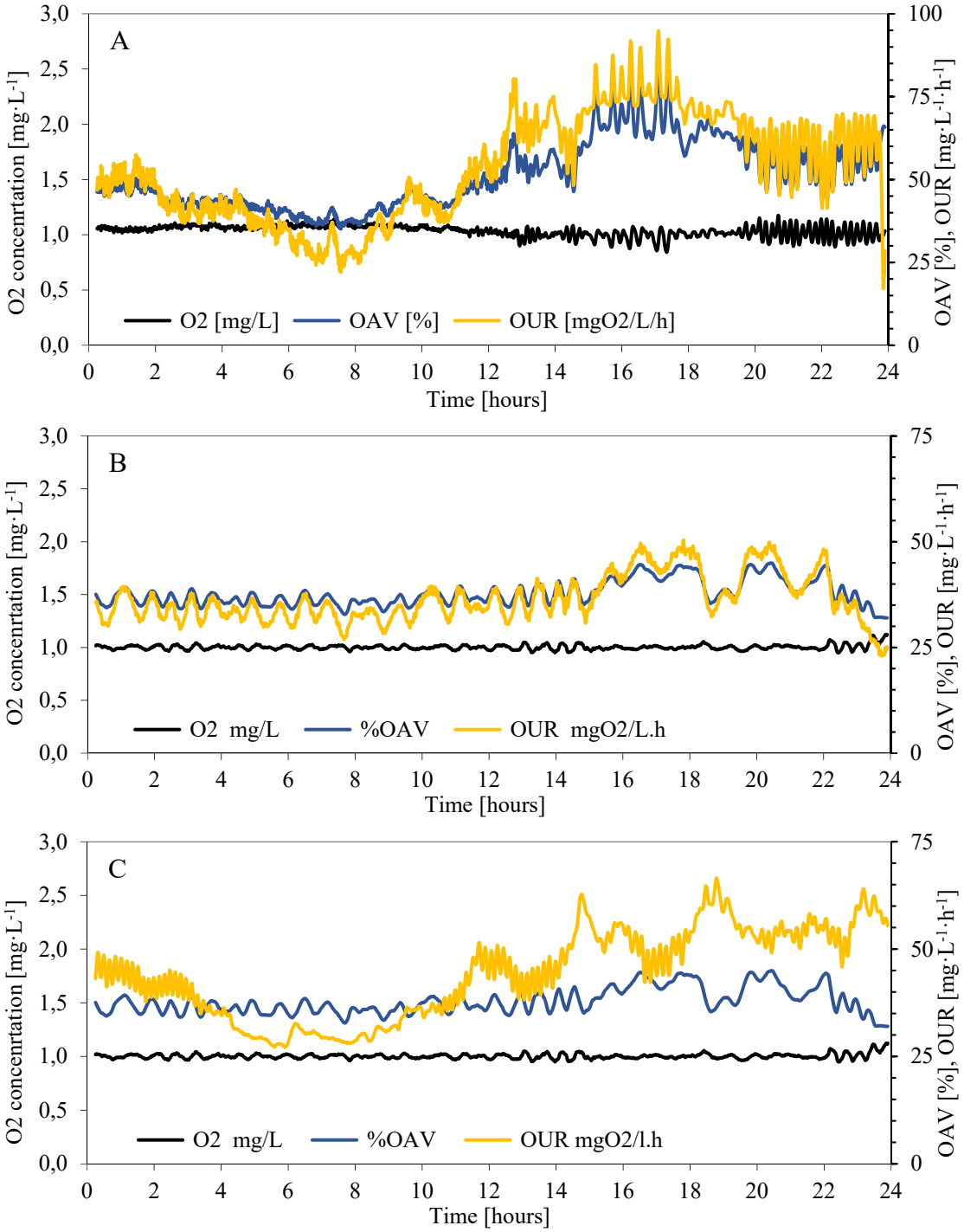

Figure 6.6 24 h monitoring of DO, OUR and % of opening of the air valve (OAV) in during three days: A) average influent load, B) constant low influent load, C) modulated low influent load

Table 6.2 Maximum and minimum OUR peak values referred to average values in a 24 hours period

	$sCOD_{in}$ [$mg \cdot L^{-1}$]	$sCOD_{rem}$ [$mg \cdot L^{-1}$]	OUR [$mg_{O2} \cdot L^{-1} \cdot h^{-1}$]				
Day	average	average	average	maximum	minimum	max/aver	min/aver
03/11/2020	110	16	55	81	20	1.7	0.4
05/11/2020	120	41	59	95	17	1.8	0.3
10/11/2020	120	41	40	60	28	1.5	0.7
12/11/2020	120	59	49	66	27	1.5	0.6
Average	117.5	39.3	51	75.5	23	1.6	0.5
16/12/2020	100	7	30	41	23	1.3	0.7
17/12/2020	63	6	38	50	23	1.4	0.6
Average	81.5	6.5	34	45.5	23	1.35	0.65

6.3.5 Daily COD removal and oxidation

To gain deeper insights into the hourly load variations along the day in the oxygen consumption and OUR demand, this study includes COD analysis in six-hour periods, COD fraction removals, and CODoxid, as an indication of oxygen consumption. Table 6.3 provides the main operational characteristics for each period. Figure 6.7A provides a comprehensive COD analysis in six-hour periods, revealing distinct daily patterns for each COD fraction.

i) The percentual pCOD removal remains consistently high, irrespective of influent load. This suggests that the operational conditions do not impose limitations on pCOD removal capacity, and it remains unaffected by the OFR.

ii) Removal of cCOD is observed predominantly during six-hour periods with elevated cCOD influent loads (13-18h and 19-24h), indicating a dependency on the influent concentration for effective removal.

iii) The sCOD removal demonstrates a peak capacity (Kg_{sCOD} in six-hour periods), from 7-12h and 13-18h, regardless of influent load. This phenomenon may be attributed to factors such as low HRT or a diminished concentration of active MLSS, rather than inadequate oxygen supply (Table 6.3). That is, oxygen concentration does not seem to be the limiting factor for the elimination of sCOD.

Moreover, Figure 6.7B illustrates the balance between COD_{OUT}, COD_W and COD_{OXID} for each six-hour period, highlighting notable variations. During high COD_{IN} load periods (13-18h), there is a pronounced increase in COD_W, resulting in maximum of 69% and a decrease in COD_{OXID} up to 1%. Low COD_{IN} load periods (0-6h) exhibited minimal COD_W (0%) and maximal COD_{OXID} (56%). This emphasizes the significant influence of influent load variations along the day in the oxygen consumption.

One way to reduce daily COD_{OXID}, and consequently the oxygen consumption, is to install a high-efficiency mechanical agitation system in the reactor to keep the biomass in suspension without sCOD oxidation during low influent COD load periods. Simultaneously, the MLSS set point concentration in the reactor could be reduced during this period to increase COD_W.

Table 6.3 Operational characteristics for each 6-hour period

Time	HRT	SRT	DO	MLSS	OLR (at 6 hr)	OLR (at 24 h)	OFR (Q_{averg})	OFR (Q_{max})
	[hour]	[day]	[mg·L^{-1}]	[mg·L^{-1}]	[Kg_{COD}·Kg_{MLSS}^{-1}.6h^{-1}]	[Kg_{COD}·Kg_{MLSS}^{-1}.d^{-1}]	[m·h^{-1}]	[m·h^{-1}]
0-6	1.4	0.2	0.3	2.528	1.8	7.3	1.5	1.7
7-12	1.3	0.2	0.5	2.608	2.1	8.5	1.6	1.9
13-18	1.1	0.2	0.4	2.610	3.6	14.2	1.9	2.2
19-24	1.2	0.2	0.3	2.546	3.0	12.0	1.8	2.1

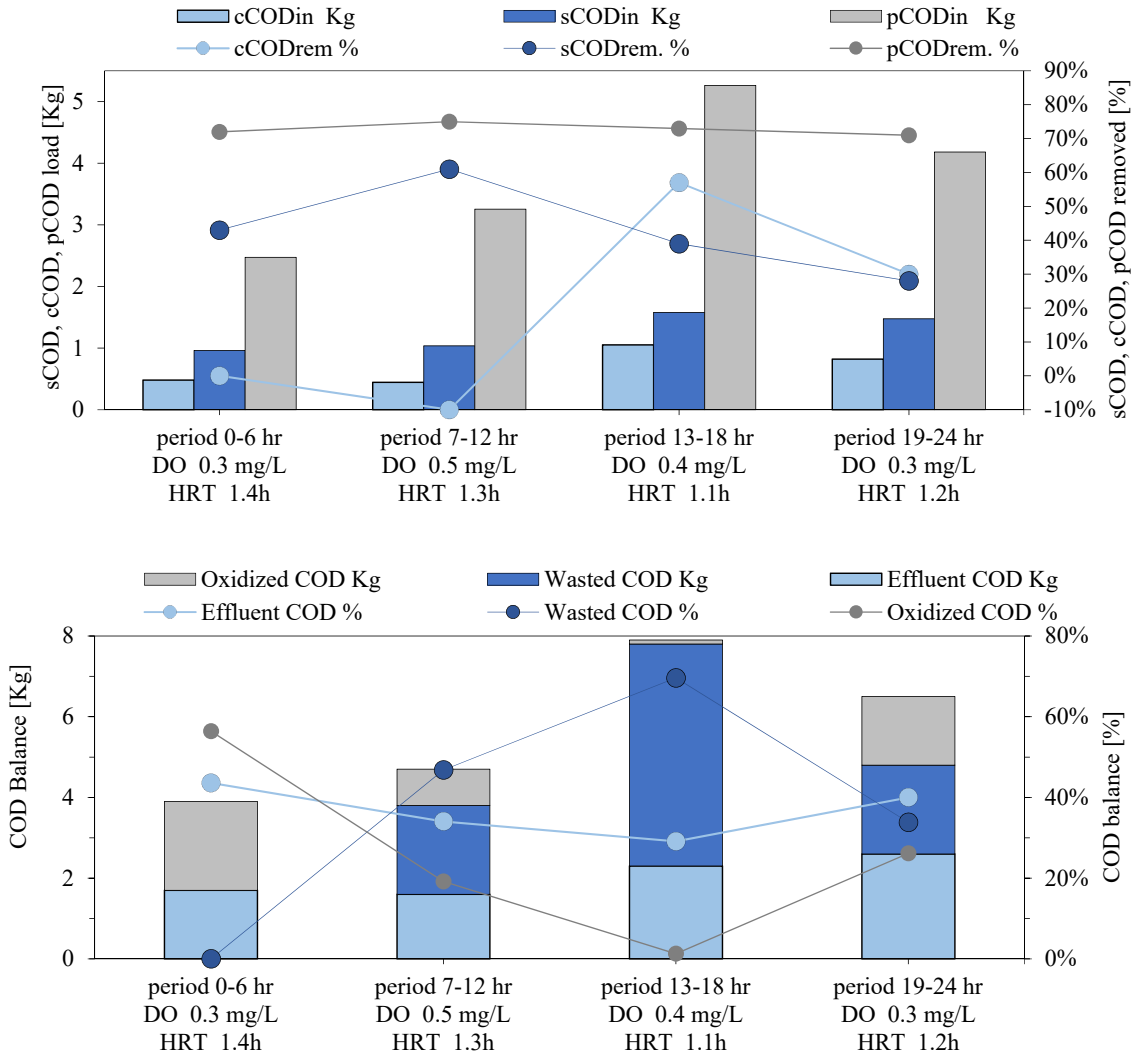

Figure 6.7 A) Influent load of COD fractions and removal percentage and B) COD balance in the six-hour periods per day.

6.3.6 Experimental and modelling SOC values

Process modelling was carried out using SUMO software according to the process model configuration with the goal to compare the real pilot plant SOC with that obtained through the model. The parameters used to run the model for the growth of AHO and OHO are shown in the Table 3.6. The COD, sCOD and BOD_5 used were determined according to the values of the pilot plant Table 6.1. The sCOD split

and AHO and OHO fraction in the total COD were according the model default values. The influent biomass considered in the model represented the 10% of the total COD_{IN}.

The pilot plant exhibited two specific characteristics distinct from full-scale facilities: lower reactor flocculation due to wall effects and a low ratio of surface-water depth in the reactor. Additionally, the recirculation line featured lower deflocculation due to the use of helicoidal pumps at low speeds, as opposed to centrifugal pumps at higher speeds used in municipal wastewater treatment plants. Therefore, the most sensitive parameters requiring adjustment in the model were the flocculation factor in the reactor, ηFLOC, Process set to 0.4 for Reactor R1 and 0.2 for Reactor R2, and the deflocculation factor, f_r, in the recirculation line set to 10%. The first parameter accounts for all hydrodynamic effects that influence shear force on the flocs (e.g., reactor geometry, type of aerators, and mixers) acting on residual colloids. The second parameter relates to the deflocculation factor in the recirculation line, as discussed by Hauduc et al. (2019). For the settling model, a non-reactive three-compartment clarifier was used, featuring a flocculation factor of 0.9 in a sludge blanket and in the feed well. Finally, a topic of the utmost importance is the possible biological activity in the clarifier. (Rosso et al., 2019) highlighted that at the bottom of clarifier, in an anoxic condition, part of the carbon stored in the cells could be redissolved. However, no biological activity has considered in the clarifier model.

Figure 6.8 presents the SOC values for COD, sCOD, and BOD_5 from both the model and the experimental pilot plant at different influent concentrations. The model closely predicted SOC values as a function of influent concentration for SOC_{COD} (Figure 6.8A), SOC_{sCOD} (Figure 6.8B), and SOC_{BOD5} (Figure 6.8C), except for the lowest sCOD influent concentrations. For $sCOD_{IN}$ values below 110 $mg \cdot L^{-1}$, SOC_{sCOD} in the pilot plant was higher than that obtained in the model, while the removal efficiency in the pilot plant was lower than in the model (Figure 6.8 B). Possible explanations for this discrepancy could include: i) excessive air supplied in the pilot plant to ensure mixing conditions; ii) the presence of reduced inorganic compounds (Fe^{2+}, H_2S) in the influent wastewater of the pilot plant, which were not considered in the model; iii) low sCOD removal in the pilot plant (10%) compared to the model (26%); iv) a low biodegradability ratio of BOD_5/COD, falling below 0.22 (Table 6.1). Nevertheless, the average SOC_{sCOD} in the model was similar to the average observed in the pilot plant for days with $sCOD_{IN}$ higher than 110 $mg \cdot L^{-1}$ (0.86 and 0.68 $Kg_{O2} \cdot Kgs_{CODrem}^{-1}$ respectively).

Furthermore, the model revealed that the highest oxygen consumption in the HRAS process was attributed to the oxidation of sCOD by the AHO microorganisms (75-85%), followed by the growth of OHO microorganisms through the oxidation of VFA (volatile fatty acids) (14-17%), and finally, the growth of OHO microorganisms from truly biodegradable material (non-VFA) (2-8%) (Table 11.1). These oxygen consumption percentages corresponded to an influent sCOD split according to the model: 20% VFA, 25% monomers (non-VFA), 38% polymers, and 17% soluble non-biodegradable compounds, along with the following removal percentages: 31% sCOD, 95% VFA, 94% monomers (non-VFA), -41% polymers, and 0% soluble non-biodegradable compounds (Table 11.2).

These findings underscore the significance of studying the sCOD split and analyzing biomass composition (AHO/OHO) as they are responsible for the oxidation of various sCOD fractions and, consequently, oxygen consumption in the HRAS process. Despite these insights, further detailed research is needed to determine the effective removal of different sCOD split fractions and to conduct an hourly study in line with the HRT of the HRAS process in order to optimize energy consumption and ensure the stability of subsequent nitrification-denitrification steps in the main stream.

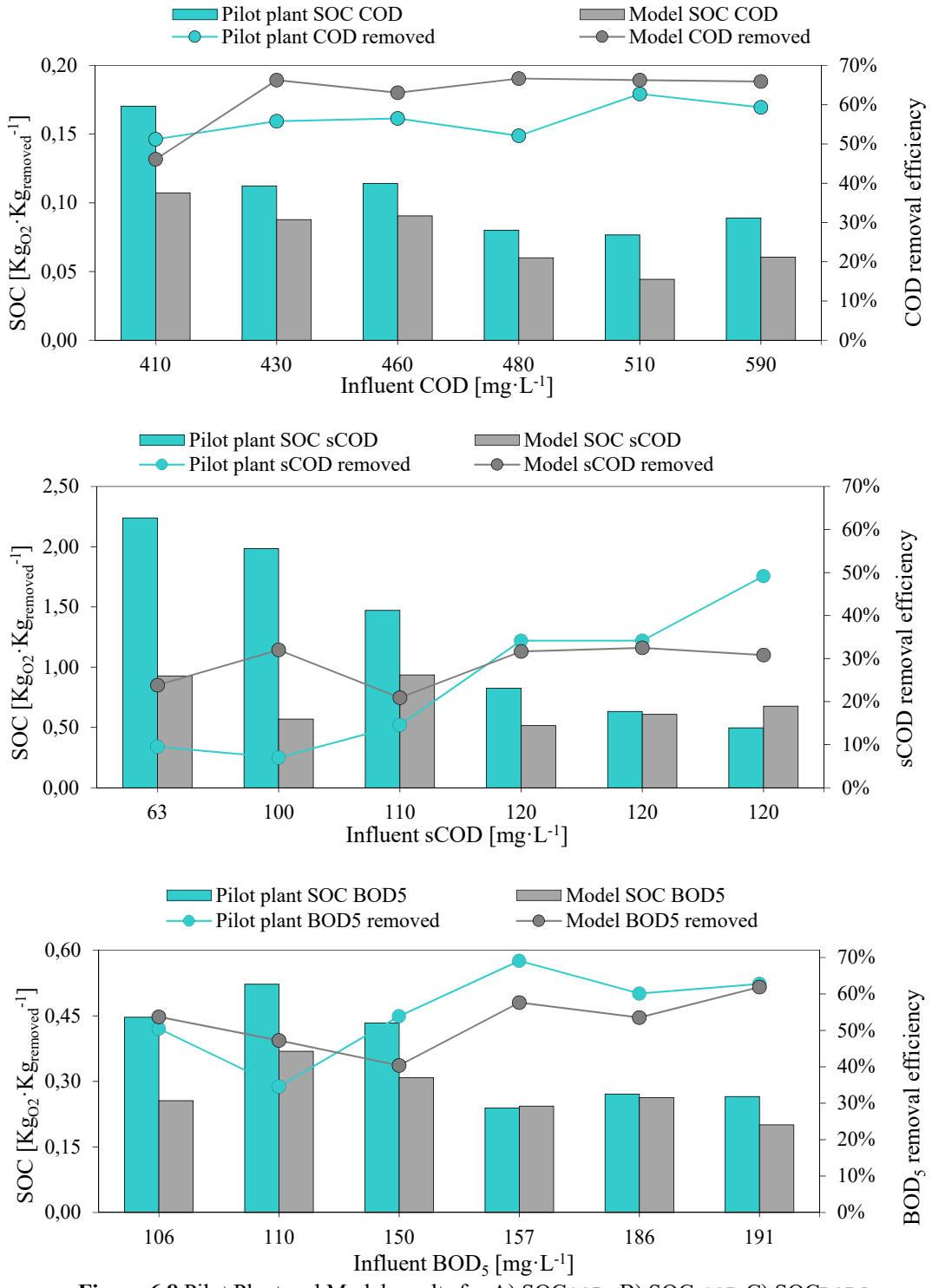

Figure 6.8 Pilot Plant and Model results for A) SOC$_{COD}$ B) SOC$_{sCOD}$ C) SOC$_{BOD5}$

6.3.7 Oxygen control system

Previous results raise one of the main questions of HRAS process design; what is the most effective method for controlling the oxygen supplied and minimalizing the SOC? The study highlights two situations that lead to high oxygen consumption, COD_{OXID}: i) days with a high sCOD influent fraction, such as Period 5 with a 32% of influent COD as $sCOD_{IN}$, resulting in a 14% COD_{OXID} (Table 4.1 and Figure 4.11), ii) hourly time periods with low COD_{IN}, like the 0-6 h periods, with only 17% of daily influent COD, promoting a 56%COD_{OXID} (Figure 6.7 B).

It is important to note that the pilot plant did not control sCODrem online and did not directly control the oxygen supplied. Instead, it controlled the oxygen concentration in reactor R2 to maintain a constant DO level and prevent anoxic and anaerobic conditions at the bottom of the clarifier. There are different approaches to control the oxygen supplied in the HRAS process: i) Maintain a constant DO in the reactor; ii) Keep the oxygen supply rate constant by fixing the position of the OAV; iii) Set a constant oxygen supply pattern for each hour based on process requirements; iv) Control the oxygen supply based on real-time sCOD measurements.

The pilot plant used the first approach, which ensures stable process operations and stability but does not guarantee a specific sCODrem value or optimize oxygen consumption. Implementing an oxygen supply control system based on real-time sCOD measurements could be a promising avenue for future studies.

Finally, the pilot plant operated with a low DO concentration of 0.5 ± 0.2 $mgO_2 \cdot L^{-1}$ to prevent deterioration of biomass settling characteristics and avoid anaerobic conditions in the settler. The concentration of oxygen in the reactor does not affect the theoretical oxygen demand but does impact oxygen transfer efficiency and reaction rates. Reported DO concentrations in HRAS reactors have ranged from 0.1 to 2 mg $mgO_2 \cdot L^{-1}$, as documented in studies by Rosso et al. (2019), Jimenez et al. (2015), and de Graaff et al. (2016). In the early stages of HRAS development, Böhnke (1997) suggested that HRAS could be operated near zero DO in a facultative mode, with the oxygen supplied solely by grit and grease removal processes in the preceding stages.

6.4 Finals remarks

The HRAS reveals a consistently low SOC across different parameters: 0.11 Kg_{O2}/Kg_{CODrem}; 0.38 $Kg_{O2}/Kg_{BOD5rem}$ and 0.65 $Kg_{O2}/KgsC_{ODrem}$, at average influent concentration of 480 $mg \cdot L^{-1}$ of COD, 150 $mg \cdot L^{-1}$ of BOD_5 and 117 $mg \cdot L^{-1}$of sCOD. A noteworthy negative correlation between SOC and COD, sCOD, and BOD_5 removal concentrations, underscores the HRAS process's heightened energy efficiency at elevated influent concentrations and his high removal associated. This positions HRAS as a potential replacement for the PC stage rather than a downstream treatment.

Operated with only 6.7% oxygen consumption of COD_{IN}, HRAS allows to send 54% of the COD_{IN} and 55% of the BOD_{5IN} to digestion. This results in a 14% increase in COD sent to digestion, increasing biogas production, and an equivalent reduction in COD sent to the CAS, reduction oxygen consumption. Operating at low DO levels (0.1 - 0.5 $mg \cdot L^{-1}$) prevents deteriorating biomass settling characteristics and the onset of anaerobic conditions in the settler.

A noteworthy negative correlation between the BOD_{IN}/COD_{IN} ratio and the SOC_{COD} and SOC_{BOD5} has detected. A higher BOD_{IN}/COD_{IN} ratio, indicative of more easily biodegradable wastewater, results in lower SOC. This implies that not only do COD_{rem} and BOD_{rem} affect the SOC, but also the biodegradability of influent wastewater plays a significant role.

The primary factor influencing the oxygen consumption COD_{OXID} is the sCODrem, while the major factor affecting the COD_W is not the COD_{OXID} but primarily the SS_{IN} and the SS_{IN} removal efficiency. High COD_{IN} loads promote maximum COD_W and minimum COD_{OXID}, and low COD_{IN} loads promote minimum COD_W and maximum COD_{OXID}.

The SOC in relation to sCOD, COD and BOD_5, is not a stoichiometric parameter like the oxygen demand for nitrification. Instead, it represents a global oxygen demand influenced by operational conditions, such as the influent concentration, which is the reason of its wide range of variation.

The study shows two situations that generate a high COD_{OXID}: i) High sCOD Influent Fraction and ii) Low COD_{IN} hourly periods. A reactor oxygen demand monitoring of 24 $h \cdot day^{-1}$ recommended to install an additional mixing system, to reduce energy and COD_{OXID} at low COD_{IN} periods.

The adopted model performs well in fitting SOC values in both pilot plant and model, with the exception of very low $sCOD_{IN}$ concentrations. While controlling oxygen supplied by reactor DO set point ensures safe operations and stability, it falls short of assuring a specific sCOD removal value or optimizing oxygen consumption. Proposing sCOD online monitoring as an oxygen supply control system presents a compelling challenge for future studies to mitigate COD_{OXID} during periods of high $sCOD_{IN}$.

Importantly, the HRAS process is positioned not as a final treatment guaranteeing permanent effluent quality but as a preliminary treatment. Its primary objective is to maximize COD sent to digestion with minimal oxygen consumption. Consequently, there is no singular operating condition meeting this objective, and the design is contingent on influent wastewater characteristics, particularly COD fractionation and subsequent nitrification-denitrification processes.

Chapter 7
RESULTS IV

Sludge Settleability in HRAS process

7.1 Overview

One of the limiting factors affecting the efficiency of the HRAS process is the settling capability of biological sludge, which correlates with carbon and nutrient harvesting. The main objective is to evaluate the settleability and thickening ability of HRAS waste sludge by analysing standardized characterization methods like SVI and zone settle velocity (ZSV) and determining the influence of clarifier biomass inventory in the HRAS process.

In order to achieve this goal, this chapter describes the results of the experimental study designed to evaluate the relationships between SVI, ZSV, OFR, and SLR concerning SS removal in the HRAS process. The pilot plant features a novel aspect with two clarifiers, 1.0 and 1.4 meters in diameter, allowing for the alteration of settling operational conditions without affecting the reactor's conditions. Maintaining a constant influent flow of 30 $m^3 \cdot d^{-1}$, the OFR for the 1.0 m diameter clarifier is set at 1.6 $m \cdot h^{-1}$, similar to PC's OFR, while for the 1.4 m diameter clarifier, it is set at 0.8 $m \cdot h^{-1}$, like to CAS clarifier's OFR.

7.2 Methodology

To quantify the effect of incoming SS in the HRAS process, we introduce the Solids Exchange Ratio (SER)**,** a rate between reactor biomass inventory and daily solids feed to the reactor, according to Equation 7.1

$$SER = \frac{MLSS_{reactor\ inventory}}{Q_{in} \cdot SS_{in}} \qquad \text{Equation 7.1}$$

To establish a clarifier model that enables the matching of sludge concentration and zone settling velocity, Zone Settling Velocity (ZSV) tests were conducted using the same sludge sample diluted to different initial MLSS concentrations. This resulted in a ZSV curve, plotted as Zone settling velocity versus initial solids concentration. The relationship between sludge concentration and ZSV can be described by the exponential decaying function, Vesilind Model (Vesilind, 1968).

$$V_{hs}(X) = V_0 \cdot e^{-r_h \cdot x} \qquad \text{Equation 7.2}$$

Where *Vhs(x)* is the ZSV of the sludge ($m \cdot h^{-1}$) at *x* solids concentration ($g \cdot L^{-1}$), V_0 is the calibration parameter corresponding to the maximum settling velocity ($m \cdot h^{-1}$) and r_h is the calibration parameter corresponding to the clarification zone ($L \cdot g^{-1}$).

Using this curve, Vesilind settling parameters V_0 and r_h were estimated by fitting the Vesilind exponential model to the experimental data. This fitting was done by minimizing the sum of the squared error between the model settling velocities and the measured settling velocities. The parameters V_0 and r_h provide information on the sludge settleability. The model calibration has been conducted with the R2 oxic sludge, following the Settling Test procedure by Torfs et al. (2016).

The total mass flux (SF_t) of solids in the clarifier is determined by combining the solids flux due to gravity (SF_g) and the solids flux resulting from bulk movement (SF_u).

$$SF_t = SF_g + SF_u \qquad \text{Equation 7.3}$$

$$SF_g = V_{hs} \cdot x \qquad \text{Equation 7.4}$$

$$SF_u = V_b \cdot x \qquad \text{Equation 7.5}$$

Where V_{hs} is ZSV of the sludges [m·h^{-1}] at X of solids concentration, Vb is the bulk downward velocity [m·h^{-1}], x is the solids initial concentration [g·L^{-1}].

Finally, to establish the Clarifier Stratification Model that allows to confirm the experimental SS stratification, a flux model with 5 layers was considered.

7.3 Results and Discussion

7.3.1 Solids Removal Performance Evaluation

This section provides an in-depth analysis of the long-term stability of the HRAS process, focusing on the daily evolution of suspended solids (SS) influent, SS effluent, and SS removal throughout the entire experimental duration.

Figure 7.1 illustrates the daily evolution of the influent and effluent concentration of SS (SSin, SSout), and the SS removal over the experimental period. Notably, the HRAS process acts as a filter for SSin peak loads, buffering these loads for subsequent activated sludge processes. Despite significant dispersion in SSin values (average 401 ± 176 mg·L^{-1}), the SSout values exhibit low dispersion (average 87±41 mg·L^{-1}). The maximum and average SS removal values are recorded at 1050 mg·L^{-1} and 315±175 mg·L^{-1}, respectively.

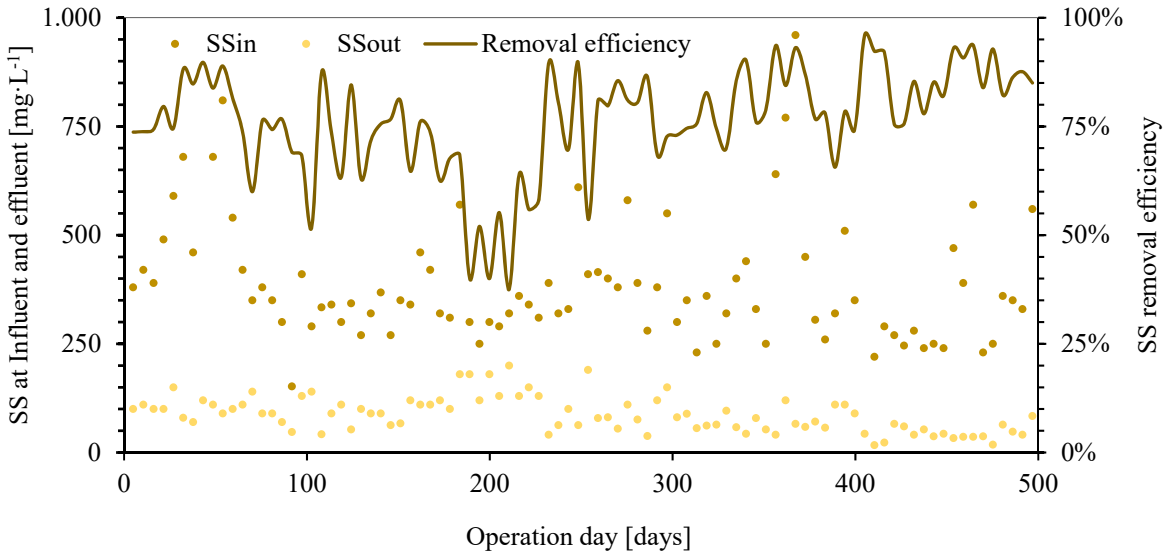

Figure 7.1 Daily variations of the SS concentration at the influent and effluent, and SS removal efficiency.

In the context of SS removal, it is essential to differentiate between the SS removal in the HRAS, named SSout and the SS removal in the clarifier. Figure 7.2 illustrates that the SS removed by HRAS exhibits lower and more dispersed values of 76 ± 11% compared to SS removed in the clarifier 96 ± 2%. This discrepancy is attributed to the relatively low variations in MLSS concentration. Interestingly, the SSout values demonstrate a low average value of 85 ± 38 mL·g^{-1} with high dispersion.

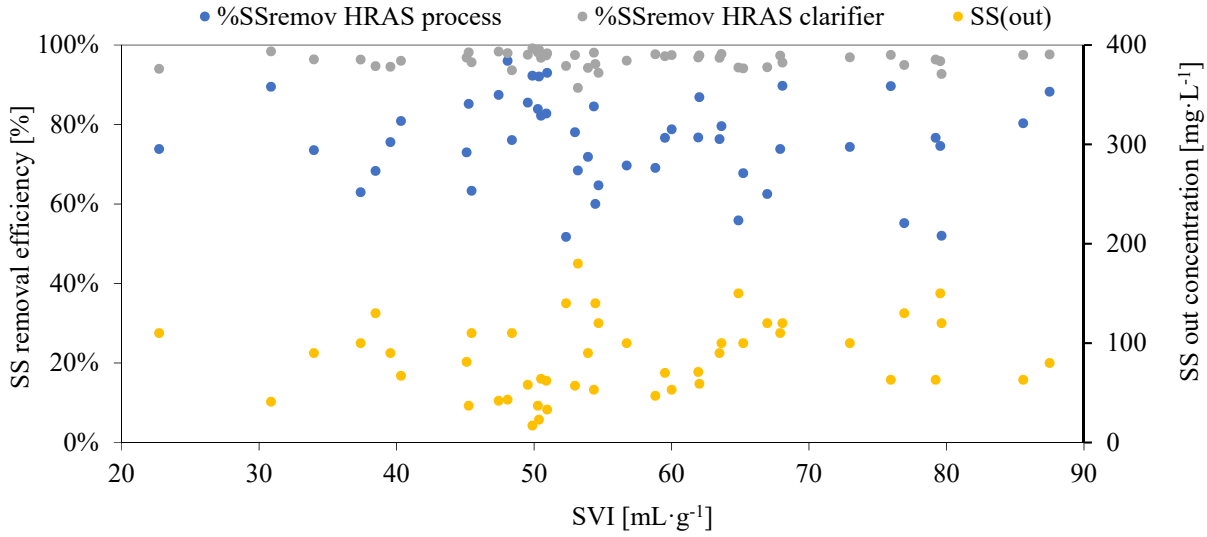

Figure 7.2. SS removal HRAS, SS removal Clarifier, and SS effluent at different SVI.

As shown in Figure 7.3, the regression line depicting the relationship between SS removal and SSin has a slope nearly m=1, which implies the existence of non-settling SS, irrespective of the SSin concentration. This observation aligns with the concept of dispersed growth, emphasizing the importance of thorough consideration of settling characteristics in the HRAS as it is observed pCOD removal (Figure 4.15b).

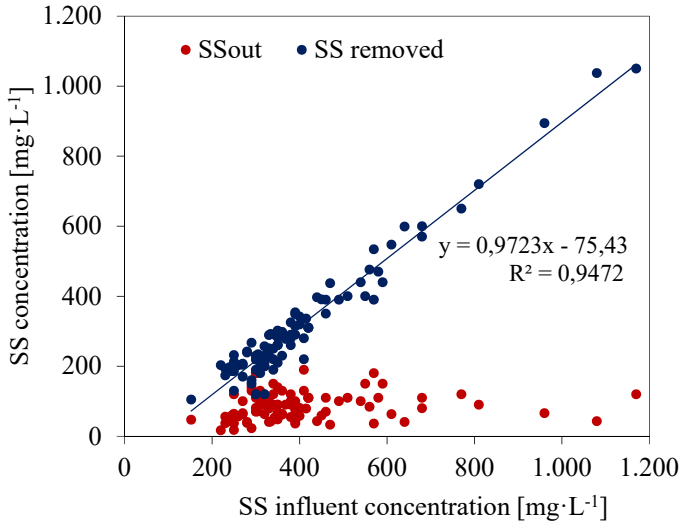

Figure 7.3 Relation between SSin concentration and SSout and SSrem

The HRAS process not only allows for the redirection of a larger SS amount to anaerobic digestion, 76 ± 12%, compared to PC (60–65%, (Crites and Tchobanoglous, 1998)), but it also effectively laminates influent SS loads to the activated sludge unit. This ensures stability and reduces the size of equipment needed to handle oxygen demand peaks in the downstream unit. The long-term stability evaluation demonstrates the adaptability of the HRAS process to handle varying SS loads, with efficient SS removal and biomass distribution. These findings contribute to a comprehensive understanding of the system's performance over extended operational periods.

7.3.2 Impact of Overflow Rate and Solids Loading on SS Removal

In this section, we delve into the crucial parameters of overflow rate (OFR), Solids Loading Rate (SL), and their impact on SS removal and effluent quality within the HRAS process. The average operating conditions and SS removal during different periods are outlined in Table 7.1. A comparison is made between the 1.0 m diameter clarifier with an OFR of 1.6 $m \cdot h^{-1}$, similar to PC's OFR, 1.2 - 2.0 $m \cdot h^{-1}$, and the 1.4 m diameter clarifier with an OFR of 0.8 $m \cdot h^{-1}$, similar to the OFR of secondary clarifier (0.66-1.6 $m \cdot h^{-1}$).

During periods with the 1.0 m diameter clarifier, SS concentrations in the effluent range from 91-119 $mg \cdot L^{-1}$, resembling those of PC (90-120 $mg \cdot L^{-1}$). Conversely, the 1.4 m diameter clarifier exhibits lower SSout concentrations of 44-69 $mg \cdot L^{-1}$ though higher than secondary clarifier in CAS systems of 20-30 $mg \cdot L^{-1}$. Particularly noteworthy is the observed increase in SS removal from 74% to 84% as the OFR decreases from 1.56 $m \cdot h^{-1}$ to 0.8 $m \cdot h^{-1}$. This trend underscores the positive impact of OFR reduction on enhancing SS removal efficiency.

The reduction in OFR is identified as a key factor in enhancing HRAS effluent quality. However, it is noted that while HRAS demonstrates improvement, it does not reach the same level as the CAS process. This phenomenon, referred to as dispersed growth, aligns with previous studies (James Bisogni and Lawrence, 1971, Miller et al., 2015) and is attributed to high SS effluent, emphasizing the importance of controlling OFR for discrete settling (class I) and flocculent settling (Class II).

Examining the impact of SL on effluent SS concentration, we observe notable variations. Periods with a 1.0 m diameter clarifier and SL of 147 $Kg \cdot m^{2} \cdot d^{-1}$, comparable to CAS's SL of 96-144 $Kg \cdot m^{2} \cdot d^{-1}$, present higher SSout concentrations of 91-119 $mg \cdot L^{-1}$ than CAS (20-30 $mg \cdot L^{-1}$). Conversely, periods with a 1.4 m diameter clarifier and lower SL of 70.7 $Kg \cdot m^{2} \cdot d^{-1}$ present a lower SSout concentrations of 44-69 $mg \cdot L^{-1}$ and very close to CAS (20-30 $mg \cdot L^{-1}$).

SL are directly correlated with OFR. However, in the pilot plant working conditions, SL has not been the limiting factor for SS effluent concentration (section 7.7.2). This highlight the greater impact of OFR reduction on enhancing SS removal efficiency.

Operating the 1.0 m diameter clarifier at specific conditions maintains clarifier stability, yielding an effluent similar to PC due to the low SVI (55±7 $mL \cdot g^{-1}$). However, it's essential to consider that

increasing the clarifier surface reduces SS effluent concentration and subsequently increases COD harvesting. A specific SSout concentration of 50 $mg \cdot L^{-1}$ aligns approximately with 70 $mg \cdot L^{-1}$ COD.

These findings underscore the importance of operational parameters in achieving desired effluent characteristics and contribute to optimizing the HRAS process for enhanced wastewater treatment.

Table 7.1. SS concentration, SSremoval efficiency, and operational clarifier parameters in each operation period.

Period	SSin [$mg \cdot L^{-1}$]	SSout [$mg \cdot L^{-1}$]	Removed [%]	Clarifier diameter [m]	OFR (Qin) [$m \cdot h^{-1}$]	SLR (Qin+Qr) [$Kg_{SS} \cdot m^{-2} \cdot d^{-1}$]	Temperature R2 [ºC]
1	586±228	103±20	81 ± 6	1.0	1.3	164	18.5
2	318±65	92±34	71 ± 10	1.0	1.6	155	22.1
3	357±89	113±37	68 ± 12	1.0	1.7	109	25.6
4	357±94	119±52	64 ± 18	1.0	1.6	156	26.3
5	387±96	91±42	77 ± 9	1.0	1.6	152	22.8
6	332±77	66±19	79 ±7	1.4	0.8	79	19.3
7	564±275	69±27	85 ± 7	1.4	0.8	75	18.9
8	411±285	65±36	81 ± 11	1.4	0.8	65	23.2
9	348±120	44±16	87 ± 5	1.4	0.8	64	20.1

7.3.3 HRAS Biomass

7.3.3.1 Solids Exchange Ratio

One pivotal distinction between HRAS and CAS lies in the impact of incoming SS on the biomass MLSS inventory (reactor). This impact can be quantified using the Solids Exchange Ratio (SER), defined as the ratio between biomass inventory and daily solids feed to the process (Equation 7.1). Under average working conditions in the HRAS pilot plant without PC, the SER ratio for HRAS was 0.17 d. In contrast, for an equivalent CAS process with PC (with an SS removal average of 60%), 8h HRT, and 3000 $mg \cdot L^{-1}$ MLSS in the reactor, the SER ratio is 4.54 d.

The significantly lower SER in HRAS of 0.17 d compared to CAS 4.54 d results in a biomass renewal in HRAS 26.7 times faster than in the CAS process. This underscores the substantial influence of influent SS in shaping the composition and concentration of biomass in the HRAS reactor. Conversely, the SRT of 0.28d in HRAS, compared to 8.0 d in the CAS process, highlights the brief duration of sludges in HRAS compared to CAS and the minimal impact of the short SRT in HRAS.

Figure 7.4 illustrates the 0.17 d of SER values for the HRAS pilot plant, indicating that incoming SS renew the biomass of 2.07 Kg SS in just 4.0 hours, and the 0.28 d SRT value, signifying that it takes 6.72 hours to renew the reactor biomass with waste sludges. As a result, the influence of incoming SS is 68% faster than the impact of SRT on the reactor biomass inventory. Consequently, the settling characteristics of the HRAS process are more governed by the settling properties of the influent SS than by those of the newly generated biomass.

In contrast, an HRAS with a PC upstream would have a greater SER, indicating that the influent HRAS has less influence on biomass composition. In this case, the new biomass produced by sCOD removal

would determine the settling characteristics. However, this strategy would necessitate the installation of two clarifiers, one for PC and one for HRAS, as well as the possibility of HRAS settleability being poorer.

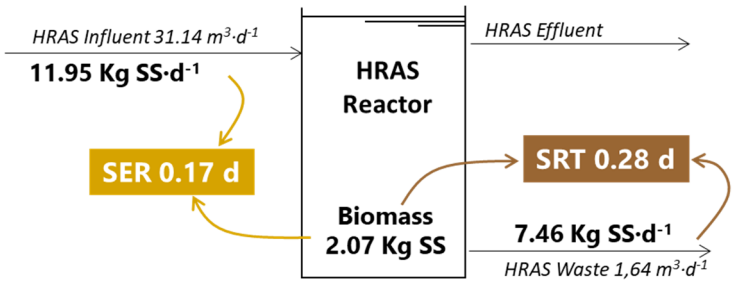

Figure 7.4 Solids Exchange Rate (SER) and Solids Retention Time (SRT) in a HRAS process

7.3.3.2 Microbial Composition of MLSS

In the course of this study, mixed liquor samples underwent microscopic examination to assess the presence of filamentous bacteria and protozoa, as depicted in Figure 7.5. Remarkably, over the 497-day operational period, no bulking phenomena were observed, even in the presence of a DO concentration of 0.2 mg·L^{-1}, aligning with the findings of Miller et al. (2016), who indicated bulking onset only below 0.1 mg·L^{-1} DO. The microbial community within the HRAS system exhibited a richness contrary to the notion proposed by Böhnke et al. (1997), who suggested that HRAS systems exclusively support the proliferation of the fastest-growing bacteria. In contrast, CAS systems were thought to support a diverse community that included bacteria, protozoa, and metazoa.

The presence of protozoa in the HRAS system could be a explained by the substantial impact of SS in the influent, encompassing both influent wastewater and the returns from sidestream solids treatment.

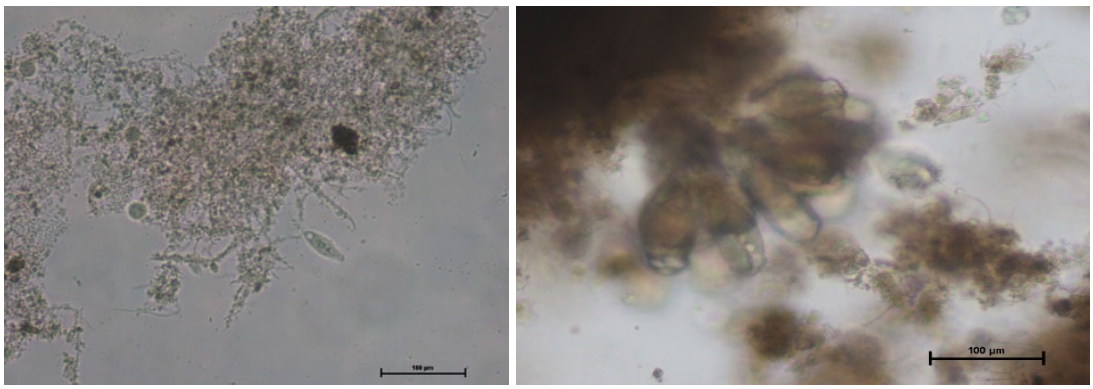

Figure.**7.5** HRAS biomass.

The low SER value can elucidate the persistence of protozoa in the HRAS system, despite a low SRT. Thus, the SER, reflecting the ratio between biomass inventory and daily solids feed, indicates a rapid turnover of incoming solids within the biomass. This revelation challenges preconceived notions about the limitations of HRAS systems in comparison to CAS systems, highlighting the resilience and diversity of the microbial community in HRAS.

7.3.3.3 Sludge Volume Index

This section delves into the significance of Sludge Volume Index (SVI) in characterizing sludge settleability, along with its impact on SS removal. SVI, a crucial parameter for assessing sludge settleability in biological processes, is examined in the context of the HRAS process.

The obtained SVI value of 55 ± 7 $mL \cdot g^{-1}$ (Table 3.4) stands in contrast to typical values in the CAS process 80-120 $mL \cdot g^{-1}$ (Crites and Tchobanoglous, 1998). This lower SVI indicates a quicker sludge settling in HRAS compared to CAS. Noteworthy references by Meerburg et al. (2016), Rahman et al. (2019), and Miller et al. (2016) support the low SVI values observed in HRAS, emphasizing its positive impact on settleability.

However, specific SVI values at 5, 10, 30 minutes time intervals of 118, 87, 56 $mL \cdot g^{-1}$ obtained in the HRAS pilot plant are higher than those for granular or heavily flocculated sludges (70, 60, 55 $mL \cdot g^{-1}$), indicating that means that HRAS settles more quickly than CAS but slower than granular sludges. This is characterized by a ratio SVI_{10}/SVI_{30} near one (Mancell-Egala et al., 2017). Figure 7.6 shows the settling test of de MLSS at 30 minutes. However, it should be considered that SVI is a good qualitative indicator of settling behavior, but does not provide quantitative information about effluent quality (Mancell-Egala et al., 2017), the effluent still contains non-settleable solids that are not characterized by SVI test.

Figure 7.6 HRAS biomass settling at 30 minutes.

7.3.4 Clarifier Sludge Stratification and Biomass inventory

A meticulous examination of sludge stratification was undertaken to ascertain the position of the sludge blanket position (SBP) within the clarifier. Figure 7.7 provides a visual representation of the main

clarifier dimensions and sample points' elevation for analysing SS concentration at different water heights.

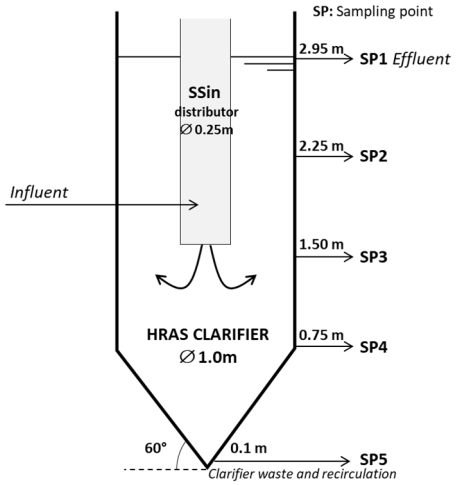

Figure 7.7 Clarifier dimensions and sample points elevation

Figure 7.8 illustrates that at an MLSS concentration of 1730 $mg \cdot L^{-1}$ in the reactor and a high ZSV of 5.8 $m \cdot h^{-1}$ (following Figure 7.10), the clarifier exhibits the SBP at a notably low height of 0.7 m, which is lower than that observed in the CAS clarifier 1.5 m.

Three different zones are identified in the HRAS clarifier. i) Upper Clarification Zone: Positioned between the sludge inlet level (1.5 m water level) and the water outlet level, this zone facilitates the removal of particles with low settling velocity. The concentration of SS transitions from 600 $mg \cdot L^{-1}$ at the lower level to 100 $mg \cdot L^{-1}$ at the higher level. ii) Sludge Settling Zone: Extending from the sludge inlet level to the beginning of the Conical Compaction Zone, this zone accommodates a concentration of SS at approximately 700 $mg \cdot L^{-1}$. iii) Sludge Compaction Zone: Located in the conical bottom of the clarifier, this zone exhibits a maximum SS concentration of approximately 5000 $mg \cdot L^{-1}$.

The ratio of MLSS (recirculation) to MLSS (reactor) was 2.9, aligning closely with the average value of 2.6 in the pilot plant, where MLSS (reactor) measured 2332 $mg \cdot L^{-1}$ and MLSS (recirculation) measured 5977 $mg \cdot L^{-1}$.

The lower waste concentration in HRAS, 0.6%, in contrast to the 1.0% in PC necessitates a more robust sludge thickening installation (Crites and Tchobanoglous, 1998). Any attempt to increase the waste concentration, be it by elevating the height of the SBP or spacing out waste times, poses the risk of potential redissolution of carbon stored in the cells, as indicated by (Rosso et al., 2019).

The sludge stratification in the clarifier allows for the quantification of the biomass inventory at 1.8 g MLSS, mirroring the biomass inventory in the reactor at 1.7 g MLSS. The overall HRAS biomass distribution, evenly split with 50% in the reactor and 50% in the clarifier, starkly contrasts with the CAS process, where 85-90% resides in the reactor and 10-15% in the clarifier. This distribution aligns with levels reported by Hauduc et al., (2019), at 60%-40%, respectively, underscoring the pivotal role

of the clarifier in the HRAS process. Furthermore, the biomass distribution in the clarifier delineates as 38% at the bottom, 28% below the influent point, 22% above the influent point, and 12% in the clarification zone, as illustrated in Figure 7.8.

Figure 7.8 also shows the SS clarifier stratification from Pilot Plant and Model, according the Chapter 11(Appendices C) and indicates the goodness of the simulation performed.

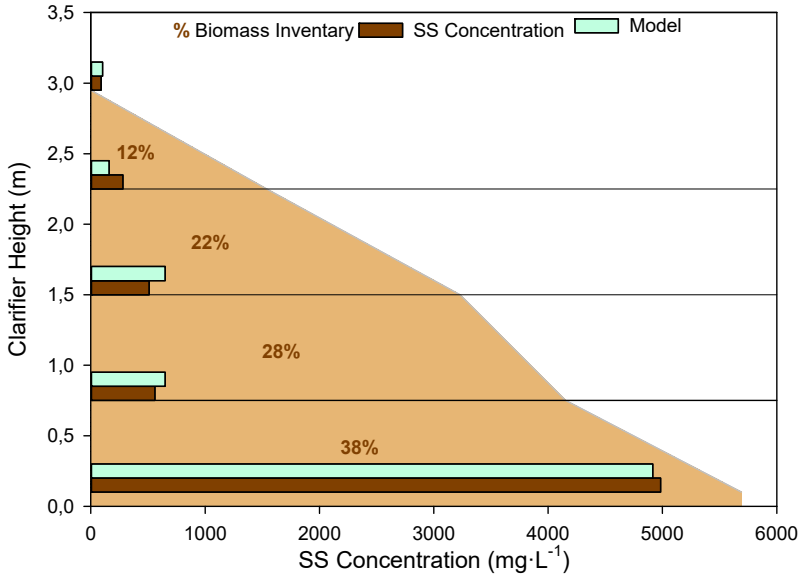

Figure 7.8 Clarifier sludge stratification and biomass inventory distribution

7.3.5 Settling Modelling and Solids Flux Analysis

7.3.5.1 Zone Settling Velocity Tests

To obtain more detailed information about the settling behaviour of a sludge sample, batch settling curve was employed. This curve allows for an investigation of the settling behaviour at various settling times (Torfs et al., 2016). ZSV tests were conducted using the same sludge sample diluted to different initial MLSS concentrations. At low initial SS concentrations, equal to or less than 1000 mgSS·L^{-1}, it is very difficult to determine solids interface, and these values are not included in the study.

Model calibration was carried out with R2 sludge reactor, following the Settling Test procedure outlined by Torfs et al. (2016). The test results are included in Tables 11.3. Figure 7.9 illustrates the interface height at different sludge concentrations and times, providing information solely on the settling behaviour at the sludge-water interface. The slope of the linear part of a batch settling curve in Figure 7.9 corresponds to the ZSV.

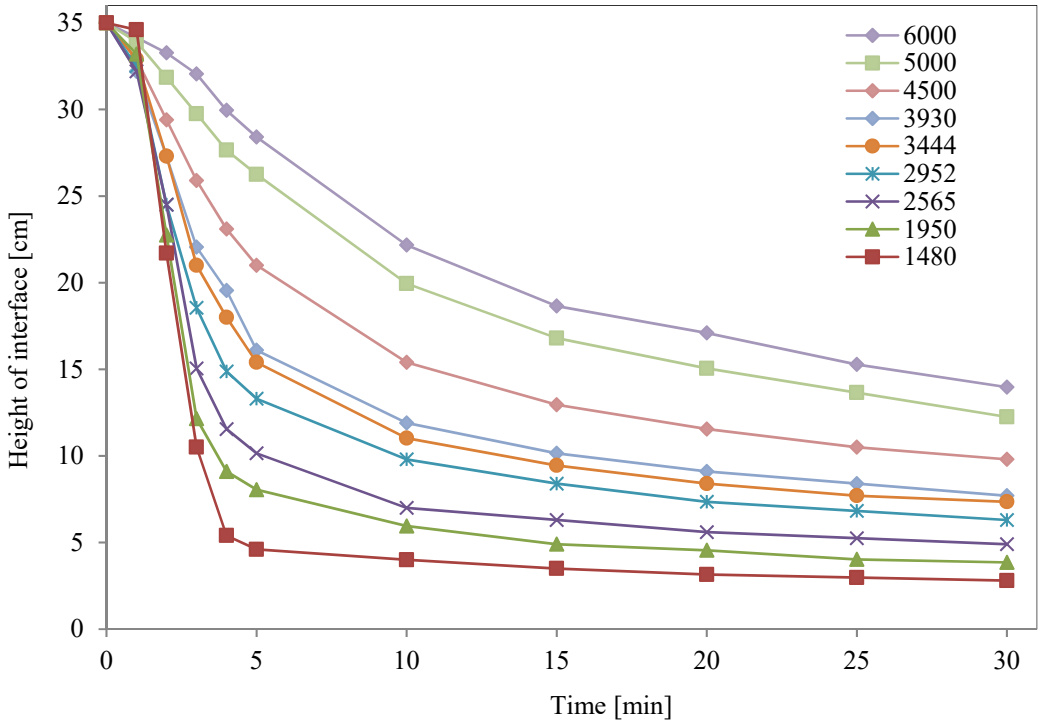

Figure 7.9 Interface height at different sludge concentration from 1480 to 6000 $mg_{MLSS} \cdot L^{-1}$ (0 - 30 minutes).

Figure 7.10 depicts the strong correlation between ZSV and MLSS sludge concentration. Circles represent experimental measurements from Figure 7.9, and the line represents the calculated ZSV after calibration of the function by Veselind Model. The calibration parameters of the Model obtained from Equation 7.2 are V_o = 12.02 $m \cdot h^{-1}$ and rh = 0.428 $m^3 \cdot kg^{-1}$, where V_o is the maximum ZSV, and rh is a model parameter. The calculated values obtained in the pilot plant are in line with those indicated by Miller et al. (2016) for a full-scale HRAS without PC.

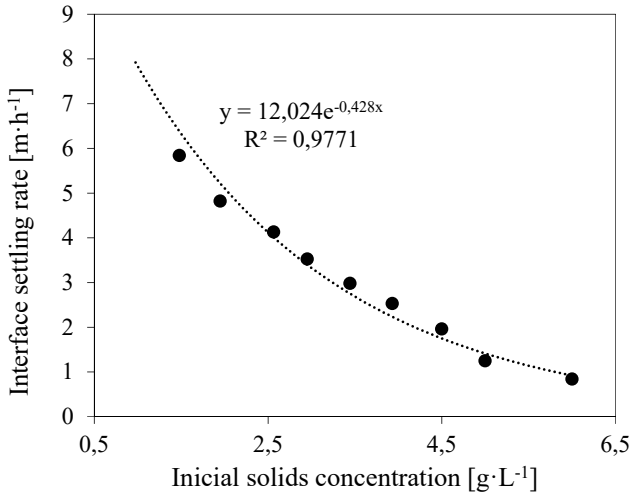

Figure 7.10 Zone settling velocity and initial sludge concentration

7.3.5.2 Solids Flux Analysis

For MLSS concentrations in the reactor ranging from 2000 to 2500 mg·L^{-1}, the corresponding ZSV calculated from the previous expression are 5.10-4.12 m·h^{-1}, respectively. These values are 54-96% higher than those reported by Torfs et al. (2016) in a CAS process (3.3-2.1 m·h^{-1}). Furthermore, an increase in MLSS concentration from 2000 to 2500 mg·L^{-1} in the reactor leads to a ZSV reduction of 36% in the CAS process and only 19 % in the HRAS process. This underscores the superior settleability of HRAS sludges compared to CAS sludges, as previously mentioned.

Additionally, the solids flux analysis was conducted using equations 7.3,7.4 and 7.5. Using the Vo and rh values obtained in the model, along with the MLSS concentration, the 0.78 m^2 surface area of the clarifier (1.0m diameter) and the recirculation rate of 0.7 m^3·h^{-1} (corresponding to 55% of Qin), a solids flux diagram for the pilot plant clarifier is depicted in Figure 7.11.

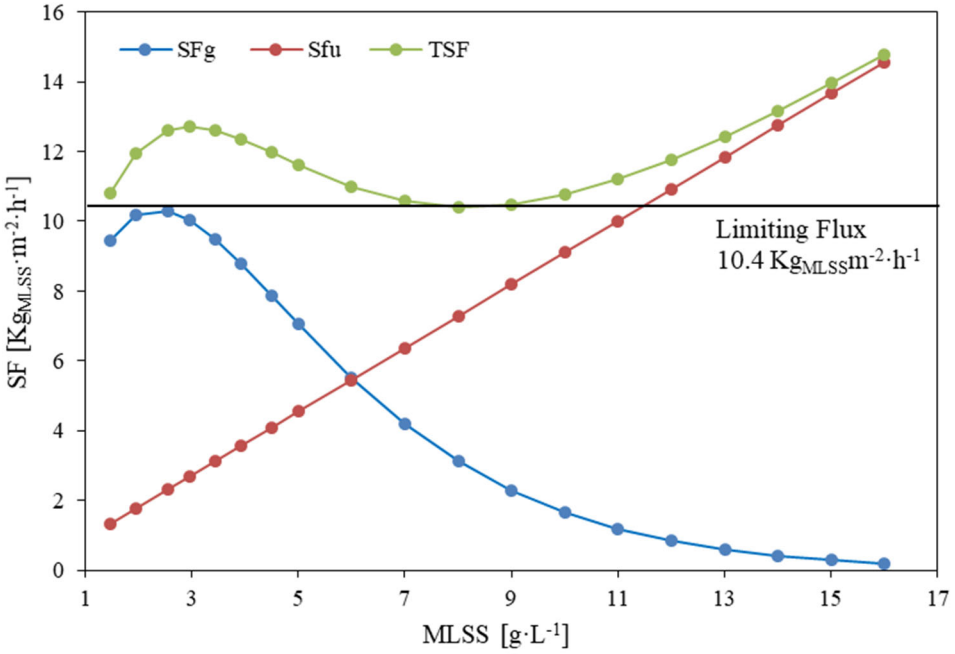

Figure 7.11 Solids Flux and Solids Concentration.

Figure 7.11 illustrates that the limiting acceptable solids flux of 10.4 Kg·m²·h^{-1} is higher than the average SL of 4.7 Kg·m²·h^{-1} and the maximum SL of 6.8 Kg·m²·h^{-1} applied in the pilot plant (Table 3.4). This confirms that the critical parameter for clarifier design is the Overflow Rate (OFR) instead of Solids Loading (SL). This opens the possibility of considering another typology of clarifier, such as a lamella clarifier, to enhance the efficiency of discrete flocculent settling in the upper part of the clarifier. Additionally, it's important to highlight that the maximum SFg occurred at an initial MLSS concentration near the operating MLSS concentration of 2000 mg·L^{-1}, a similar observation as reported by Miller et al. (2016). This high light the importance of MLSS concentration in sludge settleability and management.

7.3.6 HRAS Clarifier vs Primary and Secondary Clarifiers

The primary distinction between the HRAS clarifier, the primary clarifier (PC) and secondary clarifier (SC) lies in the nature and quantity of the SS input. Table 7.2 compares the main differences among the three clarifier technologies, including the controlling factors and influent features. In the PC, the incoming SS directly originate from the influent SS of the WWTP, ranging from 401 ± 176 $mg \cdot L^{-1}$ (Table 4.3). In contrast, the SS entering the HRAS clarifier consists of the HRAS reactor biomass, a mixture of biomass and incoming SSin, with a lower variation range of 2300 ± 400 $mg \cdot L^{-1}$ as discussed in (Table 4.3). In the SC for N/DN, the incoming SS are basically biological sludges with a lower variation range of 3200 ± 600 $mg \cdot L^{-1}$. This disparity of composition and range of variation promotes distinct settling mechanisms.

Table 7.2 Hydraulics, Load factors and Sludge characteristics for PC. HRAS clarifier and SC

Clarifier	Units	PC[a]	HRAS Clarifier[b]	SC[a]
SS in typology		WWTP SSin	WWTP (SSin + Biological)	Biological
SS in	[$mg \cdot L^{-1}$]	401±176	2311±401	3200±600
Settling class		Class I	ClassII+ClassIII+Class IV	ClassII+ClassIII+ClassIV
Gover . Settl . Class		Class I	Class II + Class IV	Class II + III
SVI	[$mL \cdot mg^{-1}$]	NA	60 – 80	80 – 120
HRT	[h]	1.5 -2.5	3	3
SL	[$KgSS \cdot m^{-2} \cdot d^{-1}$]	NA	60 – 160	100 – 150
OFR	[$m \cdot h^{-1}$]	1.2 -2-0	0.8 – 1.6	0.68 – 1.19
Q recir	[%]	NA	50 – 100	80 – 120
SS removed	[%]	55 – 60[c]	90[c]	99[c]
SS out	[$mg \cdot L^{-1}$]	100 – 200	60 – 120	20 – 25
sCOD out	[$mg \cdot L^{-1}$]	150 – 200	100 – 150	20 – 30
Controling factors		OFR+HRT	OFR+SBP	OFR+SL+SRT+SBP

[a] Clarifier Design WF (2010); [b] This thesis; [c] clarifier removal // Class I, II, III and IV according to Fig. 1.4. NA-not applicable

Another crucial difference between the technologies is the required effluent SS. While the HRAS clarifier and the PC set the SSout concentration according to the criteria of maximum harvesting of COD and minimum energy consumption, the SC must meet the legal standards ranging SSout concentration at 10-20 $mg \cdot L^{-1}$

PC design principles are based on discrete particle and flocculent settling analyses. Conversely, the HRAS settling tank, and SC, experiences different settling regimes simultaneously due to the high concentration of incoming SS and flocculated state. These regimes include discrete flocculent settling in the upper part, hindered settling (collective settling as a zone) in the incoming sludge, and compressive settling in the sludge blanket in the lower part. Consequently, SVI, ZSV, OFR, and SL exert a significant influence on SS removal in the HRAS settling tank, and SC, unlike in the PC, where the main control parameter is the OFR and the HRT.

PCs are designed to eliminate all settleable SS during average dry weather flow conditions. As settleable SS concentration is characteristic of wastewater, effective PC design starts with a thorough characterization of the wastewater. In removing settleable SS, PCs also eliminate the associated COD.

Key factors affecting PC performance include the characteristics of influent wastewater sludges basically SS concentration and percentage of settleable solids and the operational parameters, mainly the HRT and the OFR. The designer's challenge is to consistently produce PC effluent with an SS concentration equal to non-settleable SS concentration and a COD concentration equal to non-settleable COD concentration.

Key factors affecting HRAS clarifier and SC performance are: i) characteristics of reactor biomass like flocculation capacity lie to its SRT, which, in turn, influences SVI and ZSV ii) operational parameters such as SL, OFR, MLSS concentration, and recirculation flow iii) clarifier underflow concentrations that recommend operating the clarifier with a shallow sludge blanket (minimum thickening). The main difference between HRAS clarifier and SC are the higher SVI for HRAS clarifier (high ZSV), that means a quick interface settling. In the SC the key parameter is the SL, in contrast in the HRAS clarifier is the OFR. Another difference between HRAS clarifier and SC is the complexity positions the HRAS-clarifier as a system with intricate operational characteristics but with high potential for SS and COD removal associated with the adsorption of non-settleable and colloidal material, and storage of sCOD, due to the bulk higher concentration compared with CAS process.

7.4 Finals remarks

The HRAS process, characterized by a favourable settling profile with a SVI of 55±7 $mL \cdot g^{-1}$, allows for the design of a clarifier with an OFR of 1.6 $m \cdot h^{-1}$. However, for enhanced COD harvesting concerning high SS_{OUT}, it is advisable to consider a lower OFR in the range of 0.8-1.0 $m \cdot h^{-1}$.

The ZSV in HRAS, ranging from 4-5 $m \cdot h^{-1}$, surpasses that in the CAS process (2-3 $m \cdot h^{-1}$, indicating a more rapid interface settling. The effluent SS is correlated with OFR and remains independent of SVI. Notably, HRAS waste sludges exhibit a lower concentration of 0.6% compared to PC's 1.0%, emphasizing the potential benefits of the HRAS process.

Inadequate settling of sludge or undersized sedimentation processes can introduce a significant organic load downstream, limiting autotrophic nitrogen removal by fostering the growth of heterotrophic bacteria, which in turn compete with Ammonium-Oxidizing Bacteria (AOB) for dissolved oxygen and anammox bacteria for nitrite reducing nitritation rates and hinder the potential for autotrophic nitrogen removal. Caution must be taken to avoid carbon, nitrogen and phosphorous redissolution at the bottom of clarifier.

The low Solids Exchange Rate (SER) underscores that solids settling characteristics in HRAS are influenced by incoming solids rather than newly generated ones, diverging from the CAS process. The HRAS process fosters a rich community of bacteria and protozoa. Despite its observed benefits, the HRAS clarifier's intricate nature poses a challenge for full mechanistic understanding. Instead,

empirical models based on practical experience-driven rules and statistical testing are employed for describing and designing secondary settlers in HRAS.

The overall HRAS biomass distribution, split with 50% in the reactor and 50% in the clarifier, underscoring the pivotal role of the clarifier in the HRAS process.

Chapter 8
GENERAL DISCUSSION

This chapter discusses the fundamental knowledge reported in chapters 4, 5, 6 and 7, in order to consider his technical implications. To achieve this goal, within the framework of chapter 8 we have applied our results in a real case study to quantify the energy saved in a WWTP with N/DN, applying the HRAS process.

Wastewater characteristics as a key factor for HRAS design

Understanding the influent wastewater characteristic is crucial for selecting and designing the best HRAS available technology among HRAS A-stage, HRAS-CS or HRAS-SBR, in order to maximize the carbon and nutrients harvesting. Specifically, this thesis points out the direct correlation between the influent concentration and the removal of pCOD and COD, which highlights the recommendation to use the HRAS A-Stage process as a replacement of the PC and not as a downstream treatment afterward. Previous research recommendations based on the limitations of biomass inventory support the use of HRAS A-Stage for treating raw wastewater with high-strength influent, while the use of HRAS-CS is suggested for low influent COD concentrations, such as CEPT effluent and PC effluent (Rahman et al., 2017).

As presented in Chapter 5, the analysis of COD influent and fractions removal over six-hour periods reveals distinct daily patterns that affect the HRAS performance. This should be considered mainly for the design of the oxygen supply system so that the oxygen dosing is optimized as function of the COD influent. Like COD, the nutrients removal efficiency is affected by their influent concentration. The interplay between nitrogen and COD concentrations at the HRAS effluent conform the COD/TKN ratio, which is of paramount importance in the mainstream nitrogen removal technologies. Thus, COD oxidation could be adjusted to fit the most sustainable process.

This thesis points out the persistence of protozoa in the HRAS system despite the low SRT. These finding challenges previous conceptions about the limitations of HRAS systems in comparison to CAS systems. HRAS would have a resilient and divers microbial community originated from the influent wastewater, especially from the dewatering sidestream returns, as indicated by Böhnke et al., 1997 in their first studies.

The impact of influent characteristics on the HRAS performance is further emphasized by the low HRT (below 60 minutes) and the consequent low dilution factor in the reactor. Unlike CAS and N/DN process, that basically run at effluent concentration, the HRAS are more sensitive to influent variations. The operation of the pilot plant in dry and wet weather conditions, with a 1.3 peak average flow demonstrates the need for strategies to handle hydraulic overloads, which could prevent from biomass washout (Clark et al 2009).

In turn, the collecting systems and conditions (e.g. gravity, pumping and their length) have a determinant effect over the COD fractioning in the influent wastewater ((Wilén et al., 2006). Also,

temperature affects the fermentation rates and consequently increases the sCOD removal, as well as the storage of COD fractions by AHO organisms (Hauduc et al., 2019).

Therefore, a detailed characterization of the influent parameters including COD, Nitrogen and Phosphorus fractions, and their daily and seasonal variations, is essential for effective HRAS design and operation.

Operational mechanisms and removal efficiency

The primary distinction between PCs and HRAS systems lies in their operational mechanisms. PCs primarily remove settled particulate COD, nitrogen, and phosphorus through a discrete flocculant settling process (Torfs et al., 2016). In contrast, HRAS functions as a biological process with a low SRT, facilitating various mechanisms such as the adsorption of the soluble fraction in the biomass, the oxidation of the soluble fraction, the trapping of colloidal and particulate fractions in the biomass, and hindered settling of biological flocs at a constant influent MLSS concentration of 2000 $mg \cdot L^{-1}$, which enhances the flocculation. The elevated sludge concentration in HRAS fosters more collisions between particulate materials, resulting in better settling with larger flocs. Despite the low SRT of HRAS, it allows effective adsorption and trapping of colloidal and particulate fractions from the influent (Yetis and Tarlan, 2002).

HRAS proves to be a good strategy for redirecting and harvesting organic matter and nutrients, achieving a remarkable 57±9% removal of COD and 23±10% of TKN and 56±12% of TP. This redirection contributes to a substantial 20% increase in the COD sent to digestion, enhancing the biogas production, and 20.5% reduction in the TKN directed to the CAS process, resulting in decreased oxygen consumption, compared to PC efficiency.

However, the removal efficiency varies for soluble and particulate COD, TKN and TP fractions. COD and TP present high removal efficiencies in their particulate forms (74±10% and 66±12% respectively) but a lower removal efficiency in soluble form (29±12% and 23±17%). In the other hand, TKN presents low removal efficiency in in its particulate form (34±15%) and even lower in its soluble form (7±7%).

Regarding COD fractions removal, the study confirms that soluble COD removal correlates well with its influent concentration and is controlled by a biological oxidation-storage process, as reported by Hauduc et al. (2019). The study also confirm that colloidal COD removal correlates with the influent concentration according to first-order kinetics, unlike the zero-order kinetics proposed (Bunch and Griffin Jr., 1987). However, the removal efficiency of particulate COD does not correlate well with the influent concentration. The removal of particulate COD, which controls the overall COD removal because of its largest contribution, is associated with the adsorption onto biomass flocs by electrostatic interactions resulting from biological activity. Due to the high sludge settling properties of the process, the SL and the OFR do not affect the performance of particulate COD removal efficiency, but the OFR affects the effluent suspended solids concentration. While the HRAS process acts as a filter for influents

peak loads of particulate COD, it does not buffer soluble COD peak loads, which is particularly relevant for the subsequent denitrification.

Concerning the TKN fractions removal, the study confirms negative removal values for $N\text{-}NH_4^+{}_{in}$ up to 35 $mg \cdot L^{-1}$, probably due to $N\text{-}NH_4^+$ formation by sludge fermentation in the bottom of the clarifier. The $N\text{-}NH_4^+$ formation exceeds that removed by biomass growth. However, the removal becomes positive above this value, with an increasing percentage of removal. OrgN removal does not correlate with the influent concentration. The 34% OrgN removal efficiency compared to the 74% and 66% for particulate COD and phosphorous respectively, suggests that OrgN is not linked to settled materials. Thus, HRAS process does not act as a filter for particulate and soluble nitrogen fractions, like it does for particulate COD, promoting a decrease of COD/TKN ratio, and worsening the denitrification process. A challenge for future research could involve the study of mechanisms to improve the OrgN removal, which is the 45% of the incoming TKN.

Regarding TP fractions removal, the study confirms negative removal values for $P\text{-}PO_4^{3-}$: for concentrations values up to 2 $mg \cdot L^{-1}$, the $P\text{-}PO_4^3$ formation was higher than that removed by biomass growth probably due to $P\text{-}PO_4^{3-}$ formation by sludge fermentation in the bottom of the clarifier. Above this value, the removal was positive, with an increasing percentage of removal, similarly to what is reported for $N\text{-}NH_4^+$. The study also confirms that OrgP removal efficiency correlates with its influent concentration. The OrgP removal, which controls the overall TP removal because of its largest contribution, is usually associated with the adsorption onto biomass flocs, similar to particulate COD. In this case, the HRAS process filters the influent peak loads of OrgP, but it does not buffer $P\text{-}PO_4^{3-}$ peak loads, which is particularly relevant for achieving the requiered TP quality in the final WWTP effluent.

In summary, our results suggest that the removal of $N\text{-}NH_4^+$ and $P\text{-}PO_4^{3-}$ mainly occurs through assimilation, while soluble COD removal occur through bioaccumulation via intercellular storage, microbial growth, and carbon oxidation. This study reports a $sCOD/N\text{-}NH_4^+$ mass ratio of 16.6 $g \cdot g^{-1}$, higher than the 11.5 $g \cdot g^{-1}$ estimated from biomass formula $C_5H_7O_2N$ (Henze et al., 2015), suggesting a possible soluble COD intracellular storage. Furthermore, the high and similar particulate COD (74±10%) and OrgP (66±12%) removal efficiencies points out that their removal mechanisms are controlled by settling efficiency. However, the low OrgN (34±15%) removal efficiency suggests that not all the OrgN a linked to settled material, and further study should be performed to improve this nitrogen fraction elimination.

Thus, the HRAS not only saves energy by harvesting COD to anaerobic digestion, but it also saves energy by harvesting TKN for side-stream treatment with low energy consumption.

Control strategies for optimized oxygen consumption and process stability

The main objective of HRAS process, diverges from CAS and N/DN process. While the conventional approaches priorize the final effluent quality, HRAS process aims at maximizing the harvesting of COD minimizing the oxidation. Therefore, the oxygen control system is fundamental in HRAS to optimize the COD management.

The study of the Oxygen Uptake Rate (OUR) and the Specific Oxygen Consumption (SOC) shows insights of the nature of the oxygen utilization in the HRAS pilot plant. In this sense, the examination their relation with the operational parameters and the influent COD concentration permits to analyze the oxygen demand and the performance of the system. A noteworthy negative correlation between SOC and influent COD, sCOD, and BOD_5 underscores the energy efficiency of the HRAS process, particularly at elevated influent concentrations. It was also observed that BOD_{IN}/COD_{IN}, as measure of the influent wastewater biodegradability has a negative correlation with the SOC_{COD} and SOC_{BOD5}, indicating that both the concentration and the biodegradability of the organic matter influent affect the SOC.

Despite the potential of OUR as control parameter for carbon redirection and harvesting, the variability of wastewater characteristics challenges the control system. Initially, the positive correlation between OUR and COD oxidation suggests a potential alternative to MLSS control for process optimization. However, the applicability of OUR as control parameter in high-strength raw wastewater is questionable due to the significant diurnal variation in the influent loading rate, that needs a highly sensitive OUR set up (Rahman 2017).

Moreover, SOC has a dynamic nature due to the variation of the global oxygen demand influenced by operational conditions and influent COD concentration and fractions. SOC variations highlight that it is not a stoichiometric parameter like the oxygen demand for nitrification. The study points out the difference between the SOC_{COD} calculated by the OUR (from the DO monitoring) and the SOC_{COD} calculated by the COD_{OXID} (from the balance CODIN-CODOUT-CODW), controlled by the CODW, to maintain constant MLSS to ensure process stability. As a result, the process stability has been prioritized over maximizing the efficiency in the management of the COD.

The hourly variations in the COD load along the day have a significant impact on the oxygen consumption, with notable fluctuations observed in the wasted and oxidized COD. The identification of situations that generate a high percentage of COD oxidation, such as the high soluble COD influent and low COD concentration inlet, suggests the potential for the additional oxygen control strategies, including the sCOD online monitoring.

Therefore, while current control mechanisms ensure operational safety and stability, they may fail in optimizing oxygen consumption, and the proposition of sCOD online monitoring as an oxygen supply control system presents a compelling challenge for future studies to mitigate COD_{OXID} during periods

of high $sCOD_{IN}$. The reduction of the MLSS set point concentration in the reactor could increase COD_W, but MLSS below 1500 $mg \cdot L^{-1}$ worsens the sludge settleability.

The operation strategy of maintaining low DO prevented the deterioration of the biomass settling characteristics while avoiding anaerobic conditions in the settler and improving the oxygen transfer efficiency. This aligns with the goal of operating near facultative mode, with oxygen supplied solely by grit and grease removal processes in the preceding stages (Böhnke et al., 1997).

In conclusion, the HRAS pilot plant's process control strategy centers on maintaining a stable biomass concentration despite the challenging conditions, including short SRT and HRT. This self-controlling mechanism adapts to variations in influent raw wastewater composition, showcasing its resilience under extreme operational conditions. The significance of Solids Exchange Rate (SER) questions the traditional emphasis on SRT, emphasizing that solids inventory is more influenced by incoming solids than newly generated ones. The use of biomass concentration as a control parameter, as opposed to historical reliance on SRT, aligns well with SER findings, ensuring stability and adaptability in the HRAS process.

Sludge settleability and clarifier efficiency

The settleability of the biological sludge is a critical factor influencing the efficiency of the HRAS process, with implications for carbon and nutrient harvesting. While HRAS systems are generally known to present poor settling capacity, our study obtained a SVI value of 55 ± 7 mL·g-1, in contrast with typical values of 80-120 mL·g-1 observed in the CAS process. This suggests that HRAS processes may facilitate quicker sludge settling, as supported by literature references (Kinyua et al., 2017b; Meerburg, 2016; Miller et al., 2015; Rahman et al., 2019).

However, high SVI value (> 150 $mL \cdot g_{TSS}^{-1}$) was observed in HRAS with a contact-stabilization typology (CS) treating low-strength wastewater, like the PC and CEPT effluent (Miller et al., 2015; Rahman et al., 2017). This makes it advisable to use the HRAS process as a replacement of the PC stage rather than a downstream treatment.

The difference in SVI between HRAS and secondary clarifier (SC) lies in variations in the nature and quantity of the SS input. In HRAS clarifier, the incoming SS consist of a mixture of biomass and influent SS with a concentration range of 2300 ± 400 $mg \cdot L^{-1}$, whereas SCs primary receive biological sludges in a concentration range of 3200 ± 600 $mg \cdot L^{-1}$. This difference is likely to contribute to the better settling observed in HRAS, potentially due to the fact that raw influent SS are trapped in biological sludges causing densification.

The HRAS clarifier presents the same settling regime than SC, including discrete flocculent settling in the upper part, hindered settling in the incoming sludge, and compressive settling in the sludge blanket of the lower part. However, the HRAS clarifier present a higher Zone Settling Velocity compared to

SC, which could be attributed to the lower Solids Exchange Ratio (SER) of HRAS process. Increasing the SRT, that leads to increasing SER and oxidation of COD, can reduce the settling characteristics.

The clarifier's efficiency depends not only on sludge settleability and sludge harvesting but also on the SS effluent quality. The reduction in OFR is a key factor in enhancing the HRAS effluent quality, although its efficiency increase may not reach that of the CAS clarifier dues to the dispersed biomass growth and the worse flocculated sludge at low SRT. The SRT increase promotes a reduction of SS in the effluent along with an increase of COD_{OXID}, however the optimum COD harvesting corresponds with a COD_{OXID} of 3-4% and worse SS_{OUT} quality (Jiménez, 2015; Wett et al, 2020). Furthermore, the long-term stability of the HRAS process acts as a filter for influent SS peak loads, buffering its concentration to CAS process. Influent SS peaks are meanly coming from side-stream WWTP solids treatment, which constitute the main source of HRAS process instability.

Bulking sludge was not observed operating at low DO levels (0.1 - 0.5 $mg \cdot L^{-1}$), which contradicts the sludge bulking theory (Martins et al., 2004). The HRT should be limited to avoid the redissolution of COD, nitrogen and phosphorous at the bottom of clarifier. A rapid extraction of the settled sludge is recommended to prevent the formation of a sludge blanked layer.

The pilot plant was operated in dry and wet weather with a 1.3 peak average flow. Highest peak flows in wet weather could cause the washing of reactor biomass. Moreover, HRAS operates at a SRT approaching the washout SRT conditions based on the maximum growth rate of biomass (Nogaj et al., 2015). The handling of these hydraulics overloads should be studied in larger scale hydraulic work (Clark et al., 2009). Rahman *et* al. (2017) suggested the use of HRAS-CS to avoid the biomass washout reserving the biomass in the stabilizer reactor. A challenge for future research is the study of alternative clarifiers to take advantage of the high ZSV and improving the overflow quality. An inclined plate settler (IPS) (Zhang et al., 2021) could be a good alternative to improve overflow quality and footprint reduction.

Energy and footprint savings analysis

In this section, we delve into the comprehensive assessment of energy and footprint savings derived from the adoption of the High-Rate Activated Sludge (HRAS) process in wastewater treatment plants (WWTPs), particularly in comparison to conventional methods such as primary clarifiers (PC). By analyzing data obtained from pilot plant experiments and simulations using the SUMO simulator, we aim to elucidate the potential benefits of transitioning to HRAS, coupled with ancillary processes like the Anammox process in the sidestream.

Through a systematic examination of COD and nitrogen flux distribution, as well as specific energy consumption and production values, we aim to quantify the energy savings achievable with HRAS implementation, considering factors such as oxygen consumption, nutrient removal efficiency, and biogas generation.

Figure 8.1 illustrates the distribution of carbon (COD) and nitrogen (TKN) flux for a conventional WWTP comprising PC + N/DN + Anaerobic Digestion, while Figure 8.2 depicts the same for an advanced WWTP incorporating HRAS + N/DN + Anaerobic Digestion + Anammox in the sidestream. In both cases, identical influent wastewater properties (summarized in Table 8.1) and effluent quality (10 $mg \cdot L^{-1}$ of TN and 1 $mg \cdot L^{-1}$ of $N\text{-}NH_4^+$) were considered. Anaerobic digestion is presented separately from PC, HRAS, and secondary sludge to emphasize the difference in efficiency in converting sludge COD to biogas COD. The evaluation was conducted for a WWTP with a capacity of 24000 $m^3 \cdot d^{-1}$. Table 8.1 provides a summary of the main characteristics of the influent wastewater considered.

The analysis incorporates specific COD removal rates for each treatment stage: 58.7% in HRAS, based on the average value from pilot plant data, and 46% in PC, which exceeds the typical rate of 40%. For anaerobic digestion, the removal rates range from 60-65% for primary sludge and 30-45% for biological sludge. Additionally, it accounts for a 60% harvest of solids in PC, HRAS, and the biological sludge thickener.

Both solutions employ the same process and specific oxygen consumption for nitrogen removal, with no consideration of chemical phosphorus removal. The specific equivalences utilized for electrical consumption and generation are standardized: specific electrical consumption is set at 0.78 $Kwh \cdot KgO_2^{-1}$, considering conditions of 20ºC, 5 m reactor water depth, and fine bubble membrane air diffusers. Meanwhile, specific power production is calculated at 4.86 $Kwhe \cdot KgCH_4^{-1}$, factoring in a 35% electrical cogeneration efficiency and a lower CH_4 calorific value of 13.9 $Kwh \cdot KgCH_4^{-1}$.

The **c**arbon and nitrogen flux distribution show that HRAS process as an alternative to PC and Anammox in the sidestream allows:

i) 10.7% increase in the COD harvested compared to PC

ii) 9.9% reduction in the oxygen consumption for COD removal in N/DN

iii) 17.7% reduction in the TN that must be removed in N/DN

iv) 6.3% increase in the COD available for cogeneration

It is important to note the difference in the efficiency of converting sludge COD to biogas COD: 67% for HRAS sludge and 40% for N/DN sludge, highlighting the importance of maximizing COD removal in the HRAS process.

Finally, it is important to point out that the $Kwh \cdot KgCOD^{-1}$ ratio depends on the COD destination. Figure 8.3 shows that the COD harvested from the water line and sent to anaerobic digestion (10.73 $KgCOD \cdot d^{-1}$) allows to obtain 0.83 $Kwh \cdot KgCOD^{-1}$, while the COD sent to the N/DN process (7.846 $KgCOD \cdot d^{-1}$) demands 0.73 $Kwh \cdot KgCOD^{-1}$. In short, each Kg of COD harvested in the HRAS process and send to anaerobic digestion leads to a saving of 1.56 $Kwh \cdot KgCOD^{-1}$.

Total energy saves with HRAS and Anammox in the sidestream could be obtained from carbon and nitrogen flux distribution and the equivalence in electrical energy consumed and generated previously indicated. Table 8.2 shows the electricity consumption and electricity production in the two-alternative process, including all the energy consumptions in the WWTP, not only the associated with the biological process.

The implementation of the HRAS process instead of PC, together with the use of the Anammox process in the side-stream, represents an important step in the reduction of the WWTP electricity consumption, allowing a saving of 40% of the total consumption of the WWTP. This value is associated with the specific influent wastewater (Table 8.1).

Table 8.1. Influent characteristics.

Parameter	Acronym	Value	Units
Chemical Oxygen Demand	COD_{IN}	725	$mg \cdot L^{-1}$
Particulate Chemical Oxygen Demand	$pCOD_{IN}$	480	$mg \cdot L^{-1}$
Colloidal Chemical Oxygen Demand	$cCOD_{IN}$	58	$mg \cdot L^{-1}$
Soluble Chemical Oxygen Demand	$sCOD_{IN}$	187	$mg \cdot L^{-1}$
Biochemical Oxygen Demand	BOD_{5IN}	334	$mg \cdot L^{-1}$
Total Suspended Solids	TSS_{IN}	398	$mg \cdot L^{-1}$
Volatile Suspended Solids	VSS_{IN}	321	$mg \cdot L^{-1}$
Total Kjeldahl Nitrogen	$N\text{-}TKN_{IN}$	74	$mg \cdot L^{-1}$
Ammonium Nitrogen	$N\text{-}NH_4^{+}{}_{IN}$	48	$mg \cdot L^{-1}$
Total Phosphorous	TP_{IN}	9,7	$mg \cdot L^{-1}$
Orthophosphates	$P\text{-}PO_4^{3-}{}_{IN}$	2	$mg \cdot L^{-1}$
Reactor Temperature	T	20	°C

Additionally, the implementation of the HRAS Process, instead of the PC, entails modifications of the reactors volume (Table 8.3) a 34% reduction in the volume of the water line, and an increase of 9% in the volume of the anaerobic digestion. This data is important not only in terms of construction costs but also in the footprint reduction.

In conclusion, the HRAS process, with its innovative control strategies, proves effective in redirecting and harvesting organic matter, showcasing resilience under extreme conditions. The process's adaptability and stability, as evidenced by its self-controlling mechanism and adherence to biomass concentration as a control parameter, challenge conventional notions of SRT importance. The interplay of soluble and non-soluble COD removal, along with biomass efficiency, positions HRAS as a promising replacement for traditional treatment stages, providing not only effective wastewater treatment but also potential energy savings.

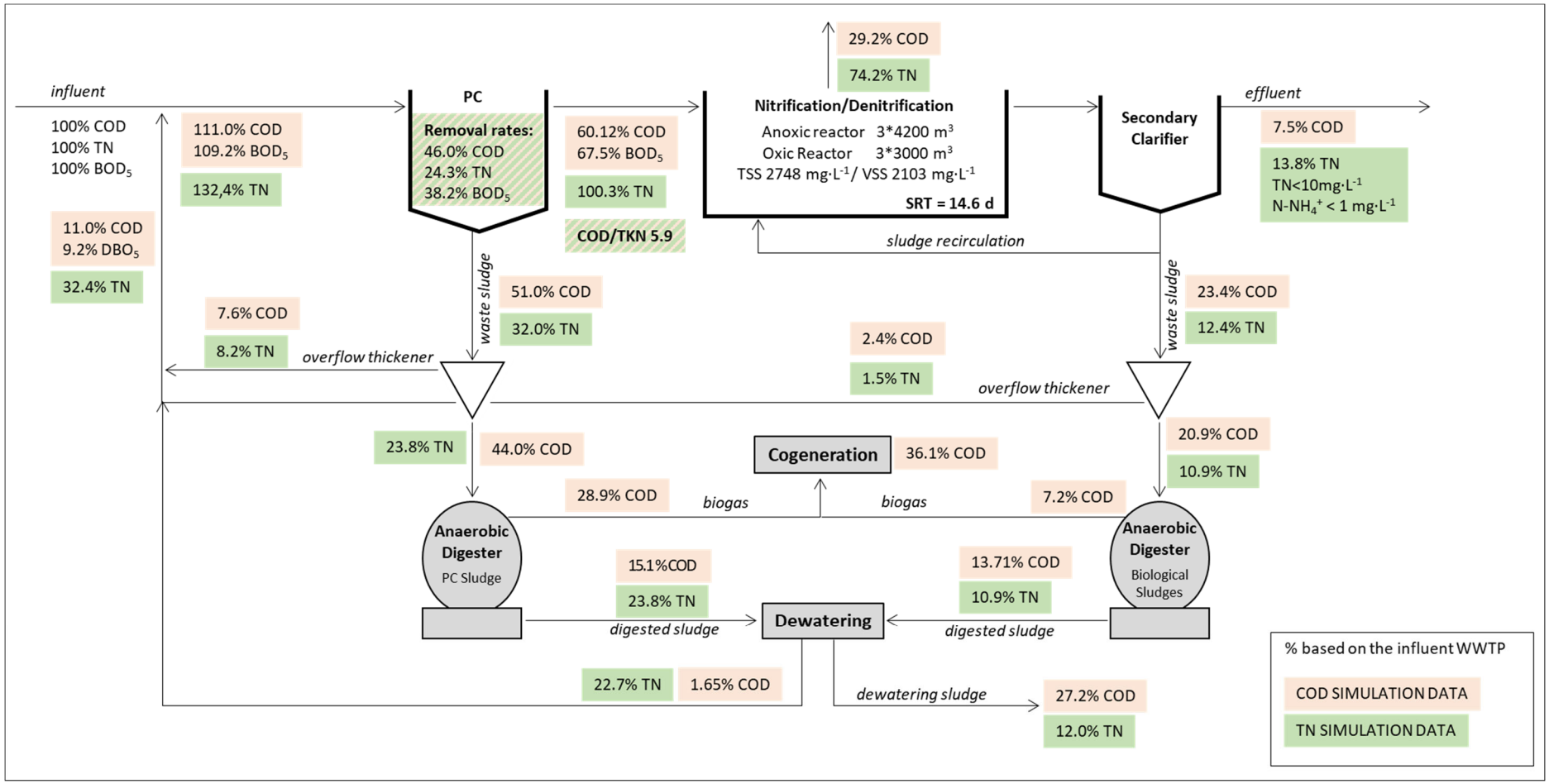

Figure 8.1. COD and TKN flux distribution for a conventional WWTP including PC, Nitrification/Denitrification and Anaerobic Digestion.

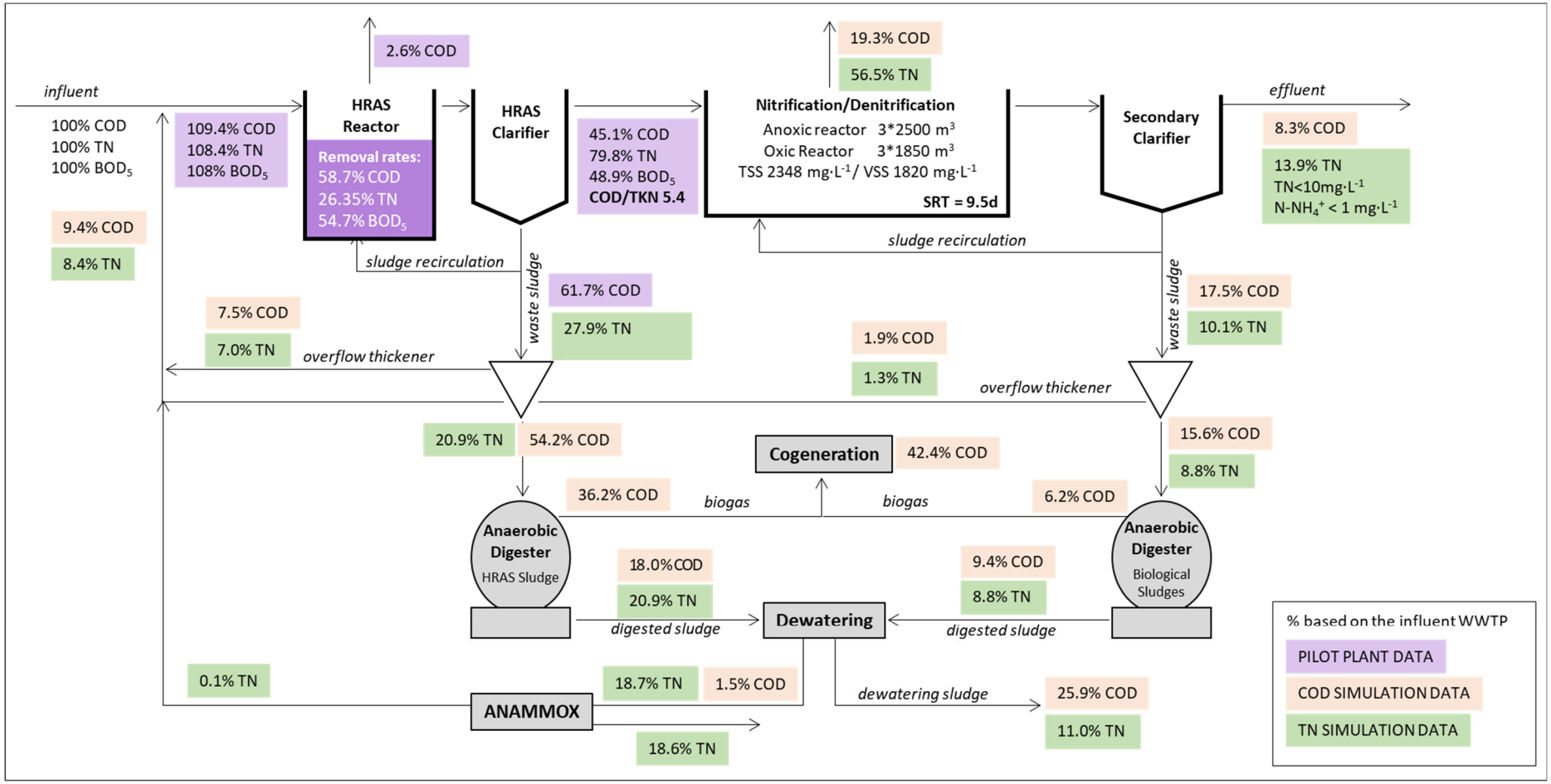

Figure 8.2. COD and TKN flux distribution for an advanced WWTP including HRAS, Nitrification-Denitrification, Anaerobic Digestion and Anammox in the side-stream

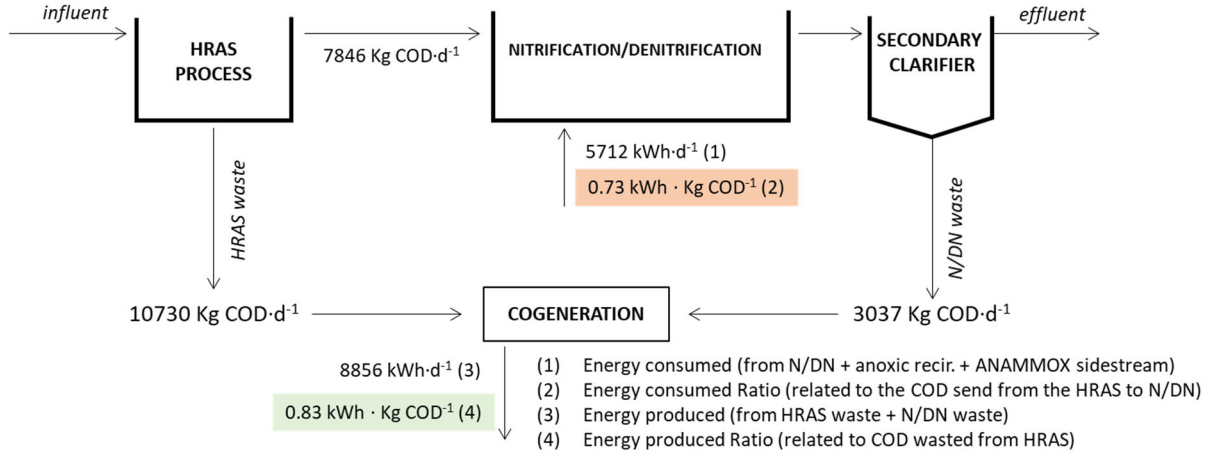

Figure 8.3. Kwh·KgCOD^{-1} ratio as a function of COD harvested o send to N/DN process.

Table 8.2. Electrical energy consumption

Configuration Sludge Treatment	PC+N/DN AD	HRAS+N/DN ANAMMOX + AD
	kWh·m^{-3}	kWh·m^{-3}
Influent WW pump station	0.053	
Pre-treatment	0.007	
PC and pumping	0.005	
HRAS-COD oxidation	-	0.014
HRAS-pumping recirculation	-	0.013
Nitrification/Denitrification	0.264	0.183
Pumping Recirculation	0.038	0.035
ANAMMOX	-	0.02
Sludge Treatment	0.06	
Sludge Dewatering	0.05	
Auxiliary Services	0.01	
Illumination	0.03	
Odor Treatment and climatization	0.03	
Specific energy consumption	0.547	0.509
Specific energy cogenerated	0.314	0.369
Specific net energy consumption	0.233	0.139
Energy Cogenerated	57.37 %	72.6 %
Saved Energy		40.2 %

Table 8.3. Reactor volumes

Configuration Sludge Treatment	PC+N/DN AD	HRAS+N/DN ANAMMOX + AD
HRAS [m^3]		1000 [m^3]
Anoxic Reactor [m^3]	12600	7500 [m^3]
Aerobic Reactor [m^3]	9000	5500 [m^3]
ANAMMOX [m^3]		230 [m^3]
Total Volume [m^3]	21600	14280 - 34 %
Anaerobic Digestor [m^3]	4888	5348 + 9 %

Chapter 9
GENERAL CONCLUSIONS

General conclusions

Regarding Process Stability and Operational Conditions:

- Maintaining a stable MLSS concentration in the reactor has ensured process stability even under large influent variations and extreme operational conditions. An increase in OLR results in increased ORR and sludge generation and waste to maintain the MLSS concentration.
- The Solids Exchange Rate (SER) emphasizes that solids inventory in HRAS is influenced by incoming solids rather than newly generated ones, questioning the importance of SRT as a critical parameter in HRAS design and control.
- Over the 497-day operation, significant variations in influent wastewater were observed due to temperature changes. An increase of 8ºC promoted a 35% of sCOD and a 30% $N\text{-}NH_4^+$ increase, needing a detailed study of seasonal variations in key parameters to ensure appropriate HRAS application and N/DN process selection for the B-Stage.

Regarding Organic Matter Removal:

- HRAS demonstrates efficient COD harvesting to digestion, outperforming PC by 14%, while also reducing COD sent to the CAS with an equivalent reduction in oxygen demand.
- The different COD fraction removal highlights the importance of settling efficiency and stability in HRAS removal efficiencies, emphasizing its use as a replacement for the PC stage.
- HRAS acts as a filter for the influent peak loads of COD, especially the particulate COD since it cannot buffer the soluble COD peak loads. The COD oxidation is primarily affected by the soluble COD removal and the COD wasted is primarily affected by the influent concentration and the removal efficiency of suspended solids.
- The simulation model adopted using SUMO resulted in a good fit for the sCOD, while for the pCOD there was a good fit except for temperatures above 23 °C.

Regarding Nutrients Removal:

- HRAS achieves higher TKN, $N\text{-}NH_4^+$, TP, and $P\text{-}PO_4^{3-}$ removal compared to PC, particularly the 50% for TKN and TP, with removal rates correlated with influent nutrient concentrations.
- HRAS acts as a filter for the influent TP peak loads, and in a lesser extent for TKN peaks.
- TKN and TP removal show positive correlations with COD and pCOD, highlighting the significance of adsorption and entrapment processes. TKN and TP removal were independent of COD_{OXID}. The superplus of sCOD removal suggests intracellular storage or the high nitrogen content in biomass in a heavily loaded HRAS.

- Long-term analysis of COD/TKN ratio in HRAS effluent reveals the presence of a short-cut nitrification/denitrification process, supplemented by Anammox in the sidestream, as the most suitable pathway for downstream nitrogen removal.

Regarding Oxygen Consumption:

- A consistently low low SOC_{COD}, SOC_{sCOD} and SOC_{BOD5} underscore HRAS's heightened energy efficiency at elevated influent concentrations, with SOC influenced by influent concentration and biodegradability.
- High oxidation of COD is generated during periods of high influent soluble COD, suggesting the potential for additional oxygen control strategies using sCOD online monitoring.
- The simulation model using SUMO fitted the SOC values with the exception of very low $sCOD_{IN}$ concentrations.

Regarding Sludge Settleability

- The primary distinction between HRAS clarifier, PC, and SC lies in the nature and quantity of the SS input, with HRAS influenced by incoming solids like PC rather than newly generated ones like SC.
- The low SVI_{30} (high ZSV) of HRAS indicates exceptional biomass settling properties, while high SS_{OUT} indicates low flocculation quality.
- HRAS clarifier could be designed with a higher OFR than SC, however, for enhanced COD harvesting and to increase process stability, it is advisable to consider a lower OFR. The SS effluent is correlated with OFR not with SL.

Regarding Energy Savings and Footprint Reduction in WWTPs.

- Implementation of HRAS instead of PC, along with Anammox in the sidestream, reduces WWTP electricity consumption by 40%. COD harvested in the water line and sent to anaerobic digestion leads to saving of 1.03 $Kwhe \cdot Kg_{COD}^{-1}$ (0.63 save in aeration and 0.4 generated by biogas combustion).
- HRAS entails a 34% reduction in the volume of the water line reactors, and 11% increase in the anaerobic digestion volumes, which decreases the construction costs and footprint

Chapter 10
REFERENCES

References

Akaboci, T.R.V., Gich, F., Ruscalleda, M., Balaguer, M.D., Colprim, J., 2018. Effects of extremely low bulk liquid DO on autotrophic nitrogen removal performance and NOB suppression in side- and mainstream one-stage PNA. Journal of Chemical Technology and Biotechnology 93, 2931–2941. https://doi.org/10.1002/JCTB.5649

A.P.H.A., 2005. Standard Methods for the Examination of Water and Wastewater, 21st ed. American Public Health Association (APHA), American Water Works Association (AWWA) & Water Environment Federation (WEF), Washington DC.

Böhnke, B., 1992. A comparative study of experimental and operational data from 2-stage AB-technology with special consideration to the microbial reaction mechanisms. IOSKOW Aachen Univ.

Böhnke, B., Diering, B., Zuckut, S., 1997. Cost-effective wastewater treatment process for removal of organics and nutrients - ScienceBase-Catalog. Water Eng Manage 144, 18–21.

Bunch, B., Griffin Jr., D.M., 1987. Rapid Removal of Colloidal Substrate from Domestic Wastewaters on JSTOR. J Water Pollut Control Fed 59, 957–963.

Canals, J., Cabrera-Codony, A., Carbó, O., Torán, J., Martín, M., Baldi, M., Gutiérrez, B., Poch, M., Ordóñez, A., Monclús, H., 2023. High-rate activated sludge at very short SRT: Key factors for process stability and performance of COD fractions removal. Water Res 231. https://doi.org/10.1016/j.watres.2023.119610

Carbó, O., Teixidó, J., Canals, J., Ordoñez, A., Magrí, A., Baldi, M., Gutiérrez, B., Colprim, J., 2024. Achieving mainstream partial nitritation with aerobic granular sludge treating high-rate activated sludge effluent.

Carrera, J., Carbó, O., Doñate, S., Suárez-Ojeda, M.E., Pérez, J., 2022. Increasing the energy production in an urban wastewater treatment plant using a high-rate activated sludge: Pilot plant demonstration and energy balance. J Clean Prod 354, 131734. https://doi.org/10.1016/j.jclepro.2022.131734

Carucci, A., Dionisi, D., Majone, M., Rolle, E., Smurra, P., 2001. Aerobic storage by activated sludge on real wastewater. Water Res 35, 3833–3844. https://doi.org/10.1016/S0043-1354(01)00108-7

Christian, S.J., Grant, S.R., Singh, K.S., Landine, R.C., 2008. Performance of a high-rate/high-shear activated sludge bioreactor treating biodegradable wastewater. Environ Technol 29, 837–846. https://doi.org/10.1080/09593330801987616

Clark, S.E., Roenning, C.D., Elligson, J.C., Mikula, J.B., 2009. Inclined Plate Settlers to Treat Storm-Water Solids. Journal of Environmental Engineering 135, 621–626. https://doi.org/10.1061/(ASCE)EE.1943-7870.0000018

Constantine, T., Houweling, D., Kraemer, J., 2012. “Doing the two-step” – Reduced energy consumption sparks renewed interest in multistage biological treatment, in: WEFTEC 2012 - 85th Annual Technical Exhibition and Conference. Water Environment Federation, pp. 5771–5783. https://doi.org/10.2175/193864712811709652

Crites, R.W., Tchobanoglous, G., 1998. Small and decentralized wastewater management systems, McGrawHill series in water resources and environmental engineering. WCB/McGraw-Hill.

Daigger, G.T., Sanjines, P., Pallansch, K., Sizemore, J., Wett, B., 2011. Implementation of a full-scale anammox-based facility to treat an anaerobic digestion sidestream at the alexandria sanitation authority water resource facility. Water Pract Technol 6. https://doi.org/10.2166/WPT.2011.033/21222

De Graaff, M.S., Van Den Brant, T., Roest, K., Van Den Brand, T.P.H., Roest, K., Zandvoort, M.H., Duin, O., Van Loosdrecht, M.C.M., Van Den Brant, T., Roest, K., 2016. Full-Scale Highly-Loaded Wastewater Treatment Processes (A-Stage) to Increase Energy Production from Wastewater: Performance and Design Guidelines. https://home.liebertpub.com/ees 33, 571–577. https://doi.org/10.1089/EES.2016.0022

Dold, P., Fairlamb, M., 2012. Estimating oxygen transfer kla, sote and air flow requirements in fine bubble diffused air systems. Proc. Water Environ. Fed. 2001, 780–791. https://doi.org/10.2175/193864701790864070

Dynamita, 2016. Sumo User Manual [WWW Document]. Sumo User Manual.

Elliot, M.S., 2016. Impacts of Operating Parameters on Extracellular Polymeric Substances Production in a High Rate Activated Sludge System with Low Solids Retention Times. Civil & Environmental Engineering Theses & Dissertations. https://doi.org/10.25777/5mmx-c139

Garrido, J.M., Fdz-Polanco, M., Fdz-Polanco, F., 2013. Working with energy and mass balances: A conceptual framework to understand the limits of municipal wastewater treatment. Water Science and Technology 67, 2294–2301. https://doi.org/10.2166/WST.2013.124

Ge, H., Batstone, D.J., Keller, J., 2015. Biological phosphorus removal from abattoir wastewater at very short sludge ages mediated bynovel PAO clade Comamonadaceae, Water Research. Elsevier Ltd. https://doi.org/10.1016/j.watres.2014.11.026

Ge, H., Batstone, D.J., Mouiche, M., Hu, S., Keller, J., 2017. Nutrient removal and energy recovery from high-rate activated sludge processes – Impact of sludge age, Bioresource Technology. Elsevier. https://doi.org/10.1016/j.biortech.2017.08.115

Goodman, B.L., Englande, A.J., 1974. A unified model of the activated sludge process. Journal of the Water Pollution Control Federation 46, 312–332.

Gori, R., Jiang, L.M., Sobhani, R., Rosso, D., 2011. Effects of soluble and particulate substrate on the carbon and energy footprint of wastewater treatment processes. Water Res 45, 5858–5872. https://doi.org/10.1016/j.watres.2011.08.036

Guisasola, A., de Haas, D., Keller, J., Yuan, Z., 2008. Methane formation in sewer systems, Water Research. Pergamon. https://doi.org/10.1016/j.watres.2007.10.014

Guven, H., Ersahin, M.E., Dereli, R.K., Ozgun, H., Isik, I., Ozturk, I., 2019a. Energy recovery potential of anaerobic digestion of excess sludge from high-rate activated sludge systems co-treating municipal wastewater and food waste. Energy 172, 1027–1036. https://doi.org/10.1016/j.energy.2019.01.150

Guven, H., Ozgun, H., Ersahin, M.E., Dereli, R.K., Sinop, I., Ozturk, I., 2019b. High-rate activated sludge processes for municipal wastewater treatment: the effect of food waste addition and hydraulic limits of the system. Environmental Science and Pollution Research 26, 1770–1780. https://doi.org/10.1007/s11356-018-3665-8

Haider, S., Svardal, K., Vanrolleghem, P.A., Kroiss, H., 2003. The effect of low sludge age on wastewater fractionation (SS, SI), in: Water Science and Technology. IWA Publishing, pp. 203–209. https://doi.org/10.2166/wst.2003.0606

Han, M., Vlaeminck, S.E., Al-Omari, A., Wett, B., Bott, C., Murthy, S., De Clippeleir, H., 2016. Uncoupling the solids retention times of flocs and granules in mainstream deammonification: A screen as effective out-selection tool for nitrite oxidizing bacteria. Bioresour Technol 221, 195–204. https://doi.org/10.1016/J.BIORTECH.2016.08.115

Hauduc, H., Al-Omari, A., Wett, B., Jimenez, J., De Clippeleir, H., Rahman, A., Wadhawan, T., Takacs, I., 2019. Colloids, flocculation and carbon capture – a comprehensive plant-wide model. Water Science and Technology 79, 15–25. https://doi.org/10.2166/WST.2018.454

Hausherr, D., Niederdorfer, R., Bürgmann, H., Lehmann, M.F., Magyar, P., Mohn, J., Morgenroth, E., Joss, A., 2022. Successful year-round mainstream partial nitritation anammox: Assessment of effluent quality, performance and N2O emissions. Water Res X 16, 100145. https://doi.org/10.1016/J.WROA.2022.100145

Henze, M., Gujer, W., Mino, T., van Loosedrecht, M., 2015. Activated Sludge Models ASM1, ASM2, ASM2d and ASM3. Water Intelligence Online 5, 9781780402369–9781780402369. https://doi.org/10.2166/9781780402369

Hertzier, P., Dufresne, L., Randall, C., Barnard, J., Stensel, D., Brown, J., 2010. Nutrient Control Design Manual. U.S. Environmental Protection Agency, Washington, DC, EPA/600/R-10/100.

Hoekstra, M., Geilvoet, S.P., Hendrickx, T.L.G., van Erp Taalman Kip, C.S., Kleerebezem, R., van Loosdrecht, M.C.M., 2019. Towards mainstream anammox: lessons learned from pilot-scale research at WWTP Dokhaven. Environmental Technology (United Kingdom) 40, 1721–1733. https://doi.org/10.1080/09593330.2018.1470204

Huang, J.C., Li, L., 2000. Enhanced primary wastewater treatment by sludge recycling. J Environ Sci Health A Tox Hazard Subst Environ Eng 35, 123–145. https://doi.org/10.1080/10934520009376958

Isanta, E., Reino, C., Carrera, J., Pérez, J., 2015. Stable partial nitritation for low-strength wastewater at low temperature in an aerobic granular reactor. Water Res 80, 149–158. https://doi.org/10.1016/j.watres.2015.04.028

James Bisogni, J., Lawrence, A.W., 1971. Relationships between biological solids retention time and settling characteristics of activated sludge. Water Res 5, 753–763. https://doi.org/10.1016/0043-1354(71)90098-4

Jenkins, D., Richard, M.G., Daigger, G.T., 2003. Manual on the Causes and Control of Activated Sludge Bulking, Foaming, and Other Solids Separation Problems. Manual on the Causes and Control of Activated Sludge Bulking, Foaming, and Other Solids Separation Problems. https://doi.org/10.1201/9780203503157

Jetten, M.S.M.M., Horn, S.J., Van Loosdrecht, M.C.M.M., 1997. Towards a more sustainable municipal wastewater treatment system. Water Science and Technology 35, 171–180. https://doi.org/10.2166/WST.1997.0341

Jia, M., Solon, K., Vandeplassche, D., Venugopal, H., Volcke, E.I.P., 2020. Model-based evaluation of an integrated high-rate activated sludge and mainstream anammox system. Chemical Engineering Journal 382, 122878. https://doi.org/10.1016/J.CEJ.2019.122878

Jiang, C., Xu, S., Wang, R., Feng, S., Zhou, S., Wu, Shimin, Zeng, X., Wu, Shanghua, Bai, Z., Zhuang, G., Zhuang, X., 2019. Achieving efficient nitrogen removal from real sewage via nitrite pathway in a continuous nitrogen removal process by combining free nitrous acid sludge treatment and DO control. Water Res 161, 590–600. https://doi.org/10.1016/j.watres.2019.06.040

Jimenez, J., Miller, M., Bott, C., Murthy, S., De Clippeleir, H., Wett, B., 2015. High-rate activated sludge system for carbon management - Evaluation of crucial process mechanisms and design parameters. Water Res 87, 476–482. https://doi.org/10.1016/j.watres.2015.07.032

Jimenez, J.A., La Motta, E.J., Parker, D.S., 2005. Kinetics of Removal of Particulate Chemical Oxygen Demand in the Activated-Sludge Process. Water Environment Research 77, 437–446. https://doi.org/10.2175/106143005X67340

Jorand, F., Block, J.-C., Palmgren, R., Nielsen, P.H., Urbain, V., Manem, J., 1995. Biosorption of wastewater organics by activated sludges, in: Récents Progrès En Génie Des Procédés.

Kinyua, M.N., Elliott, M., Wett, B., Murthy, S., Chandran, K., Bott, C.B., 2017a. The role of extracellular polymeric substances on carbon capture in a high rate activated sludge A-stage system. Chemical Engineering Journal 322, 428–434. https://doi.org/10.1016/J.CEJ.2017.04.043

Kinyua, M.N., Miller, M.W., Wett, B., Murthy, S., Chandran, K., Bott, C.B., 2017b. Polyhydroxyalkanoates, triacylglycerides and glycogen in a high rate activated sludge A-stage system. Chemical Engineering Journal 316, 350–360. https://doi.org/10.1016/j.cej.2017.01.122

Lackner, S., Gilbert, E.M., Vlaeminck, S.E., Joss, A., Horn, H., van Loosdrecht, M.C.M., 2014. Full-scale partial nitritation/anammox experiences - An application survey. Water Res 55, 292–303. https://doi.org/10.1016/J.WATRES.2014.02.032

Laureni, M., Falås, P., Robin, O., Wick, A., Weissbrodt, D.G., Nielsen, J.L., Ternes, T.A., Morgenroth, E., Joss, A., 2016. Mainstream partial nitritation and anammox: Long-term process stability and effluent quality at low temperatures. Water Res 101, 628–639. https://doi.org/10.1016/j.watres.2016.05.005

Lemaire, R., Zhao, H., Thomson, C., Christensson, M., Piveteau, S., Hemmingsen, S., Veuillet, F., Zozor, P., Ochoa, J., 2014. Mainstream deammonification with anitaTMmox process. 87th Annual Water Environment Federation Technical Exhibition and Conference, WEFTEC 2014 10, 2183–2197. https://doi.org/10.2175/193864714815942422

Li, L., 1998. Improvement of primary wastewater treatment by sludge recycling. The Hong Kong University of Science and Technology, Clear Water Bay, Kowloon, Hong Kong. https://doi.org/10.14711/THESIS-B583777

Liao, B.Q., Droppo, I.G., Leppard, G.G., Liss, S.N., 2006. Effect of solids retention time on structure and characteristics of sludge flocs in sequencing batch reactors. Water Res 40, 2583–2591. https://doi.org/10.1016/j.watres.2006.04.043

Lim, C.P., Neo, J.L., Mar'atusalihat, E., Zhou, Y., Ng, W.J., 2016. Biosorption for carbon capture on acclimated sludge—Process kinetics and microbial community. Biochem Eng J 114, 119–129. https://doi.org/10.1016/j.bej.2016.04.022

Liu, Y., Gu, J., Zhang, M., 2019. A-B Processes: Towards Energy Self-sufficient Municipal Wastewater Treatment. IWA publishing. https://doi.org/10.2166/9781789060089

Magrí, A., Ruscalleda, M., Vilà, A., Akaboci, T.R.V., Dolors Balaguer, M., Llenas, J.M., Colprim, J., 2021. Scaling-up and long-term operation of a full-scale two-stage partial nitritation-anammox system treating landfill leachate. Processes 9. https://doi.org/10.3390/PR9050800

Mamais, D., Jenkins, D., Prrr, P., 1993. A rapid physical-chemical method for the determination of readily biodegradable soluble COD in municipal wastewater. Water Res 27, 195–197. https://doi.org/10.1016/0043-1354(93)90211-Y

Mancell-Egala, W.A.S.K., Su, C., Takacs, I., Novak, J.T., Kinnear, D.J., Murthy, S.N., De Clippeleir, H., 2017. Settling regimen transitions quantify solid separation limitations through correlation with floc size and shape. Water Res 109, 54–68. https://doi.org/10.1016/j.watres.2016.10.080

Martins, A.M.P., Pagilla, K., Heijnen, J.J., Van Loosdrecht, M.C.M., 2004. Filamentous bulking sludge - A critical review. Water Res. https://doi.org/10.1016/j.watres.2003.11.005

Mccarty, P.L., Bae, J., Kim, J., 2011. Domestic Wastewater Treatment as a Net Energy ProducerÀCan This be Achieved? Environ. Sci. Technol 45, 10. https://doi.org/10.1021/es2014264

Measurements, O.N.T., 1999. Standard Methods for the Examination of Water and Wastewater Standard Methods for the Examination of Water and Wastewater, 21st ed, Public Health. American Public Health Association (APHA), American Water Works Association (AWWA) & Water Environment Federation (WEF), Washington DC.

Meerburg, F.A., 2016. High-rate activated sludge systems to maximize recovery of energy from wastewater. Gent University.

Meerburg, F.A., Boon, N., Van Winckel, T., Vercamer, J.A.R., Nopens, I., Vlaeminck, S.E., 2015. Toward energy-neutral wastewater treatment: A high-rate contact stabilization process to maximally recover sewage organics. Bioresour Technol 179, 373–381.

Metcalf, Eddy, 2003. Wastewater Engineering, 4th Editio. ed. McGraw-Hill, New York.

Miller, M., Elliott, M., Kinyua, M., B.W.-H.-R.A., 2015, U., 2015. Optimizing High-Rate Activated Sludge:Organic Substrate for Biological Nitrogen Removal and Energy Recovery. Vtechworks.Lib.Vt.Edu.

Miller, M.W., Elliott, M., DeArmond, J., Kinyua, M., Wett, B., Murthy, S., Bott, C.B., 2017. Controlling the COD removal of an A-stage pilot study with instrumentation and automatic process control. Water Science and Technology 75, 2669–2679. https://doi.org/10.2166/wst.2017.153

Miller, M.W., Jimenez, J., Murthy, S., Kinnear, D., Wett, B., Bott, C.B., 2013. Mechanisms of COD removal in the adsorption stage of the A/B process, in: 86th Annual Water Environment Federation Technical Exhibition and Conference, WEFTEC 2013. Water Environment Federation, pp. 2472–2481. https://doi.org/10.2175/193864713813673721

Modin, O., Persson, F., Wilén, B.-M., Hermansson, M., 2016. Nonoxidative removal of organics in the activated sludge process. http://dx.doi.org/10.1080/10643389.2016.1149903 46, 635–672. https://doi.org/10.1080/10643389.2016.1149903

Nogaj, T., 2015. Mathematical Modeling of Carbon Removal in the A-Stage Activated Sludge System. Electronic Theses and Dissertations.

Nogaj, T., Randall, A., Jimenez, J., Takacs, I., Bott, C., Miller, M., Murthy, S., Wett, B., 2015. Modeling of organic substrate transformation in the high-rate activated sludge process. Water Science and Technology 71, 971–979. https://doi.org/10.2166/wst.2015.051

Pedrouso, A., Val del Río, Á., Morales, N., Vázquez-Padín, J.R., Campos, J.L., Méndez, R., Mosquera-Corral, A., 2017. Nitrite oxidizing bacteria suppression based on in-situ free nitrous acid production at mainstream conditions. Sep Purif Technol 186, 55–62. https://doi.org/10.1016/j.seppur.2017.05.043

Pérez, J., Lotti, T., Kleerebezem, R., Picioreanu, C., van Loosdrecht, M.C.M., 2014. Outcompeting nitrite-oxidizing bacteria in single-stage nitrogen removal in sewage treatment plants: A model-based study. Water Res 66, 208–218. https://doi.org/10.1016/j.watres.2014.08.028

Puig, S., van Loosdrecht, M.C.M., Flameling, A.G., Colprim, J., Meijer, S.C.F., 2010. The effect of primary sedimentation on full-scale WWTP nutrient removal performance. Water Res 44, 3375–3384. https://doi.org/10.1016/J.WATRES.2010.03.024

Rahman, A., De Clippeleir, H., Thomas, W., Jimenez, J.A., Wett, B., Al-Omari, A., Murthy, S., Riffat, R., Bott, C., 2019. A-stage and high-rate contact-stabilization performance comparison for carbon and nutrient redirection from high-strength municipal wastewater. Chemical Engineering Journal 357, 737–749. https://doi.org/10.1016/J.CEJ.2018.09.206

Rahman, A., Meerburg, F., Ravadagundhi, S., Wett, B., Jimenez, J., Bott, C., Al-Omari, A., Riffat, R., Murthy, S., De Clippeleir, H., 2016. Bioflocculation management through high-rate contact-stabilization: A promising technology to recover organic carbon from low-strength wastewater. Water Res 104, 485–496. https://doi.org/10.1016/j.watres.2016.08.047

Rahman, A., Mosquera, M., Thomas, W., Jimenez, J.A., Bott, C., Wett, B., Al-Omari, A., Murthy, S., Riffat, R., De Clippeleir, H., 2017. Impact of aerobic famine and feast condition on extracellular

polymeric substance production in high-rate contact stabilization systems. Chemical Engineering Journal 328, 74–86. https://doi.org/10.1016/J.CEJ.2017.07.029

Regmi, P., Holgate, B., Fredericks, D., Miller, M.W., Wett, B., Murthy, S., Bott, C.B., 2015. Optimization of a mainstream nitritation-denitritation process and anammox polishing. Water Science and Technology 72, 632–642. https://doi.org/10.2166/WST.2015.261

Regmi, P., Miller, M.W., Holgate, B., Bunce, R., Park, H., Chandran, K., Wett, B., Murthy, S., Bott, C.B., 2014. Control of aeration, aerobic SRT and COD input for mainstream nitritation/denitritation. Water Res 57, 162–171. https://doi.org/10.1016/J.WATRES.2014.03.035

Reino, C., Suárez-Ojeda, M.E., Pérez, J., Carrera, J., 2018. Stable long-term operation of an upflow anammox sludge bed reactor at mainstream conditions. Water Res 128, 331–340. https://doi.org/10.1016/J.WATRES.2017.10.058

Rey-Martínez, N., Barreiro-López, A., Guisasola, A., Baeza, J.A., 2021. Comparing continuous and batch operation for high-rate treatment of urban wastewater. Biomass Bioenergy 149, 106077.

Ross, R.D., Crawford, G. V., 1985. INFLUENCE OF WASTE ACTIVATED SLUDGE ON PRIMARY CLARIFIER OPERATION. Journal of the Water Pollution Control Federation 57, 1022–1026.

Rosso, D., Al-Omari, A., Garrido-Baserba, M., de Clippeleir, H., 2019. Carbon Capture and Management Strategies for Energy Harvest from Wastewater | The Water Research Foundation, The Water Research Foundation.

Sancho, I., Lopez-Palau, S., Arespacochaga, N., Cortina, J.L.L., 2019. New concepts on carbon redirection in wastewater treatment plants: A review. Science of the Total Environment 647, 1373–1384. https://doi.org/10.1016/J.SCITOTENV.2018.08.070

Schwarz, M., Behnisch, J., Trippel, J., Engelhart, M., Wagner, M., 2021. Oxygen transfer in two-stage activated sludge wastewater treatment plants. Water (Switzerland) 13, 1964. https://doi.org/10.3390/w13141964

Seeley, I.H., 1992. Wastewater Engineering, in: Public Works Engineering. McGraw-Hill, New York, pp. 160–214. https://doi.org/10.1007/978-1-349-06927-9_4

Siegrist, H., Salzgeber, D., Eugster, J., Joss, A., 2008. Anammox brings WWTP closer to energy autarky due to increased biogas production and reduced aeration energy for N-removal. Water Science and Technology 57, 383–388. https://doi.org/10.2166/WST.2008.048

Taboada-Santos, A., Rivadulla, E., Paredes, L., Carballa, M., Romalde, J., Lema, J.M., 2020. Comprehensive comparison of chemically enhanced primary treatment and high-rate activated sludge in novel wastewater treatment plant configurations. Water Res 169, 115258. https://doi.org/10.1016/j.watres.2019.115258

Takács, I., Vanrolleghem, P.A., 2006. Elemental Balances in Activated Sludge Modelling, in: IWA Publishing. London, UK.

Third, K., Newland, M., Cord-Ruwisch, R., 2003. The effect of dissolved oxygen on PHB accumulation in activated sludge cultures. Biotechnol Bioeng 82, 238–250. https://doi.org/10.1002/BIT.10564

Tirkey, V., Goonesekera, E.M., Kovalovszki, A., Smets, B.F., Dechesne, A., Valverde-Pérez, B., 2022. Short sludge age denitrification as alternative process for energy and nutrient recovery. Bioresour Technol 366, 128184. https://doi.org/10.1016/j.biortech.2022.128184

Torfs, E., Balemans, S., Locatelli, F., Diehl, S., Bürger, R., Laurent, J., François, P., Nopens, I., 2016. On constitutive functions for hindered settling velocity in 1-D settler models: Selection of appropriate model structure. https://doi.org/10.1016/j.watres.2016.11.067

Van Winckel, T., Liu, X., Vlaeminck, S.E., Takács, I., Al-Omari, A., Sturm, B., Kjellerup, B. V., Murthy, S.N., De Clippeleir, H., 2019. Overcoming floc formation limitations in high-rate activated sludge systems. Chemosphere 215, 342–352. https://doi.org/10.1016/J.CHEMOSPHERE.2018.09.169

Versprille, A.I., Zuurveen, B., Stein, T., 1985. The A–B Process: A Novel two Stage Wastewater Treatment System. Water Science and Technology 17, 235–246. https://doi.org/10.2166/WST.1985.0133

Wan, J., Gu, J., Zhao, Q., Liu, Y., 2016. COD capture: A feasible option towards energy self-sufficient domestic wastewater treatment. Sci Rep 6. https://doi.org/10.1038/SREP25054

Wang, H., Xu, G., Qiu, Z., Zhou, Y., Liu, Y., 2019. NOB suppression in pilot-scale mainstream nitritation-denitritation system coupled with MBR for municipal wastewater treatment. Chemosphere 216, 633–639. https://doi.org/10.1016/J.CHEMOSPHERE.2018.10.187

Wett, B., Aichinger, P., Hell, M., Andersen, M., Wellym, L., Fukuzaki, Y., Cao, Y.S., Tao, G., Jimenez, J., Takacs, I., Bott, C., Murthy, S., 2020. Operational and structural A-stage improvements for high-rate carbon removal. Water Environment Research 92, 1983–1989. https://doi.org/10.1002/wer.1354

Wett, B., Buchauer, K., Fimml, C., 2007. Energy self-sufficiency as a feasible concept for wastewater treatment systems, in: IWA Leading Edge Technology Conference. Singapure, pp. 21–24.

Wilén, B.-M., Lumley, D., Mattsson, A., Mino, T., 2006. Rain events and their effect on effluent quality studied at a full scale activated sludge treatment plant. Water Science and Technology 54, 201–208. https://doi.org/10.2166/WST.2006.721

Wu, T., Yang, S.S., Zhong, L., Pang, J.W., Zhang, L., Xia, X.F., Yang, F., Xie, G.J., Liu, B.F., Ren, N.Q., Ding, J., 2023. Simultaneous nitrification, denitrification and phosphorus removal: What have we done so far and how do we need to do in the future?, Science of the Total Environment. Elsevier. https://doi.org/10.1016/j.scitotenv.2022.158977

Yang, Y., Zhang, L., Han, X., Zhang, S., Li, B., Peng, Y., 2016. Determine the operational boundary of a pilot-scale single-stage partial nitritation/anammox system with granular sludge. Water Science and Technology 73, 2085–2092. https://doi.org/10.2166/WST.2016.052

Yeshi, C., Leng, L.C., Li, L., Yingjie, L., Seng, L.K., Ghani, Y.A., Long, W.Y., 2014. Mass flow and energy efficiency in a large water reclamation plant in Singapore. Journal of Water Reuse and Desalination 3, 402–409. https://doi.org/10.2166/WRD.2013.012

Yetis, Tarlan, E., 2002. Improvement of primary settling performance with activated sludge. Environmental Technology (United Kingdom) 23, 363–372. https://doi.org/10.1080/09593332508618395

Zhang, C., Guisasola, A., Baeza, J.A., 2021. Achieving simultaneous biological COD and phosphorus removal in a continuous anaerobic/aerobic A-stage system, Water Research. https://doi.org/10.1016/j.watres.2020.116703

Chapter 11
APPENDICES

A. Model Information

Table 11.1 Oxygen consumption reactions from the model

Gujer kinetic matrix			03/11/2020		05/11/2020		10/11/2020		12/11/2020		16/12/2020		17/12/2020	
j	Symbol	Name	gO2/m3/d	%	gO2/m3/d	%	gO2/m3/d	%	gO2/m3/d	%	gO2/m3/d	%	gO2/m3/d	%
1	r1	OHO growth on VFAs. O2	137.86	17%	95.9	14%	135.86	16%	147.19	16%	97.9	14%	71.26	16%
4	r4	OHO growth on SB. O2	63.47	8%	11.81	2%	31.98	4%	39.36	4%	13.78	2%	33.95	8%
9	r9	OHO growth on SMEOL. O2	0.00	0%	0	0%	0	0%	0	0%	0	0%	0	0%
14	r14	AHO growth on XSTO. O2	601.40	75%	592.07	85%	689.98	80%	705.29	79%	572.09	84%	333	76%
21	r21	PAO growth on PHA. O2	0.16	0%	0.19	0%	0.27	0%	0.26	0%	0.07	0%	0	0%
24	r24	PAO growth on PHA. O2; PO4 limited	0.00	0%	0	0%	0	0%	0	0%	0	0%	0	0%
28	r28	PAO aerobic maintenance	0.02	0%	0.02	0%	0.03	0%	0.03	0%	0.01	0%	0	0%
36	r36	GAO growth on GLY. O2	0.27	0%	0.33	0%	0.36	0%	0.38	0%	0.28	0%	0.13	0%
40	r40	GAO aerobic maintenance	0.08	0%	0.1	0%	0.1	0%	0.11	0%	0.09	0%	0.04	0%
84	r84	Oxidation of Fe^{2+}	0.00	0%	0	0%	0	0%	0	0%	0	0%	0	0%
Total gO2/m3/d			803.25	100%	700.42	100%	858.58	100%	892.62	100%	684.21	100%	438.39	100%
Kg sCODrem/d			0.8		1.26		1.31		1.22		1.11		0.57	
SOCsCOD KgO2/KgsCODrem			0.9		0.5		0.59		0.66		0.55		0.69	
OUR mgO2/L/h			33.5		29.2		35.8		37.2		28.5		18.3	

Table 11.2 sCOD split and removal in the model.

	03/11/20	05/11/20	10/11/20	12/11/20	16/12/20	17/12/20	Average
sCOD							
Kg sCOD(IN)/d	3.4	3.7	3.7	3.7	3.2	1.9	3.3
Kg sCOD(OUT)/d	2.7	2.4	2.5	2.5	2.1	1.4	2.3
Kg sCOD removed/d	0.7	1.3	1.2	1.2	1.2	0.6	1.0
% sCOD removed/d	20%	35%	33%	33%	36%	29%	31%
VFA							
%VFA/sCOD	18%	17%	17%	17%	30%	32%	21%
Kg VFA(IN)/d	0.6	0.6	0.6	0.6	1.0	0.6	0.7
Kg VFA(OUT)/d	0.0	0.1	0.0	0.0	0.0	0.0	0.0
Kg VFA removed/d	0.6	0.6	0.6	0.6	0.9	0.6	0.6
% VFA removed/d	97%	90%	95%	94%	96%	99%	95%
Monomers (non-VFA)							
% monomers/sCOD	20%	29%	29%	29%	18%	17%	25%
Kg monomers(IN)/d	0.7	1.1	1.1	1.1	0.6	0.3	0.8
Kg monomers(OUT)/d	0.0	0.2	0.1	0.1	0.0	0.0	0.1
Kg monomers removed/d	0.7	1.0	1.0	1.0	0.6	0.3	0.8
% monomers removed/d	97%	86%	94%	93%	95%	99%	94%
Polymers							
% polymers/sCOD	29%	46%	46%	46%	27%	26%	38%
Kg polymers (IN)/d	1	1.7	1.7	1.7	0.87	0.5	1.2
Kg polymers (OUT)/d	1.6	1.9	2.1	2.1	1.3	0.9	1.6
Kg polymers removed /d	-0.6	-0.2	-0.4	-0.4	-0.4	-0.4	-0.4
% polymers removed/d	-60%	-12%	-24%	-24%	-49%	-76%	-41%
soluble non-biodegradable							
% non-biodeg./sCOD	32%	8%	8%	8%	25%	25%	17%
Kg (IN)/d	1.1	0.3	0.3	0.3	0.8	0.5	0.6
Kg (OUT)/d	1.1	0.3	0.3	0.3	0.7	0.5	0.5
Kg removed / d	0.0	0.0	0.0	0.0	0.1	0.0	0.0
% removed/d	0%	3%	3%	3%	12%	2%	4%

B. Settling Test

Table 11.3 Height of Interphase at different MLSS concentrations and Time.

Time [min]	975 [mg·L^{-1}]	1480 [mg·L^{-1}]	1950 [mg·L^{-1}]	2565 [mg·L^{-1}]	2952 [mg·L^{-1}]	3444 [mg·L^{-1}]	3930 [mg·L^{-1}]	4500 [mg·L^{-1}]	5000 [mg·L^{-1}]	6000 [mg·L^{-1}]
0	35	35	35	35	35	35	35	35	35	35
1	32.9	31.85	32.2	32.2	32.5	32.9	32.2	32.9	33.9	34.15
2	21	21.7	22.75	24.5	24.5	27.3	27.3	29.4	31.85	33.27
3	10.5	10.5	12.15	15.05	18.55	21	22.05	25.9	29.75	32.05
4	4.9	6.825	9.1	11.55	14.875	17.5	18.55	23.1	27.65	29.95
5	4.025	5.95	8.05	10.15	13.3	15.4	16.1	21	26.25	28.41
10	2.8	4.2	5.95	7	9.8	11.025	11.9	15.4	19.95	22.17
15	2.45	3.5	4.9	6.3	8.4	9.45	10.15	12.95	16.8	18.65
20	2.1	3.15	4.55	5.6	7.35	8.4	9.1	11.55	15.05	17.1
25	2.1	2.975	4.025	5.25	6.825	7.7	8.4	10.5	13.65	15.28
30	1.925	2.8	3.85	4.9	6.3	7.35	7.7	9.8	12.25	13.97
Vel. [cm/min]	9.3	8.3	7.7	6.9	5.9	5.1	4.6	3.3	2.1	1.4
Vel. [m/h]	5.6	5.0	4.6	4.1	3.5	3.1	2.7	2.0	1.3	0.8

C.Sludge Stratification Model

To further understand and validate the observed SS stratification in the clarifier. a flux model with five layers has been developed (Figure 11.1).

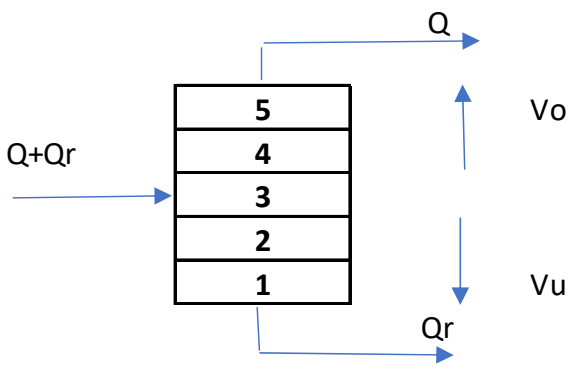

Figure 11.1 Clarifier stratifications layers

Each zone in the clarifier is described by the following differential equations:

For the first layer:

$$\frac{dX_1}{dt} = V_u \cdot (X_2 - X_1) + \frac{flux(X_2)}{h_1} \qquad \text{Equation. 11.1}$$

For the second layer: $$\frac{dX_2}{dt} = V_u \cdot (X_3 - X_2) + flux(X_3) + \frac{flux(X_2)}{h_2}$$ Equation11.2

For the third layer: $$\frac{dX_3}{dt} = (V_u + V_o) \cdot (X_{in} - X_3) + flux(X_4) + \frac{flux(X_3)}{h_3}$$ Equation11.3

For the fourth layer: $$\frac{dX_4}{dt} = V_o \cdot (X_3 - X_4) + flux(X_5) + \frac{flux(X_4)}{h_4}$$ Equation11.4

For the fifth layer: $$\frac{dX_5}{dt} = V_o \cdot (X_4 - X_5) + \frac{flux(X_5)}{h_5}$$ Equation.11.5

Where X_1 to X_5 represent the SS layer concentrations. and Xin is the SSin concentration. h_1 to h_5 are the heights of different layers (considered of the same height in this case). Vo and Vu are the fluid velocities in the clarification zone (OFR) above the inlet point and in the thickening zone below the inlet point. respectively. The product of these velocities with the concentration of SS in each layer represents the SS transport by the fluid movement.

Flux represents the SS transport by SS flocs sedimentation according to the expression:

$$flux(X_1) = V_{hs}(X_1) \cdot X_1)$$ Equation. 11.6

Where *Vhs* is the ZSV in this zone according to Equation 7.2. According to the settling tests section 7.3. $V_0 = 0.0033$ m·s^{-1}. and $r_h = 0.428$ m^3·Kg^{-1}.

The parameters used are h = 2.95 m (total clarifier height); Tt = 30h (total simulation time); X10= 0 Kg·m^3 (initial SS clarifier concentration); Qo= 1.37 m^3·h^{-1} (OFR); Qu= 0.71 m·h^{-1} (recirculation flow); A= 0.73 m^2 (surface clarifier); Xf = 1.7 Kg·m^{-3} SS (inlet SS concentration).

Figure 7.8 shows the SS clarifier stratification from Pilot Plant and Simulation and indicates the goodness of the simulation performed.